DEVELOPMENT OF CHITOSAN-BASED BLEND HOLLOW FIBER MEMBRANES FOR ADSORPTIVE SEPARATION IN ENVIRONMENTAL ENGINEERING AND BIOENGINEERING APPLICATIONS

LIU CHUNXIU

NATIONAL UNIVERSITY OF SINGAPORE

2006

DEVELOPMENT OF CHITOSAN-BASED BLEND HOLLOW FIBER MEMBRANES FOR ADSORPTIVE SEPARATION IN ENVIRONMENTAL ENGINEERING AND BIOENGINEERING APPLICATIONS

LIU CHUNXIU
(B.Sc., Nankai University)

A THESIS SUBMITTED FOR THE Ph.D. DEGREE

DEPARTMENT OF CHEMICAL AND BIOMOLECULAR ENGINEERING

NATIONAL UNIVERSITY OF SINGAPORE

2006

Acknowledgement

First and foremost, I would like to thank my supervisor Prof. Bai Renbi for giving me the chance to join his group and for encouraging me to enter into the wonderful world of hollow fiber membranes. His continuous support and enthusiasm on this project encouraged me greatly throughout this work. His integral view on research has made a deep impression on me and has helped me out immensely by keeping me and my research focused and on track. I owe him lots of gratitude for having shown me the ways of scientific research. Besides of being an excellent supervisor, Prof Bai was as close as a relative and a good friend to all the students. I am really glad that I have come to get know Prof. Bai in my life.

My next thanks go out to Prof. Neal Chung who had kindly provided help in spinning and characterizing the hollow fibers membranes. My thanks also go out to all his PhD students who had helped me a lot throughout the work.

I would like to thank all the students and staffs in particular Li Nan, Han Wei, Liu Changkun, Wee Kin Ho and Dr. Zhang Xiong who worked in the same lab with me. Over the past years, I have indeed enjoyed working with them. They are so kind and ready to help me when necessary. We also discussed and shared some knowledge and information with each other freely. Best wishes to all of them.

Finally, heartful thanks go to my family for their immense support along the way.

Table of Contents

Summary

Adsorptive separation using surface functionalized microfiltration membrane has been being increasingly studied in recent years in environmental and bio- engineering fields to selectively separate heavy metal ions and biomolecules. In this project, a novel adsorptive hollow fiber membrane, chitosan/cellulose acetate (CS/CA) blend hollow fiber membrane was prepared wherein CS provides functional groups (-NH$_2$) while CA acts as hydrophilic support. Protic solvents (>60%v/v) were able to dissolve two polymer together. The coagulant used for spinning the hollow fiber membranes was water or NaOH solution. The research scope of this study includes (1) membrane preparation method study, (2) examination of effect of spinning parameter on membrane structure, (3) application of the membranes for heavy metal ion removal and binding of BSA, and (4) modification the membranes. It was found that the two polymers were miscible in the blends. By adjusting the polymer concentration in spinning solution and composition of coagulant, a variety of CS/CA blend hollow fiber membranes with outer surface pore size in range of ~49nm-0.54µm were prepared. The blend hollow fiber membrane can be prepared to have sponge-like and macrovoids-free cross-sectional structure that is desirable for adsorptive filtration. The maximum CS content in the blend membrane that was achieved in this project was 120 mg/g. At batch mode of adsorption, maximum adsorption capacity for Cu^{2+} was 12.5mg/g and that for BSA after coupling the membrane with Cu^{2+} ligand was 60mg/g. Surface modification with CB F3GA dye improved the kinetics, adsorption amount at low concentration and low pH as well as regeneration by using HCl as desorbent of the original blend hollow fiber membrane for copper ion adsorption.

List of Tables

List of Figures

List of Symbols

1/n	Freundlich intensity parameter (dimensionless)
b	the adsorption equilibrium constant in Langmuir isotherm model (L/mg)
BE	binding energy (ev)
BFFR	bore fluid flow rate
BSA	Bovine Serun Albumin
C	concentration of solutes in the bulk solution
C_0	initial concentration of solute in the bulk solution (mg/L)
CA	cellulose acetate
CB	Cibacron Blue F3GA
C_e	equilibrium concentration of solute in the bulk solution (mg/L)
CS	chitosan
CS/CA	chitosan/cellulose acetate blend hollow fiber membranes
CS/CA-Cu	copper ion immobilized CS/CA blend hollow fiber membranes
D	dialysis
DDA	degree of *N*-deacetylation
DER	dope extrusion rate
ED	electrodialysis
ELM	emulsion liquid membrane
FA	98-100% formic acid
GS	gas separation
I.D.	inner diameter
IMA	immobilized metal ion affinity

IMAC	immobilized metal ion affinity chromatography
IMAMs	immobilized metal ion affinity membranes
K_1	rate constant of pseudo first-order kinetics model (min^{-1} or hr^{-1})
K_2	rate constant of pseudo second-order kinetics model (g · mg^{-1} · min^{-1} or g · mg^{-1} · hr^{-1})
k_d	intrinsic kinetic rate constant for diffusion-controlled adsorption (mg · g^{-1} · min$^{-0.5}$)
K_f	Henry's law constant in Freundlich isotherm model (mg/g)/(mg/L)^n
LM	liquid membrane
MF	microfiltration
MW	molecular weight
MWCO	molecular weight cut off
NF	nanofiltration
O.D.	outer diameter
PAN	polyacrylonitrile
PE	polyehtylene
PES	polyethersulfone
PP	polypropylene
PSF	polysulfone
PTFE	polytetrafluoroethylene
PV	pervaporation
PVC	polyvinylchloride
PVDF	polyvinylidene difluoride
PWF	pure water fluxes
q_e	equilibrium adsorption amount (mg/g)
q_m	the maximum adsorption amount in Langmuir isotherm model (mg/g)
q_t	the adsorption amount at time t (mg/g)
R^2	linear regression coefficients

RO	reverse osmosis
rpm	rounds per minute
SLM	supported liquid membrane
t	adsorption time (min or hr)
UF	ultrafiltration

Chapter 1 Introduction

1.1 Background

The development and application of membrane separation processes is one of the most significant advances in chemical, environmental, and biological process engineering. Currently, membrane process has been successfully applied in gas separation, desalination, water treatment, purification of biopharmaceutical products and food/beverages, and kidney dialysis, etc. Membrane separation system enjoys numerous advantages over conventional separation methods (such as coagulation plus deep bed filtration, distillation, extraction, ion exchange, and so on) including energy saving, environmentally benign, clean technology with operational ease, high quality products, and great flexibility in system design [1].

One of the most common applications for the membrane separation process is for water treatment to remove, concentrate or separate various components with different sizes or dimensions, such as particles, colloids, bacteria, viruses, proteins, humic matters, organic compounds, soluble salts, heavy metal ions, detergents, and so on. Among these components, salts or metal ions are more difficult to remove due to their smaller size (0.3-0.6nm). Among the metal ions, heavy metal ions such as Hg^{2+}, Cd^{2+}, and Cu^{2+} and so on are highly toxic to human bodies even at very low concentration (mg/L). Therefore, removal of them is more crucial. Some of the conventional membrane separation processes such as microfiltration (MF) and ultrafiltration (UF) cannot remove them because of the relatively larger pore sizes of the membrane (>50nm). In contrast, nanofiltration (NF) and reverse osmosis (RO) processes are able to reject them effectively

due to the smaller pore size (NF: ≈1nm, RO: 0.1-1nm). NF is able to retain multi-valent ions such as Ca^{2+}, Mg^{2+} and toxic heavy metal ions. RO is able to retain monovalent ions such as Na^+ and K^+. However, NF/RO processes are generally not economical because of the high operating pressures (5-80bar) and low permeate fluxes (1L membrane has pure water flux at only 70-170mL/min). Other membrane processes such as electrodialysis (ED) and liquid membranes (LM) are also effective in removal or concentration of heavy metal ions. However, ED process has low water permeate flux and is only used in a small scale because only flat membrane is adopted in ED process. Liquid membrane process is a sorption-diffusion process. It has low processing rate as solute transport is controlled by diffusion. Moreover, instability of liquid and loss of carrier from membrane support is severe and limits the wide application of this process.

It is always desirable to be able to remove heavy metal ions with membranes of larger pores (hence high permeate fluxes and low energy consumption), but to achieve high removal efficiency and high selectivity. This may be accomplished by using microporous adsorptive membranes that separate the desired or undesired substances from solutions through affinity adsorption, rather than size exclusion, sorption-diffusion, or ion exchange principles. When the feed is made to pass through the membrane thickness, the desired components to be removed or separated will interact with the functional groups on the external and internal surfaces while the liquid or other components that have low affinity with the membranes will pass through the membrane freely. When the membranes reach adsorption saturation, the adsorbed components can be washed off from the membranes with some types of desorbents and the membranes can then be reused.

Another important application of membrane filtration technology is to harvest and fractionate proteins, enzymes, microbial cells in pharmaceutical industry or to separate bio-products in bioengineering. The membrane processes used for this purpose are mainly UF membranes and dialysis membranes. However, these membrane processes are also based on size exclusion or sieving mechanism. They usually have low selectivity towards components having similar molecule weights and sizes. An alternative way to extract or separate the desired components can be usage of adsorptive membranes. Adsorption based membrane filtration has been developed since 1988 and now it has become a mature and commercial technology: membrane chromatography. The high selectivity of membrane chromatography is often achieved by coupling of specific affinity ligands, such as dyes, bioligands, and metal ions etc., onto the membrane surfaces. When a protein mixture solution passes through the membranes, only the components that have specific affinity with the ligands will be retained on the membrane surface.

Adsorptive membranes may be considered as a special type of MF membranes. The major difference between them is that adsorptive membrane bears functional groups or specific ligands on surface. The choice of MF type of membrane as adsorptive membrane substrate is based on the consideration that it can provide not only high permeate fluxes at low energy consumption but also high internal specific surface areas for binding more components. The greater pore sizes of MF type of membrane also allow the free passage of large biomacromolecules into the membranes so that the adsorption separation can fully take place in the interior of the membranes. Selective separation can be achieved by coupling different functional groups on the membrane.

The separation mechanism of adsorptive membranes is essentially same as that of adsorptive beads or resins since both configurations remove or concentrate the targets by binding them on the surfaces of a solid. However, the membrane based configurations are more efficient than the beads or resins by providing high processing rate. It is well known that the beads or resins are usually packed into a column in practice. When the feed is made to pass though the interstices of the resins in the column, the solutes in the flowing solution have to diffuse a long distance to travel to internal binding sites on the resins for separation to fully take place. Therefore, the processing rate of the resin packed column is very low. In the membrane based configuration, however, the solutes are brought to the external and internal binding sites of the membranes mainly by faster convective flow rather than molecular diffusions, and therefore higher processing rates can be achieved [2]. Schematic illustration of the solute transports in a packed bed and an adsorptive membrane is shown in Fig. 1.1. The fast processing capability of adsorptive membranes is of great importance to the industry for design of fast but low cost separation processes. In the separation of bioproducts, the fast processing rate and low operation pressure requirement is more important because it can minimize the denaturization of fragile proteins.
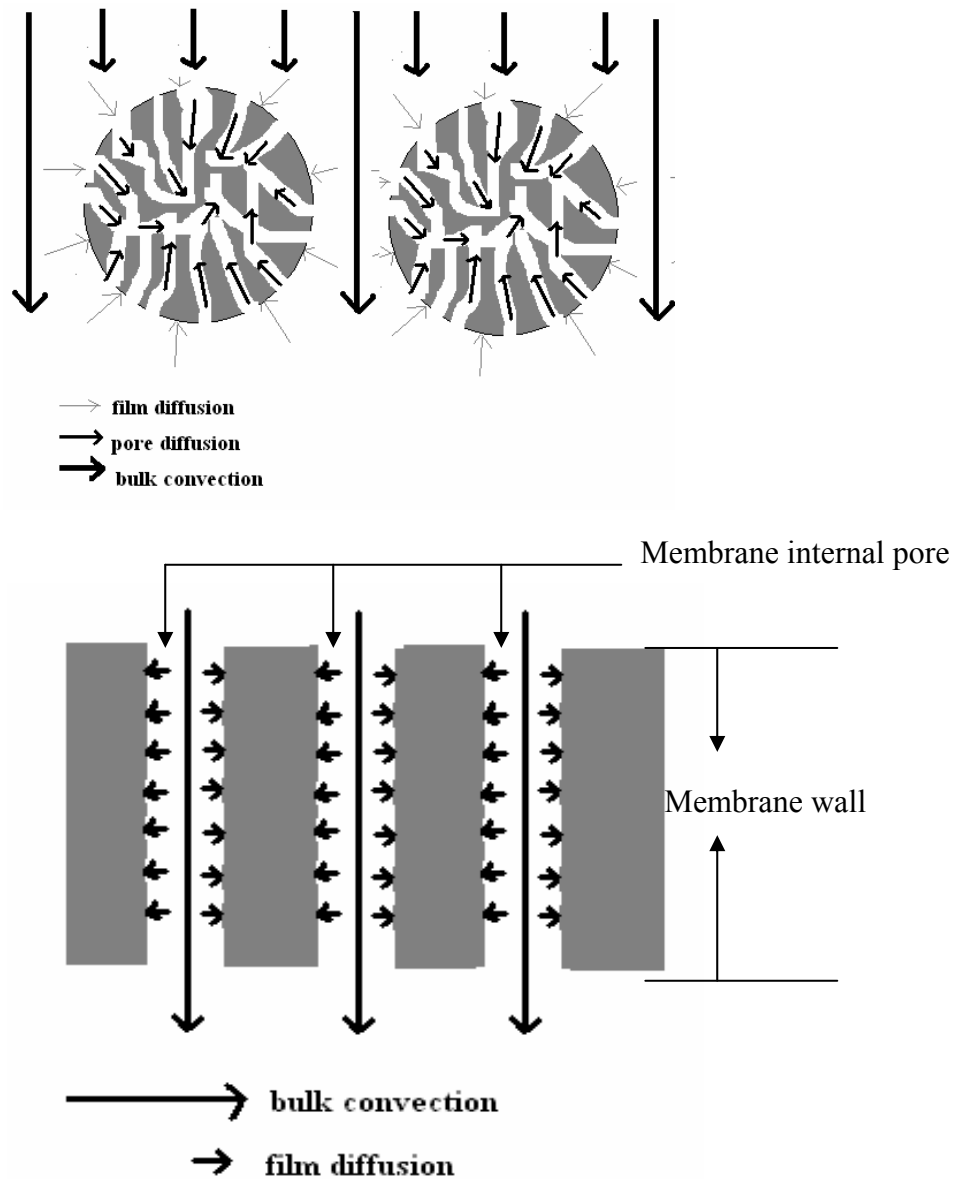
Figure 1.1 Solute transports in packed bed (top) and adsorptive membrane (bottom)
(Adopted from reference [3])

Currently, the major method for preparing adsorptive membrane is by surface modifications of the existing commercial membranes which are usually fabricated from synthetic polymers such as polysulfone (PSF), polyethersulfone (PES), polyvinylidene

difluoride (PVDF), polyethylene (PE), polypropylene (PP), polyamide (nylon), etc. These membranes are chemically inert and highly hydrophobic, usually resulting in low binding capacity and high nonspecific binding or low separation selectivity. Therefore, these conventional membranes need to be surface modified by the introduction of hydrophilic and reactive functional groups, such as -OH, $-NH_2$, $-N^+R_3$, -COOH, $-SO_3H$, epoxy and so on, to the surfaces to eliminate the nonspecific adsorption, increase the binding capacity, or facilitate other ligands coupling. The surface modification methods usually involve graft polymerization on the surfaces. However, the modifications are often conducted under harsh physical and chemical conditions, such as through oxidation with ozone, exposure to an electron or ion-beam, through ultrasonic etching, UV or laser irradiation [4-6], or by plasma treatment at low or ambient pressure [7-8], which often cause damages to the membranes structures and result in severe degradation of the polymer chains [9].

An alternative method to prepare adsorptive membranes is to use naturally occurring biopolymers or their derivatives that contain functional groups on the polymer backbones as the adsorptive membrane materials. The process to prepare adsorptive membranes is hence greatly simplified because surface modifications of the membranes made from these materials are much easier or even unnecessary. Moreover, the naturally occurring biopolymers have many other advantages over the synthetic polymers, including high hydrophilicity, good biocompatibility, nontoxicibility, low cost, and renewability, etc.

Among the biopolymers used, cellulose has been the most widely studied polymer for the preparation of adsorptive membranes. The reactivity of cellulose comes from the hydroxyl groups (-OH) on the polymer backbones. However, -OH does not show direct binding capability to heavy metal ions or proteins. It needs further derivation with other

more reactive functional groups such as $-NH_2$, $-COOH$, $-SO_3H$ and so on to overcome this problem. Recently, research has increasingly been focused on a more reactive biopolymer, chitosan. The reactivity of chitosan comes from the free amino groups ($-NH_2$). Amino groups are more reactive than hydroxyl groups [10] in that it can directly bind heavy metal ions and many charged substances. Therefore, chitosan is more attractive than cellulose as adsorptive membrane material.

1.2 Hypothesis of this research

One major problem with chitosan membrane is the poor mechanical strength including low tensile stress and low stiffness. Chitosan is often fabricated into flat sheet membranes because the flat membranes can be supported by another mechanically strong matrix. Chitosan is also blended with other biopolymers, or water-soluble synthesis or inorganic materials to improve mechanical properties, but the improvement was found to be very limited due to the poor mechanical properties of the blended polymers used, the inhomogeneous blend solution and the weak hydrogen bond or electrostatic attraction between the polymers.

In comparison with preparation of flat sheet membranes, fabrication of chitosan hollow fiber membranes is of more practical interest because hollow fiber membranes have much higher pack densities, larger surface areas and higher utilization rates in industries. Moreover, it can overcome solute lateral leakage in adsorptive filtration process that is often encountered by flat membrane. However, the fabrication of chitosan hollow fiber membranes has been less successful due to lack of self-supporting capability. The reported tensile stress for pure hollow fiber membranes is less than 1.5 Mpa, much less

than 20MPa for commercial hollow fiber membranes. To utilize chitosan with hollow fiber membrane configuration, chitosan has been coated on other mechanically stronger hollow fiber membrane supports either via surface coating or via chemical grafting to obtain composite membranes. The chitosan coated or grafted on the support are however usually small (<1.6g/m^2) in amount. Moreover, coating method results in low reproducibly of the membrane and may suffer detachment of coated layer. Grating of chitosan onto a support often needs the activation of the supports, which have to be carried out under harsh reaction conditions.

Blending two polymers together to prepare blend membrane is a very useful method to obtain membrane with advantages from each polymer. In comparison with surface coating and grafting method, blending method enjoys advantages of (1) simple (2) high reproducibly (3) homogeneous in composition and (4) achievement of high density of functional polymer. However, so far, there is no chitosan blend hollow fiber membrane available. This is due to the lack of suitable blending polymer for providing mechanical strength and corresponding common solvents for dissolving two polymers together.

1.3 Research objectives and scopes of the study

The main objectives of the research is to develop a novel chitosan based hollow fiber membrane, i.e., chitosan blend hollow fiber membranes, and examine the properties and applications of the membranes in adsorption based separation in water or wastewater treatment and bioengineering. Specifically, cellulose acetate was adopted as blending polymer in this research due to its high hydrophilicity and good compatibility with chitosan. Appropriate co-solvents to obtain chitosan and cellulose acetate blend was

identified and the process to spin the blend hollow fiber membranes were developed. The hollow fiber membranes were fully characterized. The factors that affect the structures and pore sizes of the hollow fiber membranes were investigated. The applications of the hollow fiber membranes in fields of water treatment for adsorptive removal of heavy metal ions and in bioseparation for proteins were studied. Finally, surface modification of the hollow fiber membranes with chemicals containing other functional groups was attempted to explore the possibility of further improving the separation performances of the membranes. The special scopes of the study include:

(1) The preparation and characterizations of chitosan/cellulose acetate blend hollow fiber membranes. This part presents the method to prepare chitosan/cellulose acetate blend solutions and the method to spin the blend hollow fiber membranes. As the preparation of both the blend solution and the blend hollow fiber membranes are new, experiments are to be conducted to examine the miscibility and possible interactions between the two polymers in the blends. The mechanical properties of the blend hollow fiber membranes are to be analyzed to evaluate the advantage of adding cellulose acetate into the blend to improve the mechanical strength of chitosan membranes. Adsorption of copper ions and bovine serum albumin (BSA) from aqueous solutions are to be carried out to confirm the benefits of blending a small amount of chitosan with cellulose acetate to make the blend hollow fiber membranes with high affinity or adsorptive capability.

(2) The investigation of process parameters that affect the structures, morphologies and the pore sizes of the chitosan/cellulose acetate blend hollow fiber membranes. The pore sizes of the membranes are of great importance in affinity separation because the components to be separated should have free access to the internal active sites to

maximize the capacity of the membranes. Moreover, the prevention of macrovoids formation is always desirable in fabricating affinity membranes because the formation of macrovoids could reduce the specific internal surface areas. Therefore, this part of the work aims to fabricate chitosan/cellulose acetate blend hollow fiber membranes with structures and pore sizes suitable for affinity separations. In particular, the fabrication of chitosan/cellulose acetate blend hollow fiber membranes with different structures and pore sizes will be attempted. The effects of some spinning factors such as the dope compositions and the types/compositions of the nonsolvent (coagulant) on the structures and pore sizes of the membranes will be investigated in detail.

(3) The application of the chitosan/cellulose acetate blend hollow fiber membranes for adsorptive removal of heavy metal ions from aqueous solutions. Highly porous blend hollow fiber membranes with pore sizes in the micrometer range will be prepared and the performance of the membranes in the removal of heavy metal ion, copper ion, at batch mode will be investigated. The adsorption capacity, kinetics, efficiency at low concentration, mechanism and reuse of the hollow fiber membranes are to be examined in detail.

(4) The application of the chitosan/cellulose acetate blend hollow fiber membranes in protein recovery. Metal ion ligands will be coupled onto the membranes via formation of complex with the $-NH_2$ groups of the membranes to obtain novel immobilized metal ion affinity membranes (IMAMs). A typical metal ion ligand, copper ion, will be coupled and a typical protein, bovine serum albumin, will be recovered by the novel IMAMs at batch mode. The binding performances and behaviors, including capacity, metal ion utilization, metal ion leakage, adsorption isotherm, adsorption kinetics, etc., will be studied in detail.

(5) Surface modification of the chitosan/cellulose acetate blend hollow fiber membranes to improve the heavy metal ion adsorption performance. Due to the presence of reactive –NH$_2$ and –OH groups on the membrane surfaces, the chitosan/cellulose acetate blend hollow fiber membranes may be easily modified with chemicals containing other functional groups. This opens the door to provide the membranes with other desired properties or to improve the existing property of the membranes. In this part of the work, Cibacron Blue F3GA dye as an example will be grafted onto the chitosan/cellulose acetate blend hollow fibre membranes to introduce –SO$_3^-$ groups and increase the content of –NH$_2$ and –NH groups. The adsorption performances of the surface modified membranes for copper ion will be investigated and compared with that without the surface modifications.

Chapter 2 Literature review

2.1   Membranes

A membrane is a permeable or semi-permeable phase, either solid or liquid (often a thin polymer solid), which retains certain species while permit transport of other species [11]. A membrane can be homogenous or heterogeneous, symmetric or asymmetric in structure, solid or liquid, can carry a positive or negative charge or be neutral or bipolar. Schematic drawing illustrating the cross-sections of symmetric and asymmetric membrane is shown in Fig. 2.1.

	Porous Cylinder pores (MF, UF)	Porous, with porous toplayer (UF, MF)
	Porous (MF, D)	Porous, with nonporous toplayer (RO, GS)
	Nonporous (GS, PV)	Composite, with nonporous toplayer (two step preparation) (RO, PV, GS)

Symmetric membranes   *Asymmetric membranes*
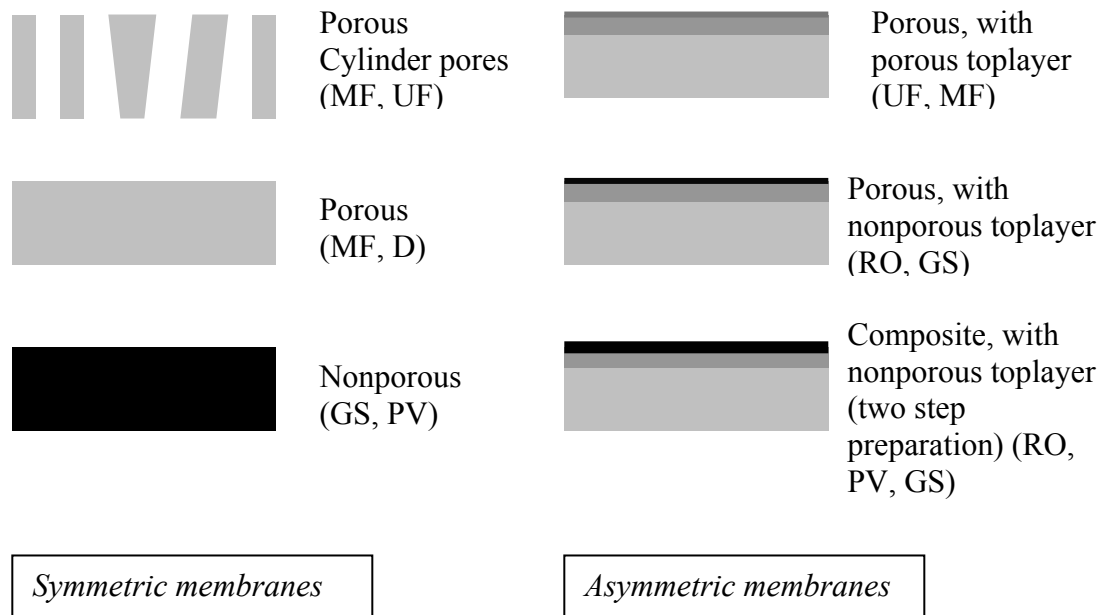
*MF-microfiltration, UF-ultrafiltration, D-dialysis, RO-reverse osmosis, GS-gas separation, PV-pervaporation

Figure 2.1 Schematic illustration of the cross-sections of symmetric and asymmetric membranes (Adopted from reference [12])

A membrane separation system separates an influent stream into two effluent streams known as the permeate and the concentrate. The permeate is the portion of the fluid that has passed through the semi-permeable membrane, whereas the concentrate stream contains the constituents that have been rejected by the membrane. The performance of a membrane is usually defined in terms of two factors: flux and selectivity [11]. Flux is the volumetric (or mass or molar) flow rate of fluid passing through the membrane per unit area of membrane per unit time. Selectivity has different definition for different influent streams. For separation of solutes and particulates in liquids and gases, selectivity is the fraction of solute or particles in the feed retained by the membrane (Eq. (2.1)). For mixtures of miscible liquids and gases, selectivity is the ratio of the concentration in the permeate divided by that in the feed for two components (Eq. (2.2)). Ideally, a membrane with both a high selectivity and a high permeability is required although attempts to maximize one factor are usually compromised by a reduction in the other.

$$R = 1 - \frac{C_p}{C_f} \qquad\qquad (2.1)$$

$$R = \frac{C_{a,f} / C_{b,f}}{C_{a,p} / C_{b,p}} \qquad\qquad (2.2)$$

Where R – selectivity

C_p, C_f – particle or solute concentration in permeate (C_p) and feed (C_f)

$C_{a,f}$, $C_{b,f}$ – concentration of component a or b in feed

$C_{a,p}$, $C_{b,p}$ – concentration of component a or b in permeate

2.2 Membrane materials and preparation methods

Membrane technology became commercially attractive with the development of asymmetric cellulose acetate (CA) reverse osmosis membranes by Loeb and Sourirajan in 1962. CA membrane is relatively inexpensive, highly hydrophilic, has a high flux and a high salt retention for reverse osmosis, a low tendency of fouling by organic macromolecules and moderate chlorine resistance (for cleaning and sanitation). However, CA is subject to rapid hydrolysis at pH <3 and pH>7, or if the temperature exceeds 30-35°C [11].

Other polymers were then introduced as membrane material. Representative polymers successfully used include polysulfone (PSF) and polyethersulfone (PES) [13]. Membranes prepared from these materials show a wide range of pH- and temperature-resistance, and are resistant to chlorine sterilization and cleaning. However, these polymers are hydrophobic and the irreversible membrane fouling by adsorption of the feed components may cause a very severe flux decline. Therefore, a number of other polymers have been investigated as alternative membrane materials, particularly hydrophilic polymers or polymer blends, for example, regenerated cellulose and polyacrylonitrile. The water contact angles that indicate the hydrophobicity of the materials used for some common commercial membranes are listed in Table 2.1. As can be seen, most of the polymers for fabrication of membranes are hydrophobic. Hydrophobic polymers are not wettable with water and needs to be pre-wetted with ethanol before aqueous separation applications.

Table 2.1 Water contact angle θ (°) for some common membrane materials

Polymer	θ	Ref.	polymer	θ	Ref.
Polytetrafluoroethylene (PTFE)	130	[14]	Polyethylene (PE)	103	[14]
Polyvinylidenedifluoride (PVDF)	84	[15]	Polypropylene (PP)	89	[19]
Polyvinylchloride (PVC)	97	[16]	Polyamide (nylon)	76	[20]
Polysulphone (PSF)	69	[17]	polyethersulphone (PES)	79	[21]
Polyacrylonitrile (PAN)	42	[18]	Cellulose acetate (CA)	54	[22]

More recently, inorganic materials are also adopted to prepare membranes, including ceramic, glass, aluminum and so on. Inorganic materials generally possess superior chemical and thermal stability, longer lifetime, and higher hydrophilicity relative to polymeric materials. The application of inorganic membranes in the past includes the enrichment of uranium hexafluoride with porous ceramic membranes [12]. Nowadays, most applications are found in the field of microfiltration and ultrafiltration for liquid phase separation and purification. The major disadvantages with inorganic membranes are that they are generally more expensive than polymeric membranes and are often quite brittle.

A number of different techniques are available to prepare membranes. A detailed description of these methods can be found in M. Mulder's book [12]. Nonporous membranes can be obtained through (1) solution casting followed by solvent evaporation and (2) extruding a melt polymer. To prepare symmetric microporous membranes, several methods are available: sintering, stretching, and track-etching etc. Sintering method involves compressing a powder consisting of particles of a given size and sintering at

elevated temperatures. This method allows microfiltration membranes with pore size of 0.1-10μm but porosity of only 10-20% to be prepared. Both polymeric and inorganic membranes can be prepared through this method. In the stretching method, an extruded film made from partial crystalline polymeric material is stretched perpendicular to the direction of the extrusion. Then small ruptures occur and a porous structure is obtained with pore sizes in the range of 0.1-3μm and porosity of up to 90%. Track-etching method can create parallel cylindrically shaped pores of uniform dimension. A polymeric or inorganic film is subjected to high-energy particle radiation applied perpendicular to the film. The film is then immersed in an acid or alkali bath to etch away the materials along the tracks. The as made membranes have pore size of 0.02-10μm and porosity of <10%.

Asymmetric porous membranes can be prepared through (1) making composite membranes or (2) phase inversion. Composite membranes can be prepared by the method of (1) dip coating or (2) various types of polymerizations such as plasma polymerization, interfacial polymerization, and in-situ polymerization etc. A basic support is needed for making composite membranes and it is often an asymmetric membrane obtained by phase inversion. Plasma polymerization is a procedure, in which gaseous monomers, stimulated through a plasma, condense on freely selectable substrates as highly cross-linked layers. Interfacial polymerization is a polymerization process that occurs at or near the interfacial boundary of two immiscible solutions, with monomer in one solvent reacting with monomer in the other solvent. In-situ polymerization is a process where substrates are dispersed in an appropriate monomer, followed by heat treatment of the mixture to induce polymerization.

The most often used and thus important class of technique for preparing asymmetric

membranes is the phase inversion technique. Phase inversion can generally be subdivided into three categories, depending on the parameters that induce phase demixing [23]: temperature induced phase separation (TIPS), reaction induced phase separation (RIPS), and diffusion induced phase separation (DIPS). Three types of techniques are developed to reach DIPS: coagulation by absorption of nonsolvent from a vapor phase, evaporation of solvent, and immersion into a nonsolvent bath. Often, a combination of the various techniques is used to achieve the desired membrane structures.

All the membranes prepared in the present work were through the immersion phase inversion method. For this reason, the phase separation process by immersion precipitation will be discussed here in more details. To prepare flat sheet membranes, a solution of the polymer is cast as a thin film on a support (glass plate or non-woven) with a casting knife, and then the film is immersed into a coagulation bath that contains a nonsolvent for the polymer for phase inversion to take place. For hollow fiber membranes, a viscous polymer solution is pumped through a spinneret and at the same time, the bore injection is pumped through the inner tube of the spinneret. The polymer solution and bore fluid are extruded into an external nonsolvent to form a hollow fiber. When in contact with nonsolvent, solvent starts to diffuse out of the homogeneous liquid polymer film, whereas non-solvent diffuses into the film. The immersion phase inversion method often results in asymmetric membranes with dense top layers (porous or nonporous) supported on a microporous sublayers. The dense top layers are formed because of the fast phase separation rate on the membrane surface since a high amount of nonsolvent is immediately available near the surface. In the sublayers of the membranes, large voids are often present. It is suggested that the growth of a macrovoid is inherent to the growth of the nucleus [24-25]. In a

nucleus of the polymer-lean phase, a mixture of solvent and non-solvent will be present. It is possible that the solvent concentration in the nucleus becomes so high, that on a local scale a delayed demixing process is favored. This means that around the nucleus the polymer solution is relatively stable and no new nuclei are formed, so that the original nucleus can grow, thereby forming a macrovoid. When the affinity between non-solvent and solvent is high, the solvent in the nascent membrane will tend to flow very quickly to the polymer-lean phase nuclei, whereby the solvent concentration in the nucleus increases drastically and macrovoid formation is favored. At a lower affinity, the solvent flows to the polymer-lean nuclei will be slower, and the propagating diffusion front will be able to form new nuclei deeper in the membrane; these new nuclei will hinder the growth of the older nuclei and macrovoid formation will be hindered. An increase in polymer concentration will slow down the indiffusion of nonsolvent, thereby promoting macrovoid formation, since on a local scale delayed demixing is promoted. On the other hand, with an increase in polymer concentration, the solvent concentration in the polymer-lean nucleus necessary to induce delayed demixing is also increased [25]. Thus, the tendency to form macrovoids will be decreased. Generally, the macrovoids can be suppressed by one or combined methods of the following [13]

-choosing a solvent/non-solvent pair with a lower affinity

-adding a nonsolvent into the solvent/polymer solution before phase immersion

- increasing the polymer concentration in the casting solution

-applying an evaporation step before the immersion in the coagulation bath

-adding solvent to the coagulation bath

For hollow fiber membranes, two coagulants are applied respectively at the outer and inner surface. The phase inversion behavior at the inner side can be significantly different from that at the outer side. As the nonsolvent amount in the lumen is small, the rapid out-diffusion of the solvent from the polymer solutions may make the lumen solution a mixture of solvent and nonsolvent. The solvent concentration in the mixture may be high enough to induce delayed phase separation, often resulting in highly porous structures at the inner surfaces.

2.3 Membrane separation processes

Although the first study of the phenomena related to membrane separations can be tracked back to 1748, it takes more than 200 years for human being to fully recognize membrane technology and make fully use of it. The scientific and systematic study on the membranes just began 40 years ago when Loeb and Souriringan developed, for the first

Table 2.2 Development of membrane processes (Adopted form reference [12])

membrane process	country	year	application
Microfiltration (MF)$^\Delta$	Germany	1920	Laboratory use (bacteria filter)
Ultrafiltration (UF) $^\Delta$	Germany	1930	Laboratory use
Hemodialysis $^\Delta$	Netherlands	1950	Artificial kidney
Electrodialysis (ED)*	USA	1955	Desalination
Reverse osmosis (RO) *	USA	1960	Sea water desalination
Ultrafiltration (UF) *	USA	1960	Concentration of macromolecules
Membrane distillation $^\Delta$	USA	1979	Hydrogen recovery
Gas Separation (GS)*	Germany	1981	Concentration of aqueous solutions
Pervaporation (PV)*	Germany/Netherlands	1982	Dehydration of organic solvents

* industrial scale $^\Delta$ small scale

time in the world, an asymmetric RO membrane. From then on, the membranes have been being widely commercialized. The history of the development of membrane technology can be listed as in Table 2.2.

In terms of the components of feed to be separated, the uses of membranes are classified as the separation of a mixture of gases/vapours, miscible liquids (organic mixtures and aqueous/organic mixtures), solid/liquid, liquid/liquid dispersions and dissolved solutes from liquids [11]. A more common classification of the membrane separation process is based on the specific industrial applications. The most commonly used membrane processes and their applications are listed in Table 2.3. Among these

Table 2.3 Applications of membrane separation processes

Process	Applications
Microfiltration (MF)	Sterile filtration, clarification of juice or beverage, remove particles
Ultrafiltration (UF)	Separation of macromolecular or removal of colloids from solutions
Nanofiltration (NF)	Removal of hardness (di-valent cations and anions) from solutions
Reverse Osmosis (RO)	Separation of monovalent cations and anions and microsolutes from solutions
Electrodialysis (ED)	Desalting of ionic solutions
Liquid membrane	Remove heavy metal ions and hydrocarbons
Gas Separation (GS)	Separation of gas mixtures
Pervaporation (PV)	Separation of azeotropic liquid mixtures

processes, gas separation (GS) is used mainly for separation of gaseous mixtures such as O_2/N_2 separation and removal of H_2S from natural gas etc. Pervaporation (PV) is a process mainly for separation of azeotropic liquid mixtures such as dehydration of alcohols. Other membrane separation processes in Table 2.3, including microfiltration (MF), ultrafiltration

(UF), nanofiltration (NF), reverse osmosis (RO), electrodialysis (ED) and liquid membranes, can be used for water treatment for separation or removal of soluble or insoluble substances, including particles, colloids, bacterial, organic macromolecules, charged solutes, salts, etc.

Different membrane separation processes are based on different separation mechanisms. Three typical types of separation mechanisms exist for the membrane separation processes. Some processes are based on the size exclusion mechanism, i.e., the membranes can retain the components having sizes larger than the pore size of the membranes while allow the free pass of other smaller components. Typical such processes include microfiltration, ultrafiltration and nanofiltraiton. Another mechanism is the sorption-diffusion model, where components that have high affinity with the membrane materials can be absorbed by the membranes at one side and then diffuse to the other side of the membranes. The selectivity is dependent on both the absorption and diffusion rate of each component in the membranes. Typical examples of such process are RO, gas separation, pervaporation and liquid membranes. In fact, some membrane separation processes, such as gas separation, are based not on a single mechanism, but on a combination of several different types of separation mechanisms. The third type is based on the charge characteristics of the components to be separated. In such process, the membranes are electrically charged and only species that have the opposite charge with that on the membranes can pass through the membranes while that with the same charge are rejected. Typical example of such process is electrodialysis. The separation mechanisms for the commonly used membrane separation processes are listed in Table 2.4.

Table 2.4 Membrane separation mechanisms

Mechanism	Membrane separation processes
Size exclusion	MF, UF, NF,GS
Sorption-diffusion (or affinity)	RO, PV, GS, liquid membrane
Charge	ED

Another classification method for the membrane separation process is based on the driving force applied in the membrane separation. They can be principally classified as pressure difference (Δp) driven, concentration difference (ΔC) driven and electrical potential difference (ΔE) driven process. A list of driving forces applied to each membrane separation process is shown in Table 2.5.

Table 2.5 Driving force applied in membrane separation process

Driving force	Membrane separation process
Pressure difference	MF, UF, NF, RO, GS
Concentration difference	PV, GS, liquid membranes
Electrical potential difference	ED

As the present study will be related to the applications of membrane in solid/liquid separation in aqueous solutions, the review will focus on the processes that are mainly used in aqueous media, such as microfiltration, ultrafiltration, nanofiltration, reverse osmosis, as well as electrodialysis and liquid membranes. A summary of the characteristics of these processes, including the membrane pore size, molecular weight cut off (MWCO), components retained, pressure difference applied, etc., are shown in Table 2.6.

Table 2.6 Characteristics of membrane separation processes for water treatment [12, 26-30]

Membrane process	Pore size	Pressure (bar)	Materials pass	examples of materials retained
MF	>50nm	<2bar	water, salts, macromolecules	particles (bacteria, yeasts)
UF	1– 100 nm MWCO: 1,000-100,000	1-10	water, salts, sugars	macromolecules, colloids, solutes MW>10,000
NF	≈1 nm MWCO: 0.2-200	5-20	water, sugars, monovalent ion	solutes MW > 300, Di- and multi- valent ions
RO	0.1-1nm	15-80	water	all dissolved and suspended solutes (salts, sugars)
ED	Not relevant	Not relative	ions with opposite charge as that fixed charges in membrane, water	ions which are same charge as that fixed in membrane
Liquid membrane	Not relevant	Not relative	solutes soluble in the extractant	components with low permeability in liquid membrane

Microfiltration (MF) is by far the most widely used membrane process with total sales greater than the combined sales of all other membrane processes. The pore size of the MF membranes is usually greater than 50nm. Attributed to the large pores, the membranes are operated at low-pressure difference, i.e., <2bar. Microfiltration is a process to separate materials of colloidal sizes and larger than true solutions. One of the main industrial applications is the sterilization and clarification of all kinds of beverages and pharmaceuticals in the food and pharmaceutical industries. A MF membrane is generally symmetric and microporous to pass water and solutes. The porosity of MF membranes is

usually high enough (>80%) to provide high permeate flux. Both polymeric and inorganic materials can be used for MF membranes [12].

Ultrafiltration (UF) covers the region between MF and NF and is used to remove particles and colloids in the size range of 1-100nm. For removal of macromolecules, the pores size of the UF membranes are mostly described by their nominal molecular weight cutoff (MWCO), which indicates the smallest molecular weight species for which the membranes have more than 90% rejection. The MWCO for UF membranes is in the range of 1,000-100,000Da. Typical rejected species by UF membrane include sugars, biomolecules, polymers, and colloidal particles. UF membranes have an asymmetric structure with a much denser toplayer (0.1-0.5µm) supported by a microporous layer. UF processes normally operate at a pressure difference of 1-10 bars. Both polymeric and inorganic materials can be used for UF membranes [12].

Nanofiltration (NF) has only recently achieved success due to developments in composite polyamide membranes [11]. The pore size of the NF membranes is about 1nm and the operation pressure difference is in the range of 5-20bar. NF is capable of concentrating sugars, divalent salts (Mg^{2+}, Ca^{2+}, SO_4^{2-}, CO_3^{2-}, etc.), bacteria, proteins, dyes and other constituents that have a MW greater than 300Da. Monovalent salts, such as Na^+ and K^+, can pass freely through the NF membranes. Membranes used for NF are usually of aromatic polyamide type made by interfacial polymerization of polyamide onto a porous sublayer [11].

Reverse osmosis (RO) is a pressure driven sorption-diffusion process. The sorption-diffusion model is that a surface layer of the membranes is a relaxed region of

amorphous polymer in which solvent and solute dissolve and diffuse. The particle size range for applications of RO separation is approximately 0.1-1nm. RO is aimed at the separation of all types of solutes from aqueous streams. All dissolved and suspended solutes (monovalent salts, sugars) can be removed from water. A much greater operating pressure than NF is required, normally in the range of 15-80bar to overcome not only the molecular friction between permeate and membrane polymer but high osmotic pressure (the osmotic pressure of seawater, for example, is about 25bar). Almost all RO membranes are asymmetric or composite membranes made of polymers with high hydrophilicity and low solute permeability such as cellulose acetate and aromatic polyamides [12].

Electrodialysis (ED) is an electrical potential (ΔE) driven process. ED process is mainly used for removal of salts or charged organics from water. Membranes in the ED units are ion selective and hence called as ion exchange membranes. The cation exchange membranes usually contain $-SO_3^-$ and $-COO^-$ groups, while the anion exchange membranes usually contain $-N^+R_3$ groups. The cation-selective membrane permits only the cations, and anion-selective membrane only the anions to pass through. Each ED unit consists of many flat membrane sheets, typically 150-400, arranged alternatively as cation- and anion-exchange membranes. The transport of ions across the membranes results in ion depletion in some cells, and ion concentration in alternate ones. The ED membranes can be prepared by (1) combining ion-exchange resins with a film-forming polymer and converting them into a film, or by (2) introducing ionic groups onto a polymer (often polystyrene) film [12].

Liquid membranes use a liquid as a membrane material. There are two basic forms of liquid membrane processes. The first is where a liquid is supported in the pores of a microporous membrane, referred to as supported liquid membranes (SLM). The polymers used in the support are hydrophobic, typically polyethylene, polypropylene and poly(vinylidene fluoride) etc. The other form of liquid membrane is the emulsion liquid membranes (ELM) where two immiscible phases, water and oil for example, are mixed vigorously to form emulsion droplets, which are stabilized by the addition of a surfactant. The thickness of the ELM is thin, usually in the range of 0.1-1μm. Solute transport in ELM can then typically proceed from a continuous aqueous phase across the organic film (membrane) and into the emulsion droplet phase (reception phase). Selectivity of liquid membrane is mainly based on the differences in the distribution coefficients of the components of feed phase with the membrane liquid and it can be greatly enhanced when a carrier with the high ability to complex with one of the solute is present inside the membrane liquid. A basic feature of carrier-mediated transport is that the complexation reaction must be reversible. Otherwise, transport will stop once all the carrier molecules have formed a complex with the solutes. Liquid membranes can be used in separation of cations, anions, gases and organic molecules. Heavy metal ions such as copper (Cu^{2+}), mercury (Hg^{2+}), nickel (Ni^{2+}), cadmium (Cd^{2+}), and lead (Pb^{2+}) can be separated. Typical anions that can be separated include nitrate (NO_3^-), chromate ($Cr_2O_7^{2-}$), and uranyl ($UO_2(SO_4)_2^{2-}$) etc. For organic molecules separations, an example is the recovery of aromatic and alphatic hydrocarbons. The major problems of liquid membranes are the loss of liquid and carrier from the support in the SLM process or instability of the emulsion droplet phase in the ELM process [12].

2.4   Adsorptive membranes

As discussed in the previous section, the separation processes that are efficient to retain salts and metal ions are reverse osmosis, nanofiltration, electrodialysis and liquid membranes. Microfiltration and ultrafiltration are not effective in the removal of those solutes although the membranes can operate at relatively lower pressures and produce higher amounts of permeate in a short time. Reverse osmosis and nanofiltration are effective in removal of mono- (RO and NF) or di-valent salts (NF), but they must operate at high-pressure difference and thus are energy intensive. Moreover, the dense or even nonporous surfaces of RO and NF membranes usually result in very low permeate flux. Electrodialysis is effective in separation of charged solutes including salts and charged organics, but it has the problem of high energy consuming, as it is an electrical potential driven process. In addition, the processing rate with ED is not high as the ED unit only consists of flat membranes that have low packing density and surface areas. Similar to RO and NF, the selectivity of ED processes is very limited. For example, selective separation of heavy metal ion from mixture containing Ca^{2+} and Mg^{2+} is sometimes desired. As all the heavy metal ions are di-valent cations, all of them can be effectively retained by RO or NF or ED. Therefore, it is difficult to get the components desired. Liquid membranes can selectively separate solutes by choosing appropriate carrier, but the liquid membranes is quite unstable as lost of the liquid and carrier or the growth of emulsion droplet phase are often observed. Due to this, the development of novel and efficient membrane technologies for various separation applications has never stopped.

In recent years, a relatively newer separation process with adsorptive membrane is increasingly used. The adsorptive membrane is derived from the concept of membrane

chromatography (or affinity membrane) which has been developed for about 20 years. In membrane chromatography, the membrane supports are functionalized with specific ligands (on both external and internal surfaces) to adsorb desired types of biomolecules from mixtures. There is a phase change in the process since adsorbed components transform from liquid to solid. After reaching adsorption saturation, the membranes are regenerated and reused by eluting the adsorbed susbstances. So far, the membrane chromatography has become a mature method and widely used in the downstream purification of biopharmaceutical products.

Replacement of conventional affinity resins by membrane chromatography overcomes many limitations associated with resin-based chromatography such as high-pressure drops, slow processing rates (due to pore diffusion), denaturalization of fragile proteins and channeling of the feed through the bed. In membrane chromatographic processes, the transport of solutes to their binding sites takes place predominantly by convection (see Fig. 1.1), thereby reducing process time. The membrane binding efficiency for protein is generally independent of the flow-rate over a wide range and therefore very high flow-rates may be obtained. For example, when residence time of stream in membrane is reduced from 10 min to 5min (velocity is doubled), there would be no significant change in the breakthrough curve and adsorption capacity. Many commercial products from well-known companies such as Pall Inc. and Sartorius Inc. are renowned to show independent binding capacity with flow rate. Moreover, as the pressure drop in adsorptive filtration is significantly lower than that in packed beds, the denaturization of protein molecules is minimized. Membrane chromatography reflects technological advances in both membrane filtration and fixed-bed liquid chromatography. Another major advantage

of membrane chromatography is its relative ease of scale-up when compared with packed beds. However, the reported binding capacities of affinity membranes for proteins (static) are in the range of 3.3-50 mg/ml membranes [31], typically lower than for porous chromatographic resins. Dynamic binding capacities are smaller than the corresponding static values because some adsorbent volumes remain unused, owing to backmixing, non-uniform flow and resistance from mass transport.

More recently, the concept of membrane chromatography has been developed in water treatment to remove soluble contaminants such as heavy metals and humic matters etc. For this reason, the concept has been widened as "adsorptive membranes". In comparison with RO and NF, the operation pressure/consumption of energy is much lower and the permeate flux is much higher as the adsorptive membranes are usually microporous or macroporous. Moreover, high selectivity can be achieved by functionalization of the membranes with groups having specific binding capability with certain components to be separated in the feed. The major advantage of adsorptive membranes over the adsorptive resin-filled column is that fast processing rate can be easily obtained because the solutes are brought to the binding sites by convective flow in membranes rather than the pore diffusions in columns.

However, drawbacks are also associated with adsorptive membrane. The main drawback for adsorptive membrane is that membrane need frequent regeneration after reaching adsorption saturation. For heavy metal ion removal, acidic and alkali solutions are often used as desorbent solution and regeneration solution respectively. However, these solutions may be corrosive to the membrane polymers. Another drawback with flat sheet adsorptive membrane is that solute lateral leakage is often observed.

The adsorptive membrane cartridge is the core of a separation process. By now, the cartridges used in adsorptive separation include sheets, hollow fibers, spiral-wound and polymer rod membranes. D. Roper and E. Lightfoot have discussed the advantages and disadvantages and kinetics properties of each configuration in a review article [31]. The schematic illustration of the configurations that have been proposed for membrane-based adsorptions is shown in Fig. 2.2. Membranes in the form of thin sheet or disks are convenient, inexpensive, and versatile. As the capacity of single adsorptive membranes

Thin sheet

Membrane stack

Polymer rod

Single hollow fiber membrane
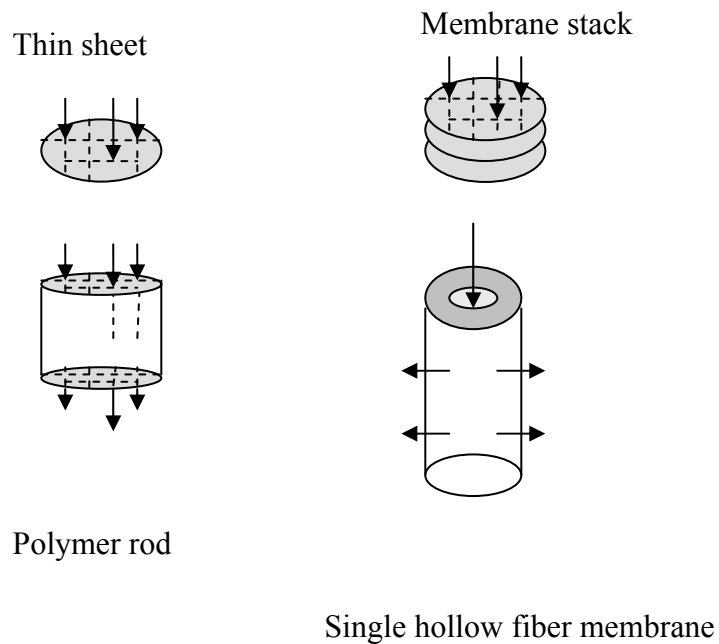
Figure 2.2 Schematic illustrations of adsorptive membrane cartridges (Adopted from reference [31])

may be limited, multiple thin sheet disk membranes are stacked in series and housed in a rigid cylindrical shell. Stacked-membrane geometries allow local variations in porosity and allow membrane thickness to be averaged out in the direction of flow. The possible

problems for the stacked disk module include fluid leakage from membrane edge. The hollow fiber membrane systems are usually considered to have high specific surface area that could lead to high relative adsorption capacity. Therefore, hollow fiber membrane has become one of the most popular shapes adopted in adsorptive membrane technique. The housing for hollow fiber membranes is typically a tube-and-shell like cartridge with a bundle of hollow fiber membranes mounted inside. Since the hollow fiber membrane cartridge is a radial-flow design, no lateral leaking problem should be concerned. A membrane-rod chromatography system involves a column with attributes of both membrane adsorbents and packed-resin beds. The polymeric matrix is a macroporous structure with thickness of 0.1–10 mm, producing a low operation pressure. The pore size distribution and the porosity of the rod can be easily controlled by selecting the proper porogen and varying the volume ratio of porogen to monomer.

2.5   Preparation of adsorptive membranes

One of the most important factors considered in the development of adsorptive membrane has been the improvement of available membrane supports. Correct choice of membrane support and the covalent coupling between the microporous membrane support and the ligand may be essential for the success of the desired adsorptive separation. An ideal supporting membrane matrix for adsorptive separations should hold the the following characteristics [32]: (1) high hydrophilicity and low nonspecific adsorption (which may be due to charged or hydrophobic groups on matrix surface); (2) high specific surface areas (to allow great amount of ligand immobilization and high adsorption capacity); (3) fairly large pore size (to allow the target biospecies easily flow through) and a narrow pore size distribution; (4) high chemical, thermal, and mechanical stabilities

(under a wide range of conditions such as high and low pH values, high and low temperatures, in situations which require organic solvents, detergents and disruptive eluents); and (5) sufficient surface functional groups (e.g., hydroxyl, carboxyl, amide, etc.) for further derivatization and immobilization of ligands. The limitation for membrane supports in adsorptive separation lies generally in the necessity for chemically active sites in the membrane matrix for bonding the ligand.

The materials used in adsorptive membrane may be subdivided into several types. The basic material is cellulose and its derivatives, which have high hydrophilicity and high density of –OH groups and have long been used to prepare matrix for affinity membrane chromatography. Another naturally occurring biopolymer, chitin and chitosan, are increasingly used as the material for adsorptive membranes recently. Chitin and chitosan are good biological materials due to their easy availability, hydrophilicity, good film forming ability and chemical reactivity. Chitosan contain both –OH and $-NH_2$ groups with the later being more reactive than the former. Amino groups ($-NH_2$) can bind proteins and heavy metal ion directly or can be more easily modified with other functional groups. Chitin contains N-acetyl-D-glucosamine units, which are affinity ligands for lysozyme and wheat germ agglutinin [33]. The major problems with chitosan are the poor mechanical strength, great swelling in aqueous solution and poor anti-acid ability. A more extensive review of chitosan and chitosan membranes will be presented latter.

Another type of materials often used for adsorptive membranes is hydrophobic and chemically inert polymers such as polysulfone, polyamide, polyethylene and polypropylene etc. These membranes need to be surface modified to improve the hydrophilicity and to introduce functional groups, such as -OH, $-NH_2$, -COOH, $-SO_3H$,

epoxy and so on. A review of the polymers used for adsorptive membranes and the modification methods have been extensively reviewed in references [2, 34]. Two general types of methods can achieve the surface modifications: physical modification and chemical modification. Physical modification involves coating functional polymers on an existing support. Chemical modification methods include graft polymerization, sulphonation and oxidation of the membrane materials. Coating hydrophilic polymers on a support is simple, but the method is irreproducible and the coated layer may suffer from detachment or dissolution in water as the coated polymers is usually highly hydrophilic. Moreover, the coated hydrophilic polymers are usually small in amount, which leads to the low reactivity of the membranes. Grafting of monomer or graft polymerization is widely used to functionalize the inert polymers by attachment of reactive monomers or polymers. Generally, the modifications are often conducted under harsh physical and chemical conditions, such as exposure to an electron or ion-beam, ultrasonic etching, UV or laser irradiation [4-6], or by plasma treatment at low or ambient pressure [7-8]. The harsh reaction conditions often cause damages to the membranes structures and result in severe degradation of the polymer chains [9]. Sulphonation reaction can introduce $-SO_3^-$ groups on supports made of hydrocarbon or containing aromatic rings. However, the reaction is usually conducted at high temperature (70-80°) and/or with concentrated H_2SO_4 as catalyst that often deteriorate the membrane structures. Oxidization of $-OH$ group containing polymers can produce aldehydes (-CHO) at the position of $-OH$ group, which facilitates the introducing of functional polymers with end $-NH_2$ groups through Schiff base reaction. However, the oxidization reaction is usually conducted with ozone (O_3) or periodate ($NaIO_4$) as the oxidant, which degrade the polymer chains severely and reduce the membrane's mechanical strength significantly.

Besides polymers, inorganic materials are also used as adsorptive membrane substrates, such as titanium dioxide and glass hollow fiber membranes. The attachment of ligands is usually carried out through the activation of –OH groups on the membrane surfaces.

Blending two polymers, one is reactive and another is not reactive, can also produce adsorptive membranes. In comparison with above mentioned coating and grafting methods, this method enjoys advantages of simple, high producibility, homogeneous in compositions and mild preparation conditions. The reactive polymer used for blend could be cellulose, chitosan, polyethylenimine, polyacrylic acid, alginate and so on. As these polymers have low mechanical strength, another polymer that has strong mechanical strength should be blended with them.

2.6   Chitosan and its applications in water treatment and bioseparation

Chitosan is manufactured from chitin, a naturally occurring biopolymer originating mainly from the exoskeleton support of crustaceans, such as lobster, crab and shrimp [35]. Chitin is second only to cellulose in terms of abundance in nature [36]. Chitin contains 2-acetamido-2-deoxy-β-d-glucose through a β (1 → 4) linkage (see Fig. 2.3) [36]. Partial
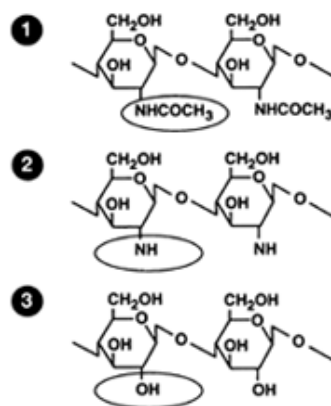
Figure 2.3 Schematic chemical structures of (1) chitin, (2) chitosan and (3) cellulose

deacetylation (>60%) of chitin in alkali solutions to remove the acetyl groups present in chitin and to expose the amino groups gives chitosan. Therefore, chitosan contains both the 2-acetamido-2-deoxy-β-d-glucopyranose and 2-amino-2-deoxy-β-d-glucopyranose residues and is more reactive than chitin. The chemical structures of cellulose, chitin and chitosan are schematically shown in Fig. 2.3.

Chitosan is insoluble in water, alkali solutions and most organic solvents, due to the strong inter- and intra- molecular hydrogen bonds and the high crystallinity [37]. However, chitosan is soluble in some dilute inorganic acid solutions such as HCl and HNO_3 (insoluble in dilute H_2SO_4 and H_3PO_4), and in some of the organic acids (formic acid, acetic acid, etc), via the protonation of the free amino groups ($NH_2 \rightarrow NH_3^+$). This has made it easy to process chitosan into various physical forms. Chitosan can also adsorb a large amount of water and form so-called hydrogels after being dissolved in an acidic solution and coagulated in an alkali solution. From the chemical aspect, chitosan can be considered as analogue of cellulose, in which the hydroxyl groups at carbon-2 are replaced by amino groups and a few acetamido groups [38]. Like cellulose, chitosan also has high hydrophilicity and biocompatibility. However, chitosan is of more commercial and research interest due to its high content of nitrogen (6-7wt%), as compared to cellulose.

Chitosan has been used in many application fields including water and wastewater treatment, medical device, healthy food, packaging, food additives, etc. In water treatment, chitosan is mainly used as adsorbents and flocculants to bind charged substances, heavy metal ions and organic compounds from aqueous solutions. Chitosan is positively charged in acidic solutions (due to the protonation of the free amino groups) and is negatively charged in alkali solutions and thus shows excellent binding capacity toward many

charged water pollutants such as anionic dyes and humic acids through the electrostatic interactions. The free amino groups ($-NH_2$) can function as heavy metal ion chelators by proving a lone pair of electrons and hence chitosan shows strong capability to capture transitional heavy metal ions. Chitosan has been found to be among the most powerful heavy metal ion binders [39]. Literature survey shows that chitosan performs significantly better than many types of commercial activated carbon (CAC) for Cr^{6+}, Hg^{2+}, Cu^{2+}, and Cd^{2+} removal, in terms of metal-loading capacity [40]. Study also shows that chitosan possesses exceptional binding capacity, normally greater than 1 mM metal/g for Cd^{2+}, Hg^{2+}, Pb^{2+} heavy metals (except for Cr), and the capacities are even greater than that of polyaminostyrene, the constituent of expensive ion exchange resins [41]. Chitosan also displays selectivity toward the adsorption of heavy metal ions and they are found to follow a order of $Pd^{2+} > Au^{2+} > Hg^{2+} > Pt^{2+} > Cu^{2+} > Ni^{2+} > Zn^{2+} > Mn^{2+} > Pb^{2+} > Co^{2+} > Cr > Cd^{2+} > Ag^+$ [42-43]. In contrast, chitosan has poor affinity towards alkaline and alkaline earth metals such as Na^+, K^+, Ca^{2+}, Mg^{2+}, etc [35, 44].

Chitosan is also widely studied in bioseparations as it is biocompatible with and shows high reactivity towards biomolecules. Chitosan can bind biomolecules directly through electrostatic or hydrophobic interactions [45-48]. Chitosan has been studied as ion exchange chromatography supports to separate protein mixtures with components having different isoelectric point (pI) values [49-50] through electrostatic interactions. Attributed to the numerous –OH and $-NH_2$ groups on chitosan, specific ligands, such as dyes [51-56], bioligands [57-59] and metal ions [60-61] are also easily coupled onto chitosan to confer it with high selectivity for bioseparations. Surface modification of chitosan to change the hydrophilicity and charge characteristics is also conducted to improve its protein binding

capacity [47, 62].

The applications of chitosan in water treatment and bioengineering is usually achieved by processing chitosan into various forms, such as hydrogel beads, resins, films, membranes, fibers, etc., via the dissolution-coagulation process. Chitosan hydrogel beads and resins have been the two most commonly studied forms for adsorptive and affinity separations in water treatment and bioengineering. The chitosan hydrogel beads have highly swollen polymer networks but poor mechanical properties. Drying the hydrogel beads to produce resins can provide them with improved hardness. However, the problem with both the chitosan hydrogel beads and resins is the low processing rates that are caused by the long diffusion distances of the solutes/solvents from the bulk solution to the internal binding sites of the beads or resins. Spherical chitosan adsorbents with greatly reduced sizes were also prepared, such as microbeads, and nanoparticles etc. [55-56, 63-64]. They usually show improved diffusion properties and hydrodamic behaviors. However, the production yield of these small particles is usually low. Moreover, it is difficult to recover these particles, particularly nanoparticles, from solutions during the particle preparation process. Another problem with them is the leakage from the columns when they are used as the separation medium.

Chitosan is also prepared into membranes for applications in water treatment and bioengineering. Most of the chitosan membranes are studied for conventional filtration process such as ultrafiltration [65], nanofiltration [66], reverse osmosis [67], dialysis [68-70], and pervaporation [71-72] etc. In contrast, the studies for adsorptive or affinity separations are rather limited. The application in heavy metal ion is less studied than in bioseparations. There are only a few reports on using chitosan membranes to remove

heavy metal ions from aqueous solutions. A highly Hg (II) selective membrane was prepared by immobilizing a dye (Procion Brown MX 5BR) on poly(hydroxyethyl methacrylate)/chitosan composite membrane [73]. Low-density vanillin-modified chitosan membrane was prepared and studied as an adsorbent for the removal of copper ions from aqueous solutions [74]. Alumina/chitosan composite membranes were fabricated and studied to remove copper ions from water. The capacity of this composite membranes was reported to reach 200 mg Cu(II)/g chitosan [75]. Chitosan was physically blended with cellulose acetate to make blend films. The capacity of the blend films was reported to be 123 mg of copper ion per gram of the hybrid [76]. In contrast heavy metal ion removal, more reference can be found on the application of chitosan membranes in bioseparations. Microporous and macroporous chitosan membranes were successfully prepared to allow the free passage of protein molecules into the membranes so that adsorption can fully take place in the membranes [51, 77-78]. Crosslinked macroporous chitosan membranes were studied as anion exchange membranes for the separation of protein mixtures with components of different pI values [49]. A few dye ligands [51-52] and bioligands [58-59] were covalently coupled on the microporous/macroporous chitosan membranes to achieve specific separation of proteins. There were studies using macroporous chitin membranes prepared from acetylation of chitosan membranes and the membranes were found to show high affinity binding toward wheat germ agglutinin [33] and lysozyme [79].

2.7   Chitosan based flat sheet membranes

So far, almost all the studies on chitosan and chitosan based membranes are focused on the flat sheet membranes. Although chitosan flat membranes have poor mechanical strength, they can be supported on another matrix to overcome this problem. In contrast,

chitosan hollow fiber membranes have to be self-supported. Therefore, the study of chitosan flat membranes is rather wide.

Chitosan membranes are usually prepared by RIP (reaction induced phase separation) and DIP (diffusion induced phase separation). In RIP, crosslinker can be added into the coagulation solution to precipitate the membranes. In DIP, alkali solution is added into coagulation tank to neutralize the chitosan to form solids. Sometimes, RIP and DIP methods are combined by using basic crosslinker solutions as the precipitation reagent. The TIP (thermally induced phase inversion) method is not applicable to prepare chitosan membranes because chitosan can degrade at the melt point T_m [38].

To prepare chitosan flat membranes, a clear and viscose chitosan solution (usually <7% m/v) is first prepared by dissolving solid chitosan in a dilute weak acid solution (acetic acid, formic acid, etc) for several hours at room temperature or an elevated temperature. The concentration of chitosan in the solution could not be high due to the formation of polyelectrolytes of chitosan in acid solutions ($NH_2 \rightarrow NH_3^+$), which significantly increases the solution viscosity. The concentration depends greatly on the molecular weight (MW) of the chitosan used. To prepare chitosan solution with high concentration, low MW chitosan should be employed. After forming viscous solution, chitosan solution is filtered to remove insoluble particles and degassed to remove small air bubbles entrapped in the solutions before casting. The treated solution is cast into a film using a casting knife. The cast film could be immediately immersed into the coagulants or nonsolvents (wet phase inversion) or may be dried partially or completely before immersion into the nonsolvent to extract the solvents (dry-wet phase inversion). The membranes prepared through the wet phase inversion method are gel-like and have poor

tensile strength. The dry-wet phase inversion method can greatly improve the tensile stress of the chitosan membranes, but the membranes are still flexible due to the lack of bulky groups on chitosan polymer chain.

The freshly prepared chitosan membranes are usually post-treated with a crosslinker to further improve the mechanical strength and enhance the antiacid ability of the membranes. The crosslinkers can also be added into the casting solutions or the coagulants during the membrane preparation process. However, crosslinking can only increase the rigidity of the membranes to some extent, and its effect is rather limited.

As the mechanical strength of chitosan membranes is poor, composite chitosan membranes are more often prepared for practical use purpose. One of the common ways to prepare composite chitosan flat membranes is by surface coating a chitosan layer on other supports with high mechanical strength. The supports reported in the literature include cellulose filter paper [80], cellulose acetate porous membrane [81], peroxyacytyl nitrate (PAN) membrane [82], polyethersulfone (PES) membrane [51], polysulfone membrane [83-85], alumina [75, 86] membrane, etc. The main problems with this method are the low reproducibility, small amount of chitosan coated and detachment of the coated chitosan layer.

Another possible method to make practical use of chitosan membrane is to fabricate membranes from chitosan blends with other materials. In comparison with the coating method, chitosan blend membranes could have more homogeneous distribution of chitosan along the membrane cross-sections, which is desirable especially for affinity

separation applications. The blending materials studied and the characteristics of the blend
membranes or films are summarized in Table 2.7.

Table 2.7 Blending materials reported in literature and characteristics of the blend
membranes or films

blending materials	solvent used	miscibility	tensile stress (MPa)	elongation (%)	Ref.
polyethylene oxide	0.1M acetic acid	m	-	<14%	[83]
bovine atelocollagen	dilute sorbic acid and HCl solution	pm	0.06-0.3	26-32%	[88]
polyacrylic acid	3.5wt% formic acid	m	2-14	1-10	[89]
	7wt% formic acid	m	20-25	4-8	[90]
polyvinyl alcohol	1v/v% acetic acid	-	26-56	8-105	[91]
	0.1M acetic acid	pm	-	<56%	[87]
	Dilute acetic acid	im	-	-	[92]
	0.2M acetic acid	pm	-	-	[93]
	1wt% acetic acid	m	-	-	[94]
polyvinylpyrrolidone	0.1M acetic acid	m	-	<7%	[87]
	1wt% acetic acid	m	-	-	[94]
	2v/v% acetic acid	m	-	-	[95]
collagen	0.5M acetic acid	m	-	-	[96]
gelatin	1v/v% acetic acid	-	-	-	[97]
konjac glucomanan	1v/v% acetic acid	pm	-	-	[98]
alginate	2v/v% acetic acid	m	21-72	6.3-7.5	[99]
	0.1M acetic acid	m	-	-	[100]
hydroxypropylmethyl cellulose	1v/v% acetic acid	pm	-	-	[101]
methylcellulose	1v/v% acetic acid	pm	-	-	[101]
polyamide 6	1wt% formic acid	im	-	-	[102]
cellulose acetate	0.1M acetic acid	m			[76]
cellulose	tetrafluoroacetic acid	pm	-	-	[103]
	tetrafluoroacetic acid	m	-	-	[104]
poly(l-lactide)	acetic acid-DMSO	-	-	-	[105]

N-methylol nylon 6	88% formic acid	-	-	-	[106]
silica	1v/v% acetic acid	im	-	-	[107]
	1v/v% HCl	im	-	-	[108]
	2wt% acetic acid	-	6-47	1-19	[109]

m - miscible;   pm - particle miscible;   im - immsicble

As chitosan is insoluble in common organic solvents but soluble in dilute acid solutions, chitosan blends are usually prepared with water-soluble polymers (synthetic or natural) by dissolving them in a dilute acid solution. Here we will put emphasis on the interactions between the polymers and the mechanical properties of the blend membranes. C. G. L. Khoo et al. [87] studied the miscibility of chitosan/PEO blends and the results showed evidence of miscibility of chitosan/PEO at all blend ratios studied. M. N. Taravel and A. Domard [88] used naturally occurring polymer, bovine atelocollagen, to make blends with chitosan and proposed that the blends were formed though either purely electrostatic interaction or hydrogen bonding. In the case of electrostatic interactions, the addition of bovine atelocollagen hardened the membranes. S. Y. Nam and Y. M. Lee   [89] prepared chitosan-poly(acrylic acid) (PAAc) complex membranes and found that the blend membranes exhibited increased tensile strength and decreased elongation at break, as compared with the average values of chitosan and PAAc. They explained the findings as a result of ionic crosslinking between the two polyelectrolyte polymers. Their results were in agreement with that of G. Dhanuja et al. [90] who also observed the increase in the tensile strength and reduction in the elongation ratio at break with increasing the PAAc content ratio in the blends. P. C. Srinivasa et al. [91] prepared chitosan–polyvinyl alcohol (PVA) blend films and found that the tensile strength of the blend films decreased while elongation ratio at break increased with the increase in PVA concentration. The miscibility between chitosan and PVA in the blends was investigated by several researchers [87,

92-94], but they gave contradictory results as shown in Table 2.7. C. G. L. Koo et al. [87], T.H.M. Abou-Aiad et al. [94] and B. Smitha et al. [95] prepared chitosan/polyvinylpyrrolidone (PVP) blend membranes and all of them found that chitosan/polyvinylpyrrolidone (PVP) blends were miscible and compatible and interactions existed between CS and PVP. However, no data on the mechanical properties of chitosan/PVP blend membranes were reported. A. Sionkowska et al. [96] prepared biopolymer blends using chitosan and collagen and found that miscibility and interactions at the molecular level between the polymers were present in the blends. Y. Huang et al. [97] prepared chitosan and gelatin blends and the study showed that the gelatin compositions greatly affect the membrane stiffness of chitosan, despite gelatin possessed very low stiffness relative to chitosan. X. Ye et al. [98] prepared chitosan/konjac glucomannan blend film and the resultant film had the highest miscibility and blend homogeneity and tensile strength at certain blend ratios due to the strong intermolecular hydrogen bonds between the two polymers. P. Kanti et al. [99] and B. Smitha et al. [100] fabricated polyelectrolyte complex membranes by blending chitosan with alginate. The membranes showed noticeably increased strength, possibly due to the ionic-crosslinking of the two polyelectrolyte polymers in the membranes. However, a marginal change in the elongation at break of the blend was noticed when compared to the homopolymers. J. Yin et al. [101] prepared blends of chitosan with two water-soluble cellulose ethers—hydroxypropylmethylcellulose and methylcellulose. The study showed that the blends were not fully miscible in a dry state although weak hydrogen bonding existed.

Besides the water-soluble polymers, water insoluble polymers are also studied to make blends with chitosan by either physically mixing the polymers together or dissolving them

in a co-solvent. A. Dufresne et al. [102] prepared blends of chitosan with polyamide 6 (PA6) by physically mixing the polymers together in 1 wt% formic acid solutions and it was found that the chitosan phase tended to sediment and to form a continuous phase on the lower face of the film if the chitosan content was high enough. I.S. Lima et al. [76] prepared chitosan and cellulose acetate blend film by physically mixing the polymers together in 0.1M acetic acid solutions and it was found that the two polymers chemically combined in a uniphased film. Y.B. Wu et al. [103] prepared chitosan and cellulose blend film using trifluoroacetic acid (TFA) as the co-solvent to dissolve both the polymers. The mechanical and dynamic mechanical thermal properties of the cellulose/chitosan blends appeared to be dominated by cellulose. Therefore, it has low mechanical strength. Study by A. Isogai and R.H. Atalla [104] who also prepared chitosan/cellulose blend films using TFA as the co-solvent suggested that cellulose and chitosan were intimately blended in the films. C. Chen et al. [105] prepared blends of poly(l-lactide) (PLLA) and chitosan by precipitating out PLLA/chitosan from acetic acid–DMSO mixtures with acetone, and reported that intermolecular hydrogen bonds existed between the two polymers in the blends. J.J. Shieh and R.Y.M. Huang [106] prepared *N*-methylol nylon 6 and chitosan blends by using 88% formic acid as the co-solvent. But nylon is very hydrophobic and not compatible with chitosan polymer.

Besides polymers, chitosan has also been blended with inorganic materials. T. Suzuki and Y. Mizushima [107] and S.B. Park et al. [108] prepared chitosan–silica hybrid materials by using tetraethoxysilane (TEOS) as the blending medium. In these blends, the silica network forms from the self-condensation reaction of the hydrolyzed Si-OH groups. Y.L. Liu et al. [109] prepared chitosan–silica hybrid membranes by in situ covalently

crosslinking chitosan with γ-glycidoxypropyltrimethoxysilane (GPTMS). The addition of GPTMS, however, did not improve the mechanical properties of the polymer as the tensile strength at break, elongation percent at break, and Young's modulus decreased with the increase of GPTMS loadings.

Among all the above mentioned blending materials, only nylon and cellulose acetate polymers are mechanically strong for preparing membranes. The blends of N-methylol nylon-6 with chitosan were prepared by dissolving them in a co-solvent, therefore the resulting blend membranes could have high mechanical strength. The blends with cellulose acetate were prepared, however, only by physical blending, leading to the poor strength of the blend membranes. The other blends have only achieved limited improvement (because the formation of only hydrogen bond or ionic crosslinking between the polymers) or even reduced mechanical properties (because the blending materials used are water-soluble and have much lower mechanical strength than chitosan).

Besides the effort in improving the mechanical properties of the chitosan flat sheet membranes, effort was also made to control the structures and the pore sizes of chitosan flat sheet membranes. E. Ruckenstein and X.F. Zeng prepared the macroporous chitosan membranes by using silica gels as the porogen [71-78]. Silica gel is compatible with the acid solutions but would dissolve in alkali solutions. Therefore, silica gel in the casting solution can be extracted in hot alkali solutions in the coagulation process and hence macropores were formed on the membranes. The macroporous chitosan membranes were reported to have pores with sizes in the range of 15-40μm [71]. Water-soluble polymers such as polyethylene glycol (PEG) were also successfully adopted as the porogen to prepare microporous chitosan membranes [51, 110-111] as PEG can be extracted by water

in the coagulation and washing process. However, some polymers which could mix and form strong interactions with chitosan at molecule level, such as PVP, were found to be hard to be extracted and ineffective in creating micropores [111]. Nanoporous chitosan membranes were prepared by a novel emulsion-mediated templating method by Y. Liu et al. and the pore sizes were reported in the ranges of 10–50 nm [112].

Although much effort has been made on the fabrication of chitosan and chitosan based flat sheet membranes, the preparations of chitosan and chitosan based hollow fiber membranes have seldom been reported. Chitosan flat sheet membranes may be used in lab or on a small scale to process small volumes of feed, due to their relatively low pack density. In the industrial, hollow fiber membranes are more frequently or preferably used. Hollow fiber membranes take the tubular form and can be self supported, thus reducing the space requirement and increasing the pack densities and water flux of the membrane ssytem. In addition, hollow fiber membranes can be more easily scaled up than flat sheet membranes for large-scale operations. Moreover, no lateral leakage will appear for hollow fiber cartridge in adsorptive filtration separation. Hence, the preparation/fabrication of chitosan based hollow fiber membranes is of great research/practical importance.

2.8   Chitosan based hollow fiber membranes

Similar to flat sheet membranes, chitosan based hollow fiber membranes can include two types: pure chitosan hollow fiber membranes and composite chitosan hollow fiber membranes. The reports on the preparation of pure chitosan hollow fiber membranes are rather limited, mainly due to the poor mechanical strength of chitosan. The first patented pure chitosn hollow fiber membrane was fabricated by F. Pittalis et al. [113] in 1984, by

the wet spinning of acid chitosan solution and by using an alkali solution as the external fiber coagulant and a gaseous phase containing ammonia as the internal fiber coagulant. The hollow fiber membranes were studied in the ultrafiltration (UF) and dialytic processes. The rupture pressure for the fiber was greater than 600 mmHg. However, the hollow fiber membranes were gel-like and soft, and their mechanical strength cannot possibly be comparable to that of commercial membranes. A long time after that, no report on the fabrication of pure chitosan hollow fiber membranes was available in the literature until 2000 when T. Vincent and E. Guibal [114] showed the use of such hollow fiber membranes for extraction of Cr (VI). The hollow fiber membranes were prepared by wet spinning of chitosan acid solutions into NaOH solutions, but the lumen was formed by blowing out the non-coagulated interior solutions using gas. To improve the mechanical strength, the fibers were partially acetylated to chitin with acetic anhydride. However, the partial acetylation of chitosan to chitin appeared not to be efficient enough to produce strong fibers as the sample hollow fiber membranes showed in the report was partially collapsed and not self-support. In 2004, Z. Modrzejewska and W. Eckstein [115] reported the preparation of pure chitosan hollow fiber membranes with improved strength, by taking advantage of the unique rheological properties of the highly viscous chitosan solutions in acetic acid. However, the tensile stress of the chitosan hollow fiber membranes at wet state was lower than 1.5 MPa. Moreover, the method needs to spin the hollow fibers at a very high shear rate, which poses great difficulties to the spinning process.

As in the case of chitosan flat sheet membranes, an alternative method is to fabricate chitosan composite hollow fiber membranes, with chitosan supported on other materials of

high mechanical strength. In general, two approaches, including the physical coating method and chemical grafting method, have been employed to fabricate the chitosan composite hollow fiber membranes.

The physical coating method is much easier and has been used in a number of studies. S. Kuniyasu et al. [116] prepared chitosan coated polyphenylenesulfide sulfone hollow fiber membranes. The composite hollow fiber membranes showed high organic solvent resistance and heat resistance and may be used in areas for pervaporation, gas separation, and reverse osmosis. C.Y. Gong and J.Y. Su [117] prepared polysulfone-chitosan hollow fiber membranes via dip coating of chitosan solution on the polysulfone support, followed by cross-linking the chitosan. The hollow fiber membranes were reported to have charged surfaces and be useful in the desalination of seawater. W. Edwards [84] developed chitosan coated polysulfone hollow fiber membranes and the membranes were used in membrane bioreactor for phenol remediation. Besides the polymeric support, some inorganic hollow fiber membranes were also used as the support. S. Tomonari [118] prepared chitosan composite hollow fiber membranes by laminating chitosan film on alumina and ceramic membranes. The hollow fiber membranes showed excellent physical properties and were used for dehumidifying organic solvents or gases.

The advantages and shortcomings of the chitosan coated hollow fiber membranes may be similar to those of chitosan coated flat sheet membranes, but in general, chitosan coated hollow fiber membranes have higher mechanical strength since a support with stronger mechanical strength is used. Besides, the coating method is simple, inexpensive and the supports can be freely selected. From the structural point of view, the chitosan coated hollow fiber membranes have heterogeneous structures, with one thin chitosan

layer supported on another porous supporting material. The thin chitosan layer, as an active layer, can improve the performances of the hollow fiber membranes in some application fields. However, the chitosan coated hollow fiber membranes can fail in fields where the adsorption capability of chitosan plays the primary role as the coated chitosan layer on the hollow fiber membranes is very thin and the amount of chitosan is very small. Another drawback of the coating method for preparing composite chitosan hollow fiber membranes is the clogging of the fiber's lumen by chitosan solution, which is difficult to be cleaned afterwards. Other drawbacks of the coating method include irreproducibility, incomplete coverage of the surfaces and easy detachment of the coated chitosan layers.

The other method to make chitosan composite hollow fiber membranes has been through surface grafting, i.e., the covalent coupling of chitosan on a support with strong mechanical strength. B. Xia et al. [119] prepared chitosan grafted nylon hollow fiber membranes for bilirubin adsorptions. The coupled chitosan amount reached 84mg/g hollow fiber membranes. W. Shi et al. [120] disclosed a process for preparing asymmetric ultrafiltration adsorptive polysulfone-chitosan membrane via chemical reaction, but the amount of chitosan grafted was not reported. P. Ye et al. [121] fabricated a dual-layer biomimetic membrane as the support for enzyme immobilization by covalently coupling chitosan on the surface of poly(acrylonitrile-co-maleic acid) (PANCMA) ultrafiltration hollow fiber membranes. The grafted chitosan amount was reported to be 0.032-1.2g/m^2.

There are disadvantages with the grafting method as well. The coupling reaction is normally carried out under harsh reaction conditions, such as acid and alkali treatment and high temperature for reaction, that are often undesirable to retain the membrane properties. Moreover, the content or density of chitosan grafted on the composite hollow fiber

membranes could not be substantial because the amount is controlled by the chitosan molecules that can diffuse into the reaction sites of the support and the reaction can usually only take place on the outer surface of the membranes.

From the above discussions, it is clear that the methods used to prepare chitosan or chitosan based hollow fiber membranes are rather limited. Therefore, the development of new or improved methods is important. A possible method that has never been attempted by researchers is to prepare chitosan based hollow fiber membranes from chitosan blends with other materials. As discussed earlier, most of the polymers or inorganic materials that have been used to prepare chitosan flat sheet membranes are poor in mechanical strength. Even though nylon, a mechanically stronger polymer, may be used as a candidate to prepare chitosan blend hollow fiber membranes, nylon is hydrophobic and incompatible with chitosan [122]. So far, the major difficulty in the fabrication of chitosan blend hollow fiber membranes has come from (1) the selection of suitable blend polymers that provide high mechanical strength and (2) the selection of co-solvents that can dissolve both chitosan and the polymer to be blended to form a homogeneous and clear blend solution. Although many commercial synthetic polymers could be chosen as the blend polymers, no suitable co-solvents can be easily found because of the significant difference in their dissolution behaviors. It is well known that the frequently used solvents for chitosan are some dilute acid solutions but those for synthetic polymers are usually non-acidic organic solvents. Therefore, finding the suitable blend polymers with chitosan and the corresponding co-solvents is the major challenge.

In this research, we studied cellulose acetate as the polymer to be blended with chitosan by using concentrated organic acid solutions as the co-solvents. This provides the

possibility to prepare chitosan/cellulose acetate blend hollow fiber membranes. The reason for choosing cellulose acetate is that it is a hydrophilic and compatible with chitosan. The preparation and examination of chitosan/cellulose acetate blend hollow fiber membranes is of great research and practical interest. This thesis summarized the major results in the preparation, characterization, and application of chitosan/cellulose acetate blend hollow fiber membranes as well as in the exploration of surface modification to enhance or improve the properties of the membranes.

2.9   Significance of this study

From the practical aspect, the main contribution of this work has been the preparation of the chitosan and cellulose acetate blend hollow fiber membranes, which is the first of its kind. The study has demonstrated the feasibility of the co-solvent selected to prepare chitosan and cellulose acetate blend solutions that have been successfully used to fabricate chitosan and cellulose acetate blend hollow fiber membranes. The developed blend hollow fiber membranes have high mechanical strength, high reactivity, and tunable hydrophilicity. The pore sizes and porosities of the membranes can be effectively controlled through some spinning parameters. The novel chitosan based blend hollow fiber membranes (with or without surface modifications) have been shown to have good adsorptive performance for heavy metal removal and protein recovery. Hence, there is practical potential of the novel hollow fiber membranes for industrial applications in environmental and biopharmaceutical engineering. Theoretically, the study on the blending mechanisms of the polymers, the binding behavior of the metal ions and albumins on the blend hollow fiber membranes provide new information and increase our

understanding in chitosan-based hollow fiber membranes for affinity separation applications.

Chapter 3 Preparation and characterization of chitosan/cellulose acetate (CS/CA) blend hollow fiber membranes

Summary

Cellulose acetate (CA) was chosen as the blending polymer to provide the blend membrane with high mechanical strength. Another important reason for choosing CA is that CA has similar molecular structure to CS, giving the possibility that good compatibility between the two polymers can be achieved. The suitable common solvents for both CS and CA were found to be a series of protic solvents with acid concentration higher than 60%v/v. Alkali solution (3wt% NaOH) was employed as external and internal coagulants for spinning hollow fiber membranes in this chapter. The membranes prepared in this part of the work were mechanically strong (tensile stress: 22-26 MPa) due to high concentration of CA (26-26.5%wt.) in spinning solution. However, they possessed low concentration of CS (1.7-3.5%wt). FTIR and XRD experimental results suggested good miscibility between the two polymers. The membranes showed sponge-like and macrovoids-free open porous structure, which are desirable for adsorptive filtration. In spite of small amount of CS blended, copper ion binding was significantly improved (maximum: 4mg/g at pH 6 at batch mode) as compared to 0mg/g for pure CA membrane.

3.1 Introduction

The production of chitosan (CS) based blend hollow fiber membranes has never been reported so far, largely due to the lack of the desired blending polymers and co-solvents known. In this work, we developed the method to make cellulose acetate (CA) and CS blend solutions through a co-solvent, protic solvent (60-100%v/v), which made it possible to prepare CS blend hollow fiber membranes.

The membranes made from CA normally have high mechanical strength and hydrophilicity. CA membranes have been widely used as reverse osmosis (RO) membranes in industry. Moreover, since CA has similar chemical structure (see Fig. 3.1) to CS, it provides the possibility for good miscibility with CS. However, the solvents used for CA are usually organic and aprotic solutions such as acetone, N, N-dimethylformamide (DMF), N-Methyl-2-Pyrrolidone (NMP), tetrahydrofuran (THF), and dimethyl sulfoxane (DMSO), etc, but that for CS is dilute acid solution. Therefore, co-solvent for both CS and CA is not available.
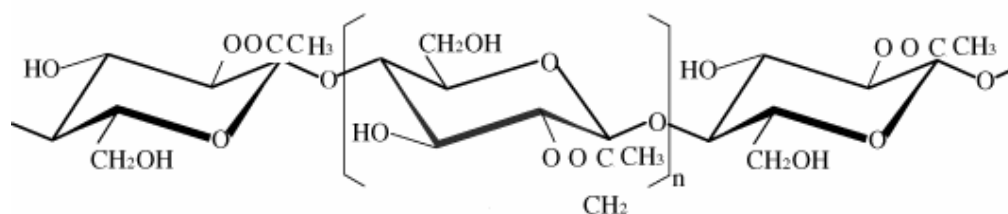
Figure 3.1 Schematic chemical structure of cellulose acetate

After many tests, we found that highly concentrated organic acid (such as formic acid and acetic acid) solutions can be selected as solvents for both CS and CA polymers. The

produced blend solution is clear, homogeneous and transparent. We varied the concentrations of the acid solutions and found a minimum of 60% v/v is required. Mixtures of acids with organic solvents were also found to be able to dissolve the polymers together. Some of these solvents proven effective for dissolving CS and CA are listed below:

1. Formic acid aqueous solutions (60-100% by volume)

2. Acetic acid aqueous solutions (60-100% by volume)

3. Mixture (at any ratio) of 1 and 2

4. Formic acid in acetone (60-100% by volume)

5. Acetic acid in acetone (60-100% by volume)

6. Mixture (at any ratio) of items 4 and 5.

In this chapter, a typical co-solvent, 98-100% formic acid (FA), was used to prepare the CS/CA blend solutions. The CS/CA blend hollow fiber membranes were fabricated by wet spinning the CS/CA blend solutions into an alkali solution that has been found to be effective in solidifying the hollow fiber membranes. Three types of hollow fiber membranes were prepared from the blend solutions with a compositions of CS/CA/FA=0/27/73, 0.5/26.5/73 or 1/26/73 by weight, denoted as Pure CA hollow fiber membranes, 0.5-26.5-73 and 1-26-73 CS/CA blend hollow fiber membranes, respectively. The miscibility and possible interaction of the two polymers in the blend hollow fiber membranes were investigated through FTIR and XRD analyses. The morphologies, water permeate fluxes, contact angle, and mechanical strength of the blend hollow fiber membranes were examined. The adsorption performance of the blend hollow fiber

membranes was investigated through the adsorption of copper (II) ions and bovine serum albumin (BSA) in a series of batch experiments.

3.2   Experimental

3.2.1   Materials

CS, practical grade from crab shells, was supplied by Aldrich and used as received. The viscosity-averaged molecular weight of CS, as determined from the Mark–Houwink equation [123] in the study, was 319,000 g/mol. The degree of N-deacetylation (DDA) of CS was measured with the titration method [124] and was found to be 79%. CA, with MW of 37,000 g/mole and acetyl content of 40%, was purchased from Fluka. 98-100% formic acid (FA) from Fluka was used as the co-solvent for both the CS and CA polymers. Copper sulphate ($CuSO_4 \cdot 5H_2O$) and bovine serum albumin (BSA) from Sigma were used in the adsorption experiments.

3.2.2   Fabrication of CS/CA blend hollow fiber membranes

CA and CS were first dried at 65°C to remove extra moisture. The blend solution was prepared by mechanically stirring CA and CS together in FA at 200 rounds per minute (rpm) overnight at room temperature. The resultant solutions were clear and homogeneous. The blend solution was then degassed by leaving it in the dope tank overnight without stirring to free the air bubbles entrapped in the dope solution, and it was finally filtered through a 15 μm stainless steel filter to remove any insoluble particles under the force of high pressure of N_2 gas. Then the blend hollow fiber membranes were spun from the blend solutions using the spinning setup shown in Fig. 3.2.
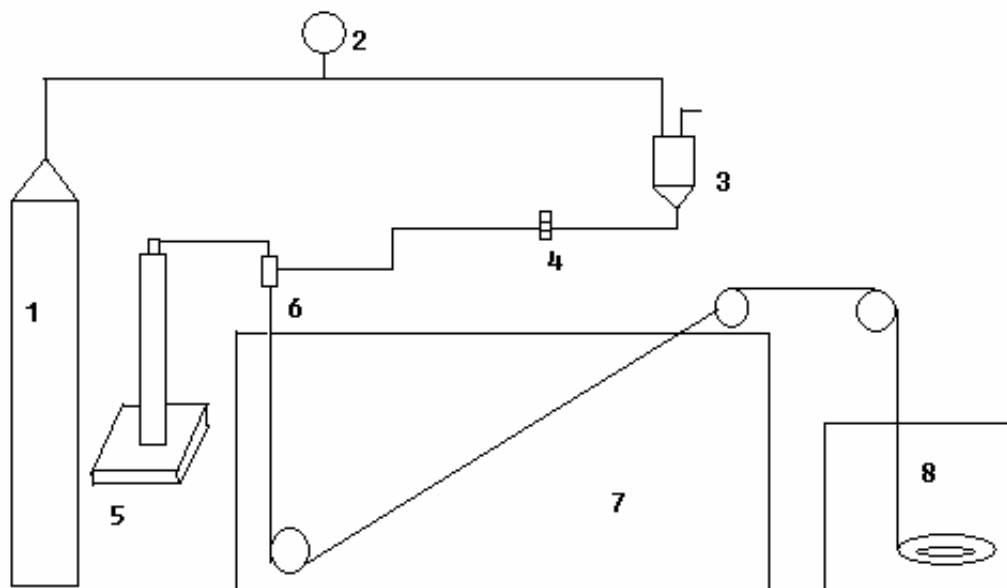
(1) Nitrogen gas cylinder (2) Digital pressure meter (3) Dope tank (4) Filter (5) High pressure syringe pump (6) Spinneret (7) Coagulation bath (8) Rinsing tank

Figure 3.2 Schematic diagram of the experimental setup for hollow fiber membrane fabrication

The hollow fiber membranes were spun through a wet spinning process. The viscous and clear spinning dope solution was forced through a stainless steel spinneret comprising an annular ring (with O.D. and I.D. of 1.3 mm and 0.5 mm respectively) under the force of high pressure of N_2 gas (2.0-6.9 bar), and was protruded into the coagulation bath (without air gap). The dope extrusions rate (0.4-0.5g/min) was controlled by the pressure of the nitrogen gas. A core liquid coagulant (1/3 of the dope flow rate, i.e., 0.13-0.17ml/min) was delivered simultaneously through the inner core by a high pressure syringe pump (ISCO 100DX). NaOH solution (3 wt%) was used as both the external (in the coagulation tank) and internal fiber coagulants (the bore flow). The hollow fiber membranes were formed and solidified in the coagulation bath and collected by a drum. The collection rate of the hollow fiber membrane was carefully controlled so that there was no excess drag force

imposed on the fibers. Upon collection, the fibers were rinsed with tap water to leach out excess solvents and the external/internal coagulation solution. The clean hollow fiber membranes was then stored in DI water for further use.

To get dry membranes for analysis, water in the wet hollow fiber membranes was exchanged with solvents of low surface tensions because the high surface tension of water can cause pore collapse of the membranes. The solvent exchange was conducted with 1-propanol followed with 1-heptane. The fibers were firstly rinsed with 1-propanol (100%) for 2 hours to extract the water and then they were rinsed with 1-heptane (100%) for another 2 hours to extract the 1-propanol [125]. Finally the fibers were dried at room temperature (22-23ºC), without causing any damages to the membrane structures [126-127].

3.2.3   Characterization of hollow fiber membranes

Fourier transform infrared spectroscopy (FTIR) studies were conducted with a Shimadzu H8400 spectrometer in the wavenumber range of 500-4000 cm^{-1}. The hollow fiber membranes were dried and ground into fine powder. Approximately, 1 mg sample powder was homogenously mixed with 99 mg of KBr and the mixture was then pressed into a tablet. FTIR analyses were done on pure CA hollow fiber membranes, pure CS films, and CA/CS blend hollow fiber membranes. Pure CS film was prepared from a solution with 1.5 g CS dissolved in 100mL 98-100% formic acid and coagulated in 3 wt% NaOH solution.

X-ray diffraction (XRD) measurements were carried out on a diffractometer (Lab XRD-6000) with the Cu $K\alpha$ ray source (λ =1.54 Å). Scanning diffraction angle range was

set at 2–40° and scanning rate was 2° (2ɵ) per minute. The spectra were recorded at 40 kV, 25 mA. The samples, including CS, CA and CS/CA blends, were prepared by grinding them into powder for measurement.

The structure and morphology of the hollow fiber membranes were investigated through FESEM (JEOL JSM -6700F FESEM) and SEM (JEOL JSM -5600 SEM). The dried hollow fiber membranes were snapped in liquid nitrogen to give a generally clean break of the cross-section. As the polymers were non-conductive, the hollow fiber membranes were coated with platinum powder on the surface for 40 seconds at 40 mbar vacuum. For FESEM/SEM analyses, the electrical voltage was controlled at below 15 kV to prevent possible collapse of the membrane surface caused by electron beam scanning. The dimensions (O.D. and I.D.) of the hollow fiber membranes and the average pore size of the membrane surfaces were measured by the software supplied by the manufacturers of the SEM/FESEM.

Pure water fluxes (PWF) measurements of the hollow fiber membranes were carried out in a dead end filtration set-up at room temperature. Ten dry fibers (length: 20 cm) were assembled into the test module with glue. Pressure drop across the hollow fiber membranes was controlled by compressed N_2 gas and maintained at 5.8 bars in all runs. Pure water was loaded into the lumen side and permeated out from the outer side. After the flux through the membrane was stabilized, the permeate was collected and measured at desired time intervals. Each type of hollow fiber membranes was tested three times and the average flux was calculated. The PWF was determined from the following expression (Eq. (3.1)):

$$J_w = \frac{Q}{A(\Delta T)(\Delta p)} \qquad\qquad (3.1)$$

where J_w is the water flux (L/m^2·hr·bar), Q the quantity of water permeated (L) during ΔT, ΔT the sampling time (hr), A the membrane outer surface area (m^2), and Δp the pressure drop across the hollow fiber membranes (bar).

The water contact angle of the membrane surfaces was measured in an automated contact angle goniometer (Model 100-0-230, Rame-Hart, Inc.) equipped with digital imaging software. The sessile drop method was used. After the dried fiber was mounted in the telescope, 0.5 μl DI water was dropped on the surface to measure the contact angle. The relative humidity and temperature in the test were 60% and 22-23°C, respectively. For each contact angle value reported, 5 readings from different parts of the fiber surface were measured and averaged.

The mechanical property of the wet hollow fiber membrane was evaluated through the measurement of tensile stress, elongation ratio, and Young's modulus at break. Tests were conducted with Instron 5542 Material Testing Machine at a temperature of 22-23°C and a relative humidity of 60%. The initial gauge length was set to be 25 mm and the draw speed was set at 10 mm/min. In each measurement, sample of each fiber was cut into 5 cm length, and attached onto the 2 clamps of the machine. Values of breaking force and elongation at break were then recorded. For reliability, five readings were taken for each sample, and the average value was reported in this work.

The internal surface areas of the CS/CA blend hollow fiber membranes were determined by N$_2$-sorption employing the Brunauer-Emmet-Teller (BET) method and

using a Quanta Chrome Nova 3000 series instrument. The actual contents of CS in the blend hollow fiber membranes were analyzed with the ninhydrin method [128].

Adsorption experiments with Pure CA or CS/CA blend hollow fiber membranes were conducted for the adsorption of copper ions and bovine serum albumin (BSA) at 22-23ºC in a batch mode. DI water was used to prepare all the solutions. All the adsorption experiments were conducted on an orbital shaker operated at 150 rpm. The dry hollow fiber membranes were cut into about 0.5 cm length. For copper adsorption experiments, approximately 2 g of the hollow fiber membrane pieces were added into 50 mL of the copper solution with initial concentration of 50 mg/L. The initial pH of the copper solution was adjusted to 5 or 6, respectively by adding a small amount of 0.1M HCl or NaOH solution. The choice of pH 5-6 was to maintain copper in its ionic form [129]. At pH above 6, copper precipitates out from solution to form $Cu(OH)_2$. Adsorption at pH lower than 5 was not conducted as it is not a common condition for intended applications and the adsorption amount will decrease significantly at lower pH due to the fact that most NH_2 groups convert to $-NH_3^+$ which causes unfavorable interaction for metal cation adsorption.. For the isotherm study, the initial concentrations of copper solution varied from 10 to 300 mg/L and the initial solution pH was set at 6. The concentrations of copper ions in the samples were measured using an inductive coupled plasma spectrometer (ICP-OES, Perkin Elmer Optimer 3000DV).

For the BSA adsorption experiment, approximately 4.5 g of the fiber pieces were added into 50 mL BSA solution with an initial concentration of 0.5 g/L and an initial solution pH of 6.3. At pH 6.3, the adsorption capacity of BSA by chitosan is high [130] and the deformation and agglomeration of BSA molecules is less. The amount of BSA

adsorbed on the hollow fiber membranes was determined from the absorbance difference of the samples before and after adsorption with a UV-Vis spectrometer at the wavelength of 278 nm. For isotherm study, the concentrations of BSA were varied from 0.2 to 1.3 g/L.

3.3   Results and discussion

3.3.1   Hollow fiber membranes

Two CS/CA blend hollow fiber membranes and Pure CA hollow fiber membranes were prepared and the detailed information is summarized in Table 3.1. The dope composition plays an important role in the mechanical properties of the hollow fiber membranes. Being the supporting matrix material, CA content in the dope determines the strength of the blend hollow fiber membranes. In industrial fabrication process, the spinning solution with CA content of 23-29% by weight is normally used to fabricate CA hollow fiber membranes. It is well known that an increase in the polymer content in the

Table 3.1 Dope compositions and other information for the Pure CA hollow fibers and CS/CA blend hollow fibers 0.5-26.5-OH and 1-26-OH

hollow fiber ID	CS/CA/FA (g/g/g)	DER (g/min)	BFFR (ml/min)	O.D. (μm)	I.D. (μm)	Wall thickness (μm)
Pure CA	0.0/27.0/73	0.488	0.167	611	350	131
0.5-26.5-OH[*]	0.5/26.5/73	0.402	0.133	671	429	121
1-26-OH[*]	1.0/26.0/73	0.411	0.133	644	362	141

*OH means that the CS/CA blend hollow fiber membranes was externally and internally coagulated with 3 wt% NaOH solutions. DER: Dope extrusion rate, BFFR: Bore fluid flow rate, O.D.: outer diameter, I.D.: inner diameter

dope leads to an increase in the mechanical strength, but too concentrated dope can make the spinning of hollow fiber membranes impossible due to the high viscosity. For the present study, we set the total weight percentage of the polymers in the dope at 27%. The weight ratio between the polymers of CS and CA were at 0:27, 0.5:26.5, and 1:26, respectively (The attempt to spin hollow fiber membranes at a high CS content was difficult due to the high viscosity of CS and the non-flow behavior of the resulting dope). The prepared three types of hollow fiber membranes were given the name of Pure CA, 0.5-26.5-OH, and 1-26-OH respectively, where OH indicates that the hollow fiber membranes were externally and internally coagulated with 3wt% NaOH solutions. As can be found in Table 1, the resultant hollow fiber membranes had an outer diameter between 0.6-0.7mm.

3.3.2 FTIR analysis of the hollow fiber membranes

The nature of mixing between the two polymers is of great interest to the study. FTIR has often been used as a useful tool in determining specific functional groups or chemical bonds that exists in a material. The presence of a peak at a specific wavenumber would indicate the presence of a specific chemical bond. For CS and CA blending, if specific interactions took place between the two polymers, the most obvious and significant difference would be the appearance of new peaks or shift of existing peaks. Fig. 3.3 shows the FTIR spectra of CS, Pure CA hollow fiber membranes and CS/CA blend hollow fiber membranes. The FTIR spectrum of CS shows peaks assigned to the saccharide structure at 899 and 1153 cm^{-1}, the amine group peak at around 1601 cm^{-1}, N-acetylated chitin at 1655 cm^{-1} and the OH and NH peaks centered at 3418 cm^{-1}. The FTIR spectrum of CA shows peaks for the C=O functional groups at 1755 cm^{-1}, the OH functional groups at

3528 cm^{-1}, the CH$_3$ groups at 1384 and 1249 cm^{-1}, and the ether C-O-C functional groups at 1060 cm^{-1}. The FTIR spectra for CS/CA blend hollow fiber membranes (0.5-26.5-OH and 1-26-OH) are very similar to that of CA, probably due to the small percentage of CS in the blend hollow fiber membranes. A most obvious difference in the spectra for CA and CS/CA blend hollow fiber membranes is observed to be the shift of the broad peak for OH and NH groups from 3528 to 3483 and to 3479 cm^{-1} with the increase of CS content in the hollow fiber membranes, indicating that an increased amount of amine groups or nitrogen atoms were incorporated into the CA matrix and interacted with the OH groups in the hollow fiber membranes.
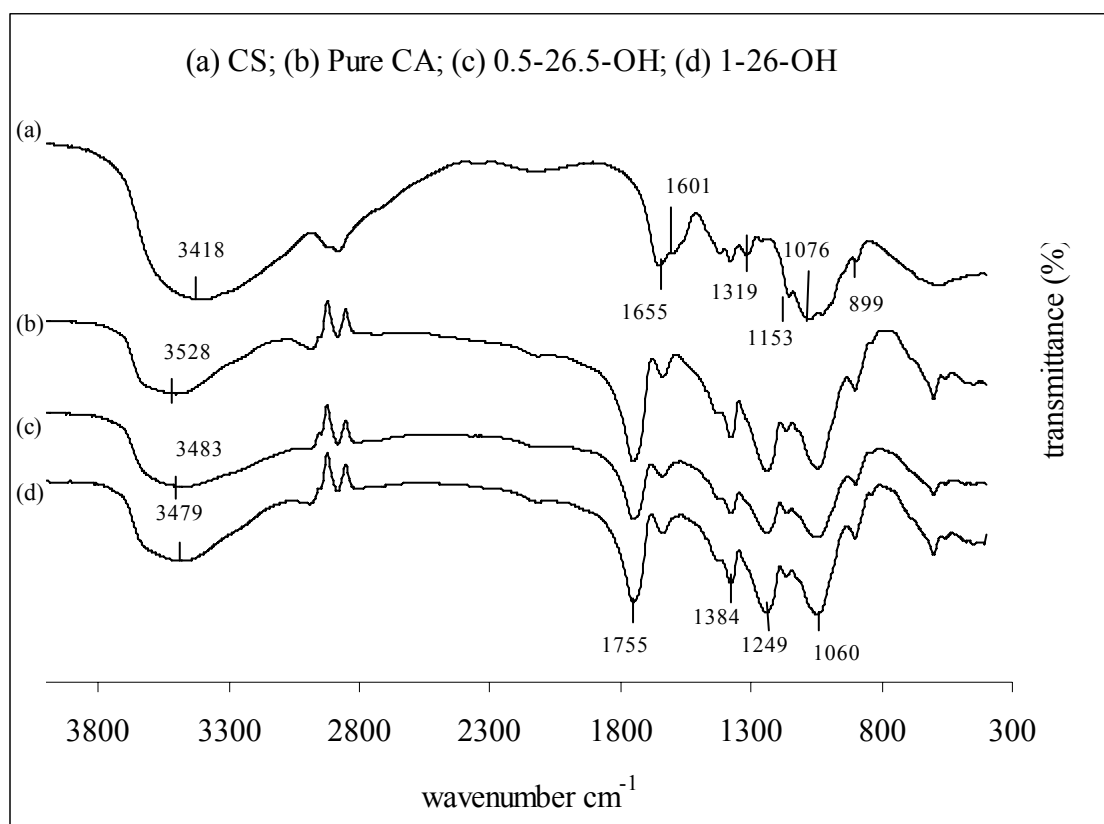
Figure 3.3 FTIR spectra of CS and Pure CA hollow fiber membranes and CS/CA blend hollow fiber membranes 0.5-26.5-OH and 1-26-OH

3.3.3   XRD analysis of the hollow fiber membranes

The XRD spectra of CS, Pure CA hollow fiber membranes and the two blend hollow fiber membranes are shown in Fig. 3.4. As observed, CS showed two peaks at the two diffraction angles of $2\theta=10.26$ and $19.86°$, in agreement with the finding reported in the literature [131], and Pure CA fibers displayed a single crystalline peak at $2\theta=13.06°$. The diffractograms of the two blend hollow fiber membranes (0.5-26.5-OH and 1-26-OH) however showed nearly no obvious difference from that of Pure CA. Since no other new peaks and the peaks of CS were present in CS/CA blends, the results indicate that CA structure was not significantly affected by the addition of a small amount of CS and CS
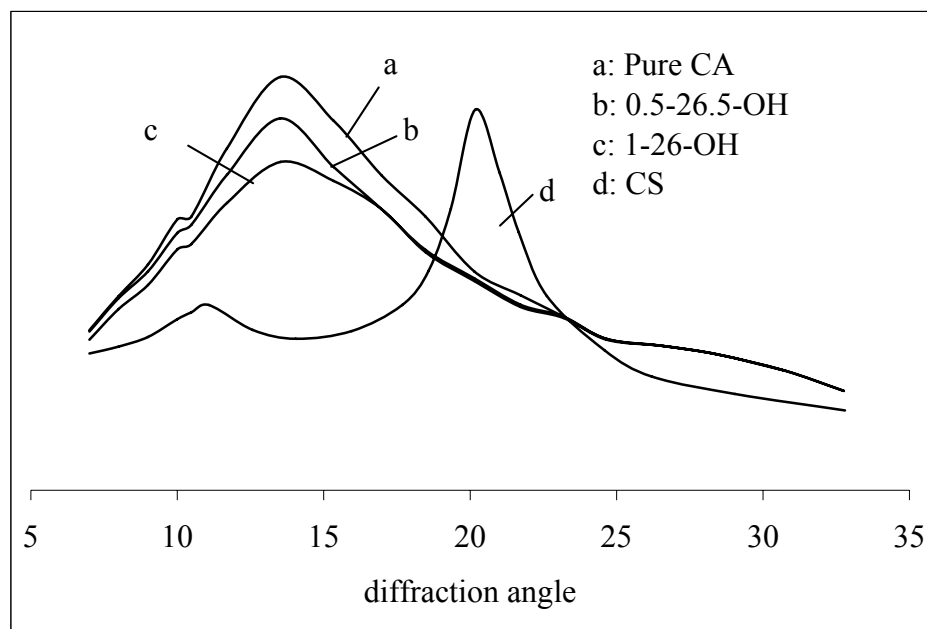
Figure 3.4 XRD diffractograms of CS and Pure CA hollow fiber membranes and CS/CA blend hollow fiber membranes 0.5-26.5-OH and 1-26-OH

did not form its own crystalline region in the blend. The XRD results therefore confirm the good compatibility and miscibility between CS and CA in the blends studied, because,

if CS and CA had low compatibility in the blend hollow fiber membranes, each component would show its own crystal region in the blend hollow fiber membranes and the X-ray diffraction patterns should show a simply mixed pattern of CS and CA.

The crystallinity and peak diffraction angles of CS, Pure CA and the two blends are listed in Table 3.2. It can be found that the crystallinity was slightly suppressed when CS content in the blends was increased. The diffraction angles also shifted slightly to a lower value for CA in the two blends with the increase of CS content in the blends. The XRD results thus provide supporting evidence to the FTIR result that some specific chemical interaction between CA and CS existed in the blend.

Table 3.2 Crystallinity and peak diffraction angles of CS and Pure CA hollow fiber membrane and CS/CA blend hollow fiber membranes 0.5-26.5-OH and 1-26-OH

Smaples	CS	Pure CA	0.5-26.5-OH	1-26-OH
Crystallinity (%)	7.28	6.65	6.42	6.34
Peak diffraction angle (°)	10.26/19.86	13.24	13.06	13.00

3.3.4   Surface morphology

The Pure CA hollow fiber membranes were transparent and colorless and the CS/CA blend hollow fiber membranes were translucent and had a milk-white color. Both Pure CA and CS/CA blend hollow fiber membranes displayed a sponge-like and macrovoids-free cross-section, which are desirable for adsorptive membranes. Fig. 3.5 shows the typical cross-section morphologies of the Pure CA and CS/CA blend hollow fiber membranes

1-26-OH. The cross-sections are full of highly interconnected micropores which would provide high internal surface areas for the membranes.

Pure CA

(a)

(b)

1-26-OH

(c)

(d)
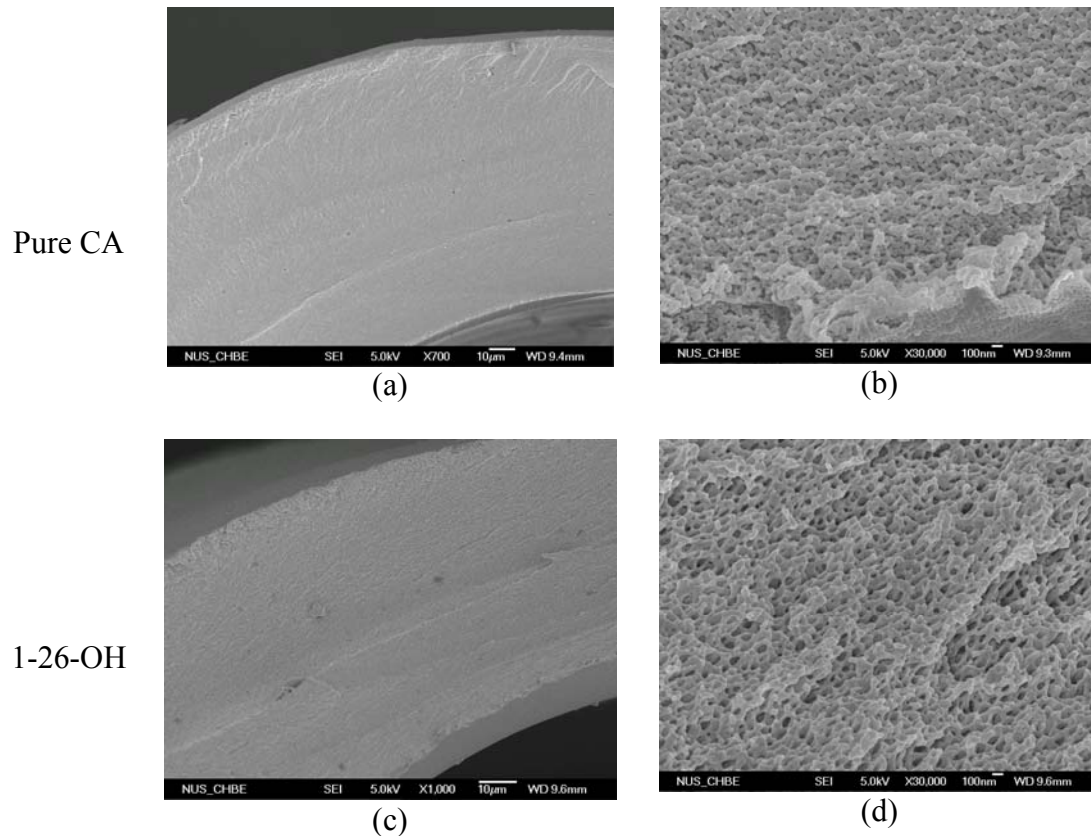
Figure 3.5 Cross-sectional morphologies of Pure CA hollow fiber membranes and CS/CA blend hollow fiber membranes 1-26-OH

Heterogeneous structure with top skin supported by finger-like macrovoid substrate is often observed in other hollow fiber membranes fabricated through the wet phase inversion method, due to the fast solvent and nonsolvent exchange rate. Macrovoids need to be avoided for adsorptive membranes because the macrovoids not only decrease the internal surface areas of membranes but also lead to non-uniform flow behavior of solutions in the membranes. Many studies have been devoted to the methods that can

depress macrovoids, or reduce macrovoids, to yield a sponge-like porous structure, including the use of high polymer concentrations [132], the addition of high viscosity component [133], and the induction of delayed demixing of dope [134]. The macrovoids-free structure of the hollow fiber membranes prepared in this study may be mainly attributed to the high polymer concentration and the high viscosity of the dopes.

Outer surface Inner surface

(a) (b)

(c) (d)
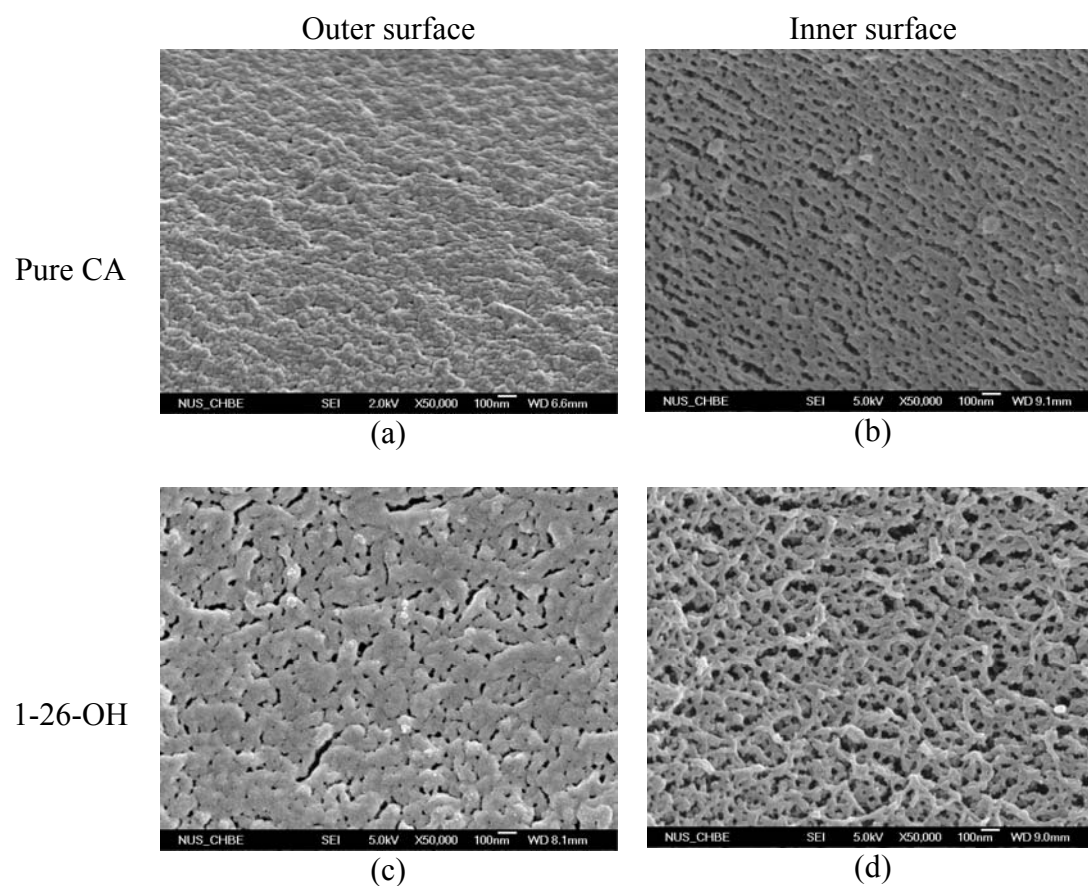
Pure CA

1-26-OH

Figure 3.6 Outer and inner surface morphologies of Pure CA hollow fiber membranes and CS/CA blend hollow fiber membranes 1-26-OH

The SEM images in Fig. 3.5b and Fig. 3.5d clearly show that the cross-sections of CS/CA blend hollow fiber membranes became much more porous and had larger pores

than that of the Pure CA hollow fiber membranes. The outer and inner surfaces of the Pure CA and CS/CA blend hollow fiber membranes 1-26-OH are shown in Fig. 3.6. It can be found that the blend hollow fiber membranes exhibited a porous outer surface while the Pure CA hollow fiber membranes showed a relatively denser outer surface. Analyses indicated that the outer surface pore size and porosity of the hollow fiber membranes increased in the order of Pure CA, followed by 0.5-26.5-OH (image not shown) and 1-26-OH, with average surface pore size of 50 nm for Pure CA and 72 nm and 80 nm for 0.5-26.5-OH and 1-26-OH blend hollow fiber membranes, respectively. The inner surfaces of Pure CA and CS/CA blend hollow fiber membranes showed even more significant difference in the pore size and porosity. In comparison with the outer surfaces, the inner surfaces of both CA and CS/CA blend hollow fiber membranes had much larger pore sizes. Unlike in the fabrication of flat membrane where only one coagulation process is involved, hollow fiber membrane fabrication involves two coagulation processes at the same time. One is through the continuous flow of bore fluid in the lumen of the fiber, while the other is through the outside contact with the coagulant as the hollow fiber membranes enter the coagulation bath. Although both the external and internal coagulants used in this study were 3 wt% NaOH solutions, the coagulation behavior in the lumen side was different from that at outside. The NaOH solution in the bore fluid, which was of very small quantity, can be quickly neutralized by the formic acid diffused from the polymer dope. Therefore, the coagulation rate of the fiber at the lumen side was slower than that at outside, leading to a delayed phase separation and therefore more porous inner surfaces. This result also indicate that a more dilute NaOH solution (<3 wt%) should be used as the external coagulant in order to have the outer surfaces to be as porous as the inner surfaces or in order to make the outer surface be more porous.

3.3.5 Pure water fluxes (PWF) and contact angles

Table 3.3 presents the water flux results and the contact angles of the different types of hollow fiber membranes. It can be found that the water fluxes of the CS/CA blend hollow fiber membranes were comparable to that of Pure CA hollow fiber membranes, even though the results in Fig. 3.5 and Fig. 3.6 show that the CS/CA blend hollow fiber membranes being much more porous than the Pure CA hollow fiber membranes. This phenomenon may be explained by the change in the hydrophilic nature of the hollow fiber membranes upon the addition of chitosan. As can be found in Table 3.3, CA is relatively more hydrophilic than CS which has a higher contact angle value than CA. The blending of CS with CA therefore resulted in an increase of the contact angle values of the blend hollow fiber membranes, as compared to that of CA. Thus, the blend hollow fiber membranes became more hydrophobic than the CA hollow fiber membranes, which can lower the water flux of the blend hollow fiber membranes.

Table 3.3 Pure water fluxes and water contact angles of CS and Pure CA hollow fiber membranes and CS/CA blend hollow fiber membranes 0.5-26.5-OH and 1-26-OH

Samples	PWF ($\times 10^{-2}$L/m^2·hr·bar)	Water contact angle (°)
CS	-	63.0±3.0
Pure CA	9.06±0.41	36.5±1.1
0.5-26.5-OH	9.22±0.36	40.0±1.7
1-26-OH	9.14±0.45	47.5±2.0

3.3.6   Mechanical property

The tensile stress, elongation ratio, and Young's modulus values at break for the three types of hollow fiber membranes are summarized in Table 3.4. Stress is defined as the force per unit area, normal to the direction of the applied force, and elongation as the extension per gauge length at break. It is found that the CS/CA blend hollow fiber membranes displayed high tensile stress (22.1-38.8 MPa) and Young's modulus values (0.09-0.1145 GPa) although these values tended to decrease with the increase of CS in the blend hollow fiber membranes. The elongation ratios at break were in the range of 24.36-33.9% and decreased with CS content in the blend hollow fiber membranes.

Table 3.4 Mechanical test results for Pure CA hollow fiber membranes and CS/CA blend hollow fiber membranes 0.5-26.5-OH and 1-26-OH

Hollow fiber membranes	Tensile stress (MPa)	Elongation ratio (%)	Young's Modulus (GPa)
Pure CA	38.80	33.90	0.1145
0.5-26.5-OH	26.16	27.97	0.0935
1-26-OH	22.10	24.36	0.0900

The tensile stress values of the Pure CA and CS/CA blend hollow fiber membranes appear to be slightly greater than that of many other hollow fiber membranes in literature and the values of elongation ratio and Young's modulus are generally comparable with that of other hollow fiber membranes, suggesting that the CS/CA blend hollow fiber membranes prepared in this work have high mechanical strength and can be used in the industrial level.

3.3.7   Adsorption performances

The three types of hollow fiber membranes, i.e., Pure CA, CS/CA blend hollow fiber membranes 0.5-26.5-OH and 1-26-OH, were used as adsorbents to adsorb copper ions and BSA from aqueous solutions. As given in Table 3.5, the specific surface areas were found to be 18.6 m^2/g for Pure CA hollow fiber membranes, 23.5 m^2/g and 28.6 m^2/g for CS/CA blend hollow fiber membranes 0.5-26.5-OH and 1-26-OH, respectively. The CS content on the CS/CA blend hollow fiber membranes were analyzed with the ninhydrin method and was found to be 1.7 wt% (17mg/g) and 3.5 wt% (35mg/g) for fibers 0.5-26.5-OH and 1-26-OH respectively. These values are very close to the weight ratios of CS: (CS+CA) in the spinning solutions (1.85% for 0.5-26.5-OH and 3.7% for 1-26-OH).

Table 3.5 Internal surface areas and CS contents on the Pure CA hollow fiber membranes and CS/CA blend hollow fiber membranes 0.5-26.5-OH and 1-26-OH

Hollow fiber membranes	Internal surface areas (m^2/g)	CS content (wt %) on membrane	CS/(CS+CA) in spinning solution (wt%)
Pure CA	18.6±0. 5	-	0
0.5-26.5-OH	23.5±0. 5	1.7±0. 2	1.85
1-26-OH	28.6±0. 3	3.5±0. 3	3.70

3.3.7.1   Adsorption of copper ions

The mechanism for chitosan to adsorb copper ion is reported in many literature to be a complexation between copper ion and NH_2 groups or sometimes involving –OH groups on CS polymer. In the complexation process, N atom on CS provides a pair of lone electrons to the empty 3d orbit of copper ion. Therefore, the adsorption should be primarily assigned as chemical adsorption. However, adsorption may also take place through Van

der Vall force interaction since it is commonly seen on solid surface. Therefore, physical adsorption through Van der Wall force interaction may also be involved in the adsorption. Ion exchange between copper ion and chitosan does not take place because both Cu^{2+} and NH_2 are positively charged at pH<6.3-6.6. Therefore, the overall interaction between copper ion and CS/CA membrane surface include at least two mechanisms: (1) formation of complex and (2) Van der Vall force induced physical adsorption.

The adsorption was only conducted at pH 5 and 6. This is because chitosan performs better at neutral pH than at low pH due to the fact that $-NH_2$ converts to $-NH_3^+$ at low pH and lose complex formation capability with copper ion. The adsorption amounts of copper ions on the three types of hollow fiber membranes at pH 5 and 6 are presented in Table 3.6. The uptakes of copper ions by Pure CA hollow fiber membranes were almost negligible. The CS/CA blend hollow fiber membranes showed greatly enhanced adsorption of copper ions even though the amount of CS in the blend hollow fiber membranes was very small, indicating that CS is indeed effective in chelating copper ions from solutions and thus improving the adsorption performance of CA hollow fiber membranes. The solution pH also influenced the adsorption performance and all the three types of hollow fiber membranes showed an increase in the adsorption amounts for pH change from 5 to 6. This may be an indication of the effect of electrostatic repulsion force at low pH on adsorption since at a lower pH the fibers were also electrically positively charged as like copper ion.

Table 3.6 Experimental adsorption amounts of copper ions on Pure CA hollow fiber membranes and CS/CA blend hollow fiber membranes 0.5-26.5-OH and 1-26-OH

Hollow fiber membranes	Cu^{2+} removal efficiency by blend hollow fiber membranes				Cu^{2+} removal efficiency contributed by CS	
	pH=5		pH=6		pH=5	pH=6
	Q_{ads} (mg/g)	Remove percent (%)	Q_{ads} (mg/g)	Remove percent (%)	Q_{ads} (mg/g)	Q_{ads} (mg/g)
Pure CA	0.00	0	0.04	3		
0.5-26.5-OH	0.38	22	0.55	44	0.38	0.51
1-26-OH	0.74	59	1.09	87	0.74	1.05

Adsorption isotherm of copper ion on CS/CA blend hollow fiber membrane was also studied. Only the 1-26-OH membrane was investigated as it was the desired type with higher adsorption amount between the two types of blend membranes. Isotherm study was conducted at pH 6 as an illustration.

The Langmuir isotherm model and Freundlich isotherm model were used to fit the experimental results. The Langmuir isotherm model assumes that the adsorbed layer is one molecule in thickness and that all adsorption sites have equal energies and enthalpies of adsorption and that no interactions exists between the adsorbed molecules. The Freundlich model is based on an assumption of adsorption on heterogeneous surfaces and also possibly in multi-layer adsorption pattern. The Langmuir and Freundlich isotherm models are usually given as in Eq. (3.2) and Eq. (3.3) respectively and their linearized forms of these two models can be given in Eq. (3.4) and Eq. (3.5) respectively.

$$q_e = \frac{bC_e q_m}{bC_e + 1} \qquad\qquad (3.2)$$

$$q_e = K_f C_e^{\frac{1}{n}}$$
(3.3)

$$\frac{1}{q_e} = \frac{1}{q_m} + \frac{1}{bq_m C_e}$$
(3.4)

$$\log q_e = \frac{1}{n} \log C_e + \log K_f$$
(3.5)

where q_e is the equilibrium adsorption uptake (mg/g), q_m the maximum monolayer adsorption amount (mg/g), b the Langmuir adsorption equilibrium constant (L/mg), C_e the equilibrium concentration of adsorbate in solution (mg/L), $1/n$ Freundlich intensity parameter (dimensionless), and K_f Henry's law constant, $(mg/g)/(mg/L)^n$.

The plots of the experimental $1/q_e$ against $1/C_e$ and $\log q_e$ against $\log C_e$ for the adsorption data of copper ions on the CS/CA blend hollow fiber membranes 1-26-OH are shown in Fig. 3.7a and Fig. 3.7b respectively. It is found that the adsorption can be better fitted by the Langmuir model, giving the R^2 value of 0.994. The maximum copper ion adsorption capacity (q_m) and the adsorption equilibrium constant (b) were found to be 4.146 mg/g (equivalent to 118 mg/gCS) and 5.85×10^{-2} L/mg respectively. The fitted results from the Langmuir model (dotted line in Fig. 3.7c) were in good agreement with the experimental results. In contrast, the Freundlich isotherm model could not describe the adsorptions as well as that of the Langmuir model, with the R^2 value being only 0.938, and the fitted results are also shown by the solid line in Fig. 3.7c.

Figure 3.7 Isotherm adsorption data of copper ions on CS/CA blend hollow fiber
membranes 1-26-OH and data fitting with the Langmuir and Freundlich isotherm models

The regeneration and reuse of the blend hollow fiber membranes 1-26-OH were also evaluated. The hollow fiber membranes were pre-adsorbed with copper ions under the conditions of an initial pH 6 and at initial concentration of 50 mg/L and then the adsorbed copper ions were desorbed in 50 mL of 50 mM HCl solution. Upon desorption completed, residual HCl solution was washed off by DI water. Some residual HCl attached on $-NH_3^+$ was neutralized by addition of very small amount of dilute NaOH. The adsorption-desorption process was repeated for three cycle. It can be found that except a reduction of 24.7% in the first cycle, the hollow fiber membranes showed almost no further reduction in the adsorption performance in the subsequent cycles, indicating that the blend hollow fiber membranes can be regenerated and reused as an effective adsorbent.

Table 3.7 Reuse of CS/CA blend hollow fiber membranes 1-26-OH for copper ions adsorption

Reuse cycle	1	2	3
Adsorption amount (mg/g fiber)	1.09	0.82	0.81

3.3.7.2   Adsorption of BSA

The mechanism for BSA adsorption on CS/CA membrane surface is dependent on solution pH. However, it is primarily an electrostatic interaction. BSA has PI value at about 4.7. Above this pH it is negatively charged and below this pH it is positively charged. As for CS/CA membrane, the CS polymer has PI value at pH 6.3-6.6. At pH lower than 6.3-6.6 it is positively charged and at pH higher than 6.3-6.6 it is negatively charged. Therefore, in solution pH range of 4.7-6.3 or 4.7-6.6, electrostatic attraction takes

place between negatively charged BSA and positively charged $-NH_3^+$ groups on membrane surface. Beyond this pH range, hydrophobic interaction, formation of hydrogen bond and other physical adsorptions such as Van der Vall force interaction may contribute to the adsorption. Hydrophobic interaction may take place between hydrophobic segments on BSA molecules and CS polymer chains. Formation of hydrogen bond is possible because both BSA and membrane surface contain O, N, H atoms.

The adsorption of BSA on Pure CA and CA/CS blend hollow fiber membranes were investigated at pH 6.3. The reason for us to conduct BSA adsorption at pH 6.3 is that protein molecules prefer staying in neutral solutions to acidic or alkali solutions because in acidic or alkali solutions severe denaturization of proteins could occur, which will result in the loss of activity of proteins. Therefore, this study examined a more preferred condition. The equilibrium adsorption uptakes of BSA on the three types of hollow fiber membranes obtained at pH 6.3 are given in Table 3.8. Similar to the results in copper ion adsorption, the blend hollow fiber membranes showed significantly enhanced adsorption performance for BSA than the Pure CA hollow fiber membranes. The equilibrium adsorption amount, for example, for hollow fiber membranes 1-26-OH is 3.411 mg/g, in comparison with 0.292 mg/g for Pure CA hollow fiber membranes.

Table 3.8 Experimental adsorption amounts of BSA on Pure CA hollow fiber membranes and CS/CA blend hollow fiber membranes 0.5-26.5-OH and 1-26-OH

Hollow fiber membranes	BSA adsorption amounts (mg/g)	BSA removal percent (%)	BSA adsorption amounts contributed by addition of CS (mg/g)
Pure CA	0.292	5	0
0.5-26.5-OH	1.117	20	0.825
1-26-OH	3.411	61	3.119

The fitting of Langmuir and Freundlich isotherm models to the adsorption of BSA on the blend hollow fiber membranes 1-26-OH is illustrated in Fig. 3.8. Here we only studied the adsorption isotherm on the 1-26-OH as it was the desired type with the highest BSA binding amount among the three types of membranes at pH 6.3. Both the Langmuir and Freundlich isotherm models can be fitted to the experimental results reasonably well, giving the R^2 value of 0.988 (see Fig. 8a) and 0.9455 (see Fig. 8b) for the Langmuir and Freundlich models, respectively. The fitted results from both the isotherm models are in good agreement with the experimental results, as shown in Fig. 8c. The values of q_m and b for the Langmuir model were calculated to be 13.85 mg/g (equivalent to 396 mg/gCS) and 1.69×10^{-3} L/mg, respectively. The values of K_f and $1/n$ for the Freundlich model were calculated to be 8.58 $(mg/g)/(mg/mL)^{1.69}$ and 0.5905, respectively. The value of $1/n$ was less than 1 (or $n>1$), indicating that the adsorption of BSA would eventually reach saturation.
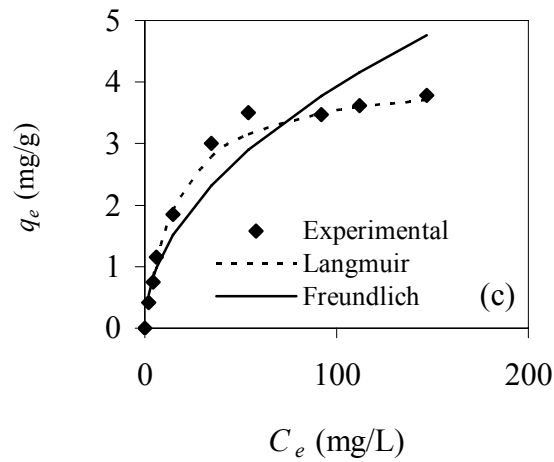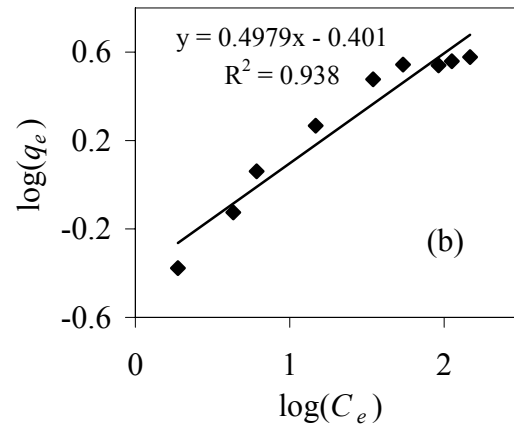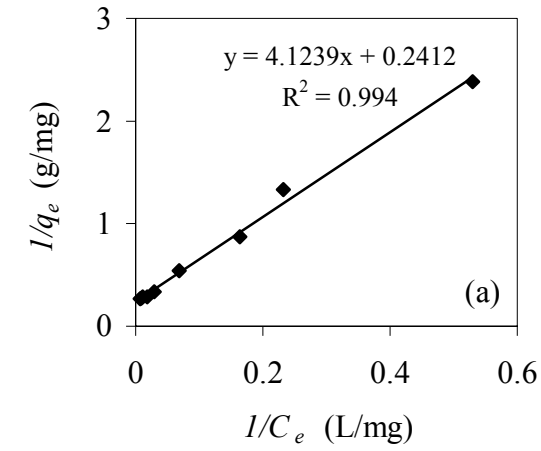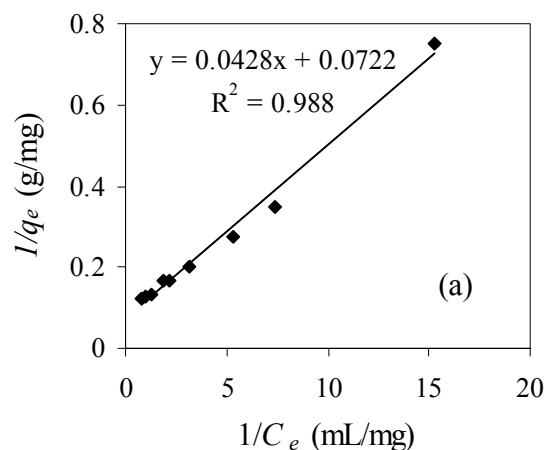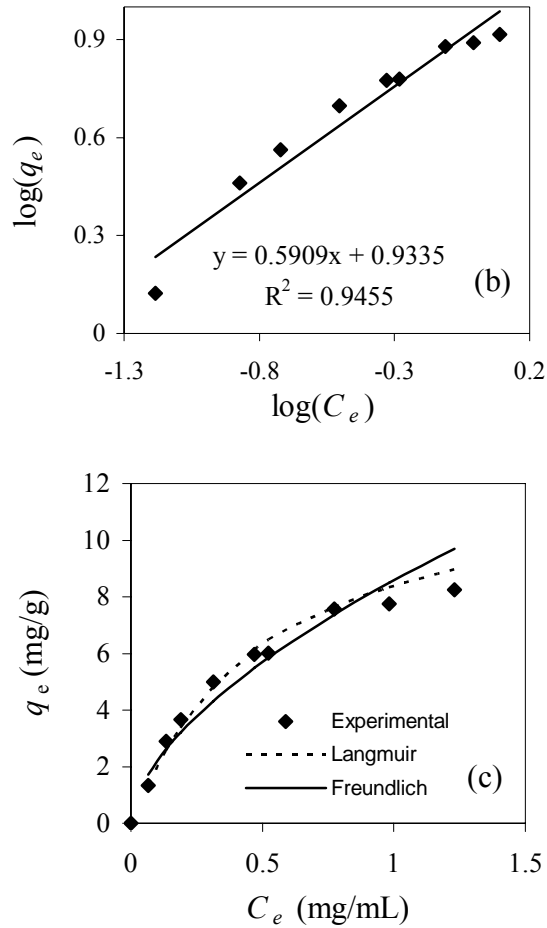
Figure 3.8 Isotherm adsorption data of BSA on CS/CA blend hollow fiber membranes 1-26-OH and data fitting with the Langmuir and Freundlich isotherm models

Again, the regeneration and reuse of the hollow fiber membranes for BSA adsorption were examined. BSA adsorbed on the fibers was desorbed in 15 ml of 50 mM KSCN solution. Table 3.9 shows the adsorption results from three cycles. Similar to that in copper adsorption, there was a reduction (8.5%) in the adsorption amount after the first cycle, but the adsorption performance stabilized in subsequent cycles.

Table 3.9 Reuse of CS/CA blend hollow fiber membranes 1-26-OH for BSA adsorption

Reuse cycle	1	2	3
Adsorption amount (mg/g)	3.411	3.120	3.106

3.3.7.3　Comments on adsorption performance

Although all the adsorption experiments in this part of the work were conducted in batch mode, they are able to indicate the adsorption performance of the blend membrane. The blend membrane1-26-OH that has greater amount of CS showed maximum binding capacity of about 4mg/g for Cu2+ at pH 6 and 14mg/g for BSA at pH 6.3.

Although it is desirable to investigate dynamic mode of adsorption including saturation capacity and binding kinetics, we did not intend to do this because the purpose of this research was to find method to prepare chitosan blend hollow fiber membranes and to examine its potential in heavy metal ion retention and BSA binding.

3.4 Conclusions

In this study, novel CS/CA blend hollow fiber membranes were successfully fabricated via the wet spinning method, with protic solvents as the co-solvents and alkali solutions as the external and internal coagulants. CA was chosen to be the polymer matrix providing high mechanical strength and CS to be the reactive polymer contributing to the functionality of adsorptive property of the blend hollow fiber membranes. FTIR and XRD

analyses revealed that the two polymers were well miscible in the blends in the ratio range studied (CS/CA=0.5/26.5 and 1/26) and chemical interactions existed between them. The prepared CS/CA blend hollow fiber membranes had high mechanical strength, comparable to that of commercial hollow fiber membranes. The hydrophilicity and hydrophobicity of the blend membranes can be adjusted through the change of the CS/CA ratios. The blend hollow fiber membranes showed microporous and macrovoids-free structures, with highly interconnected pores that are desirable for affinity based separations. The outer surface pore sizes and specific surface areas for the two types of CS/CA blend hollow fiber membranes were in the range of 72-80nm and 23.5-28.6m^2/g respectively. The blending of CS into CA, even though at a small CS amount, significantly improved the adsorption performance of the blend hollow fiber membranes for copper ions (4.146mg/g for fibers 1-26-OH) and BSA (13.85mg/g for fibers 1-26-OH) from aqueous solutions.

Chapter 4 Effect of polymer concentrations and coagulant compositions on the structures and morphologies of the CS/CA blend hollow fiber membranes

Summary

Although the membrane prepared in last chapter was mechanically strong, CS content in the spinning solution was quite low (0.5-1.0wt%), resulting in low CS density on the blend membranes (<3.5%wt). To make more CS that provides binding sites be blended into the membrane, blend membranes were spun from spinning solutions with higher concentration of CS (2-4%wt.) and lower concentration of CA (12-18%wt). It was found that with changing polymer concentration the membrane structure changed significantly. Besides increasing CS polymer concentration, it was also found that using different coagulant also could improve the CS content on the blend membranes. However, it was also found that different coagulant has significantly different effect on membrane structure. Therefore, in this part of the work, we studied the effect of spinning parameters on the membrane morphologies and structures. The CS content in membranes prepared under different conditions will be presented in next chapter. By varying spinning parameters mentioned above, highly porous CS/CA blend hollow fiber membranes were prepared with outer surface pore sizes and bulk porosities in the range of 0.54 to 0.049 μm and 80.6 to 70.4%, respectively. All the membranes prepared with water as coagulant showed sponge-like, macrovoids-free, and relatively uniform porous structures. When NaOH solutions (2 to 3 wt%) were used as the internal coagulant, macrovoids formed in the membranes that are spun from solution with low polymer concentration. With increasing

CS concentration from 2%wt to 3%wt in spinning solution, the macrovoids were effectively eliminated.

4.1 Introduction

In the previous chapter (Chapter 3), CS/CA blend hollow fiber membranes were successfully prepared by wet spinning the CS/CA blend solution, with 98-100% formic acid as the co-solvent, into NaOH solutions. The previous study also showed that the blend hollow fiber membranes have high mechanical strength, tunable hydrophilicity, sponge-like structures, and good binding or adsorption capabilities toward heavy metal ions or albumins even at the presence of a small amount of CS.

However, the major problem associated with the blend membrane prepared in Chapter 3 is the low CS content (<3.5wt%), due to the fact that CS concentration in spinning solution was quite low. To improve this, we tried to increase CS concentration in spinning solution from 0.5-1wt% to 2-3wt% while reduce CA concentration from 26-26.5wt% to 12-18wt%. Moreover, we also tried to use different coagulants to improve CS content in the blend membranes. However, we found the membrane structure changed significantly by changing these spinning parameters. Therefore, a further study on effect of spinning parameters on the structures and morphologies of the CS/CA blend hollow fiber membranes is of research and practical interest since the membrane structures can have significant impact on the separation performances. For example, for binding of large biomolecules, the membranes should have large pore sizes to allow adequately free passage of the solutes into the membranes, but at the same time, the pore size should be as small as possible to maximize the membrane surface area and adsorption capacity. Moreover, macrovoids-free membranes are desirable for affinity separations because they can provide large specific surface areas for adsorption [135] and uniform flow across the

membranes for process efficiency. Study on the structures and morphologies of the CS/CA blend hollow fiber membranes is also of interest in expanding the application of the novel adsorptive membranes with filtration function as that in UF, NF, RO, dialysis processes and so on.

In this part of the work, the investigated factors included CA and CS concentrations in the spinning solutions and the compositions of the external and internal coagulants. To add more CS in the spinning solutions, CS with a low molecular weight of 75,000 g/mol (as compared to 319,000g/mol in previous work) was used and CA concentration was reduced from 26-26.5 wt% in previous study to 12-18 wt% in the present study.

4.2   Experimental

4.2.1   Materials

CS was purchased from Aldrich (labeled as low molecular weight) and used as received. The DDA and the MW of CS were determined to be 73.5% and 75,000 g/mol respectively. The reason in choosing CS with low molecule weight was to allow that a greater amount of chitosan could be added into the CS/CA blend dope solution and the CS and CA concentration in the blend dope solution could be changed in a greater range. CA and formic acid (FA) were the same as those used in previous study.

4.2.2   Fabrication of CS/CA blend hollow fiber membranes

The blend hollow fiber membranes were fabricated through the wet spinning process. However, in the present study, the hollow fiber membranes, upon collection, were rinsed with 10 wt% sodium acetate (NaAc) solution, instead of water as used in previous study. This was to prevent and minimize the dissolution of CS in the rinsing solution because the

prepared blend hollow fiber membranes in this study were highly porous on the outer surface. Other procedures in the membrane preparation were the same as those described in Chapter 3.

Table 4.1 Parameters investigated for spinning CS/CA blend hollow fiber membranes

	Hollow fiber membrane identity	CS/CA/FA (g/g/g) in the dope	External coagulant	Internal coagulant
Effect of CA concentrations	2-12-w 2-14-w 2-16-w 2-18-w	2.0/12.0/86.0 2.0/14.0/84.0 2.0/16.0/82.0 2.0/18.0/80.0	Tap water	DI water
Effect of CS concentrations	2-12-w 3-12-w 4-12-w	2.0/12.0/86.0 3.0/12.0/85.0 4.0/12.0/84.0	Tap water	DI water
Effect of external coagulant	2-12-OH/w 2-12-NaAc/w 2-12-FA/w	2.0/12.0/86.0	3% NaOH 10% NaAc 3.6×10^{-2}% FA	DI water
Effect of internal coagulant	2-12-w/OH2% 2-12-w/OH	2.0/12.0/86.0	Tap water	2% NaOH 3% NaOH
	3-12-w/OH2% 3-12-w/OH	3.0/12.0/85.0	Tap water	2% NaOH 3% NaOH

* The concentrations of all the internal and external coagulants were based on weight percents

A number of experiments were conducted with different dope compositions and external and internal coagulants and the conditions are summarized in Table 4.1. The total weight of the three components in each dope, i.e., CS, CA and FA, was set at 100 g while the CA concentrations in the dopes varied from 12 to 18 wt% and the CS concentrations varied from 2 to 4 wt%. Water was first examined as both the external and internal coagulants to prepare the highly porous membranes. Then, the composition of the external coagulant was adjusted by adding an adequate amount of NaOH or sodium acetate or a

small amount of FA in tap water, and that of the internal coagulant was adjusted by the addition of a different amount of NaOH in DI water.

4.2.3 Cloud point study

Cloud points of the dope solutions were measured by titration method. CA solution, CS solution and CS/CA blend solutions were prepared by dissolving them in FA, respectively, with mechanical stirring. Then, nonsolvent or coagulant (i.e., DI water or NaOH solution in this case) was added slowly into each of the solutions through a syringe pump. The cloud point was observed visually from the sudden occurrence of the turbidity of the solutions (indicating the production of polymer solid particles due to phase separation/inversion).

4.2.4 Other analyses of the blend hollow fiber membranes

The structures and morphologies of the blend hollow fiber membranes were investigated through SEM and FESEM. The pore sizes on the surfaces of the hollow fiber membranes were measured with the software supplied by the manufacturers of the SEM/FESEM.

The specific surface areas of the blend hollow fiber membranes were measured with the BET method.

The porosities of the hollow fiber membranes at wet state were measured by the dry-wet weighing method. The dried hollow fiber membranes were equilibrated with DI water for 24 hours. The porosity was then determined by dividing the amount of water

adsorbed (mL) with the amount (mL) of the wet hollow fiber membranes. The experiment was done for 5 samples and the average porosity was used for each type of the blend hollow fiber membranes.

The mechanical properties of the wet hollow fiber membranes were evaluated through the measurement of tensile stress and elongation ratio at break. Tests were conducted with Instron 3345 Material Tester. Other operation conditions were the same as those described in Chapter 3.

4.3 Results and discussion

4.3.1 Cloud point data

The cloud point data provide useful thermodynamic information about the phase separation/inversion process of the polymer solutions. Table 4.2 shows the experimental results of the cloud points for a few types of spinning solutions containing CA/FA,

Table 4.2 Cloud point data of different spinning solution compositions at 25ºC

CS (g)	CA (g)	FA (g)	Nonsolvent concentration at cloud point (wt%)	
			Water as nonsolvent	NaOH (3 wt%) solution as nonsolvent
0	12	88	39.3	34.5
2	12	86	32.7	30.2
3	12	85	29.6	27.3
2	0	98	Not observed	95.6

CS/CA/FA, and CS/FA, respectively. The results indicate that both the ternary CS/CA/FA blend solutions and the binary CA/FA solution had high tolerance with the addition of the

nonsolvent (or coagulant), i.e., water or NaOH solutions in this case, because the nonsolvent added to obtain the cloud point was as high as 27-40% by weight. This suggests that FA was indeed a good solvent with high solubility for both CS and CA polymers. The cloud point for the CS/FA binary solution was however not observed with the addition of water up to 100% by weight, and was only observed when the addition of NaOH solution (3 wt%) reached about 95% by weight. Since CS can dissolve in solutions of pH<4, the cloud point (or phase separation/inversion) of the CS/FA solution would only occur when the addition of water or NaOH solution raised the solution pH to a value of 4 or above. The results in Table 4.2 also suggest that, though both the tap water and the NaOH solution may be used as the coagulants for the fabrication of the CS/CA blend hollow fiber membranes, higher pH coagulant (e.g., NaOH solution) would serve as a stronger coagulant since the amount of the NaOH solution to be added was less than that of tap water to obtain the cloud point. With the increase of the polymer concentrations (consequently a reduction of FA), the phase separation/inversion also appeared to be easier as the cloud point occurred at a less amount of addition of the water or NaOH solution. The CS concentration seemed to have a significant impact on the cloud point since a slight increase of the CS concentration caused a large reduction in the need of the addition of water or NaOH solution to obtain the cloud point (e.g. the dope solution of 12% CA, 2% CS and 86% FA needed 39.3% water, and that of 12% CA, 3% CS and 85% FA needed only 29.6% water, see Table 4.2). This trend of change indicates that thermodynamically CS may work favorably in enhancing the demixing of the polymers with FA in the CS/CA/FA spinning dope solutions.

The difference in cloudy point data between CA/FA system and CS/FA system indicates their different phase separation behavior. CA/FA system has much faster phase separation than CS/FA system. When the polymer blend solution is in contact with nonsolvent, CA precipitates out quickly and forms a matrix. However, CS is not solidified at the initial stage because only small amount of nonsolvent penetrates into the membrane. Therefore, CS flows freely with solvent to the liquid phase that contains a large portion of solvent and a small portion of nonsolvent. Before the solidification of CS, more CS polymer gathers into the liquid phase. Therefore, when the nonsolvent concentration reaches high enough to induce phase separation for CS, a phase rich of CS may have already been formed. Therefore, CS and CA would preferably form its own phase in the solid blends. This is also supported by the fact that pure CA membrane is transparent while CS/CA blend membrane is translucent and has a milky-white color, indicating two phases are present in blends.

However, the phase separation into two different phases (CS rich phase and CA rich phase) was not observed from FESEM images at magnification of 50,000. Therefore, it indicates the size of CS rich phase is very small and may be less than 10nm that can be detected by FESEM at magnification of 50,000.

Although it is possible that CS forms a different phase, we cannot exclude the case where a few CS polymer chains are entangled by CA polymer and wrapped into CA matrix. This is because CS is polymer and its diffusion in viscous solution is quite slow.

4.3.2   Effect of cellulose acetate (CA) concentrations

CS/CA blend solutions with a constant CS (2 wt%) and different CA concentrations (i.e., 12, 14, 16, and 18 wt%) were used to spin the hollow fiber membranes and water was used as both the external and internal coagulants (non-solvent). Some typical results showing the overall and the cross-sectional structures of the hollow fiber membranes are given in Fig.4.1, and those showing the effect of CA concentrations on the specific surface areas, porosities, and surface pore sizes of the hollow fiber membranes are given in Fig. 4.2.

Overall view	Cross-section
(a): 12%	(b): 12%
(b): 18%	(d): 18%
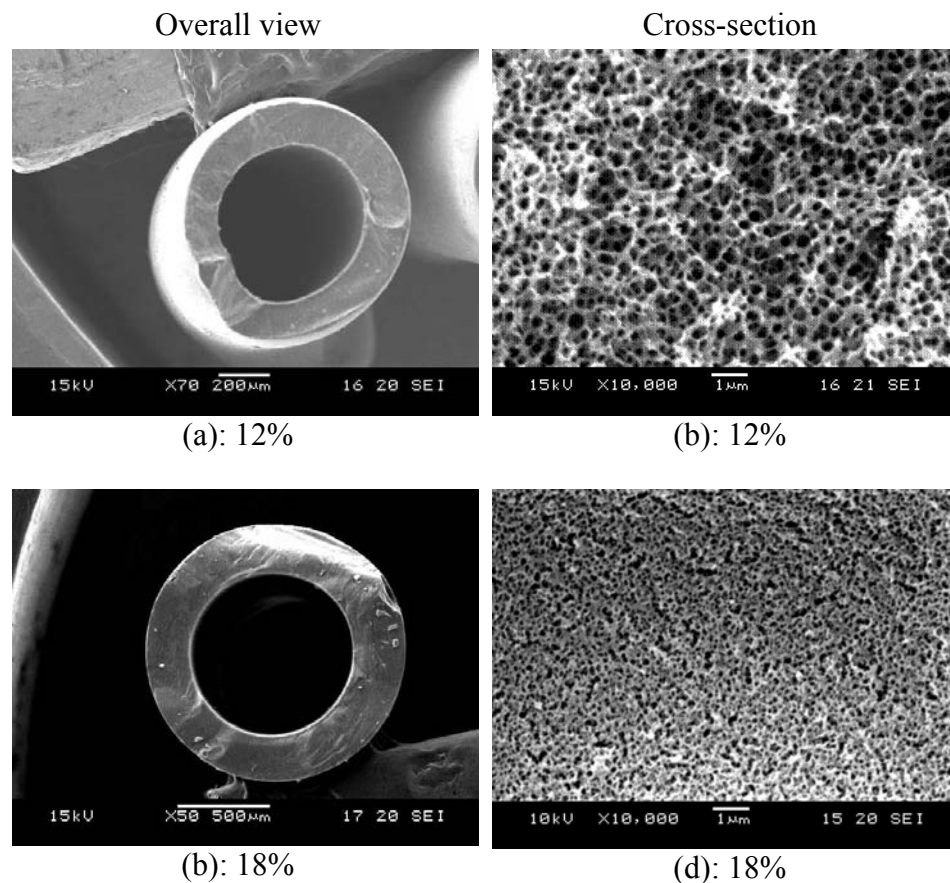
Figure 4.1 Effect of CA concentrations in the spinning solutions on the overall and cross-sectional structures of the CS/CA blend hollow fiber membranes

It has been found that all the hollow fiber membranes had sponge-like and macrovoids-free structures, with the pores in the cross-sections being highly interconnected and displaying open porous networks, which is the desirable structure for adsorptive membranes to achieve large specific surface areas and uniform fluid flow. As indicated in Fig. 4.2, the porosities and surface pore sizes of the hollow fiber membranes decreased but the specific surface areas of the hollow fiber membranes increased with the increase of the CA concentrations in the dope solutions. For example, for CA from 12 to 18 wt%, the porosity reduced from 80.6 to 70.4%, and the outer surface pore size from 0.54 to 0.09 μm, but the specific surface area increased from 10.4 to 14.5m^2/g. Since CA acted as the matrix polymer, it is easy to understand that more CA in the spinning dope solution resulted in the formation of denser matrix networks, hence lower porosity, smaller pore sizes but greater specific surface areas.
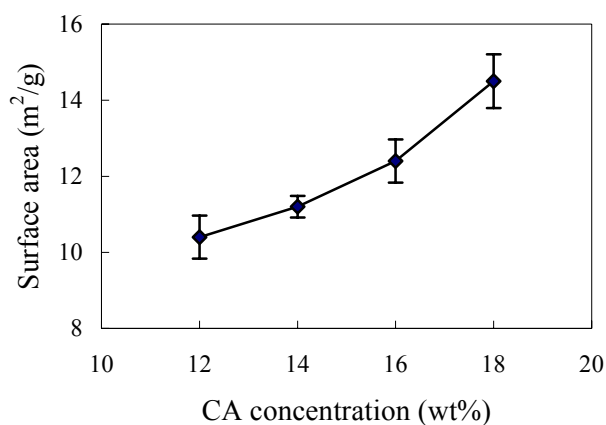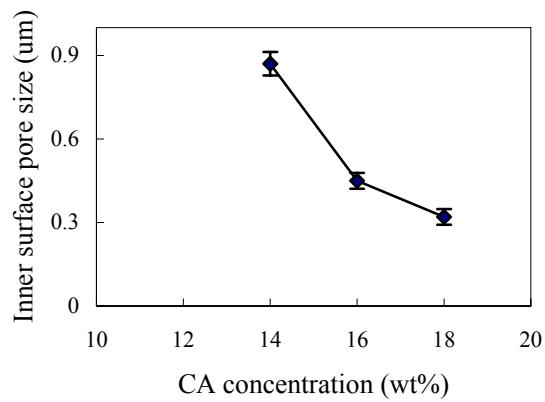
Figure 4.2 Effect of CA concentrations in the spinning solutions on the structural characteristics of the CS/CA blend hollow fiber membranes

To further illustrate the effect of the CA concentrations on the morphologies of the hollow fiber membranes, Fig. 4.3 and Fig. 4.4 show the SEM images of the outer and inner surfaces of the hollow fiber membranes fabricated at different CA concentrations. Extremely open porous outer surfaces with a latex structure were obtained in the CA concentrations ranging from 12 to 16 wt% (see Fig. 4.3a-c) while a much less porous surface was obtained at the CA concentration of 18 wt% (see Fig. 4.3d). Although water was used as both the external and internal coagulants, the inner surfaces appeared to be even more porous with much larger pore sizes than the corresponding outer surfaces, with beak-like structure at the CA concentration of 12 wt% (see Fig. 4.4a) or latex structure at the CA concentrations of 14-18 wt% (see Fig. 4.4b-d). The larger inner surface pore sizes than the outer surface are also clearly shown in Fig. 4.2. As seen in both Fig. 4.4 and Fig. 4.2, the average pore sizes of the inner surfaces also decreased with the increase of the CA concentrations.

| (a): 12% | (b): 14% |
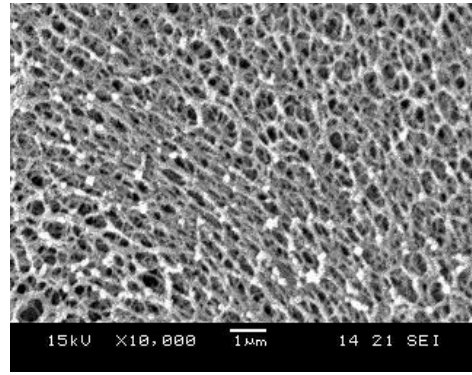
<center>(c): 16%   (d): 18%</center>

Figure 4.3 Effect of CA concentrations in the spinning solutions on the outer surface morphologies of the CS/CA blend hollow fiber membranes
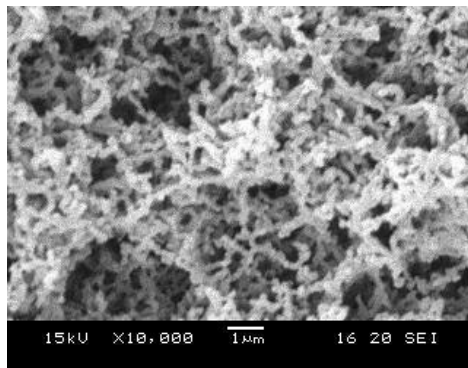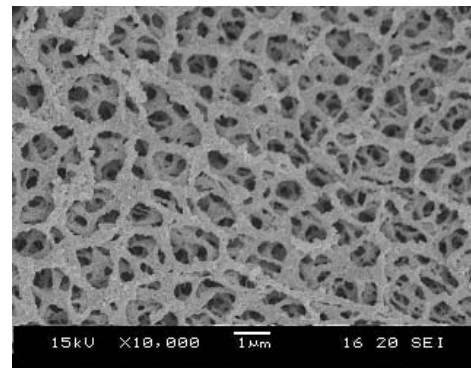
<center>(a): 12%   (b): 14%</center>
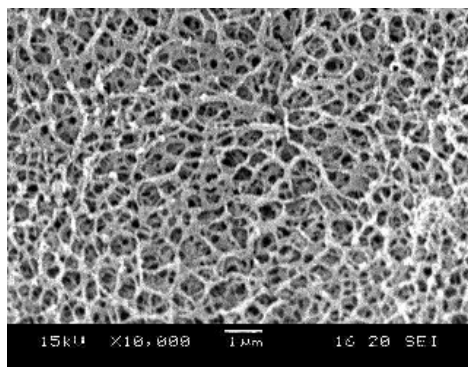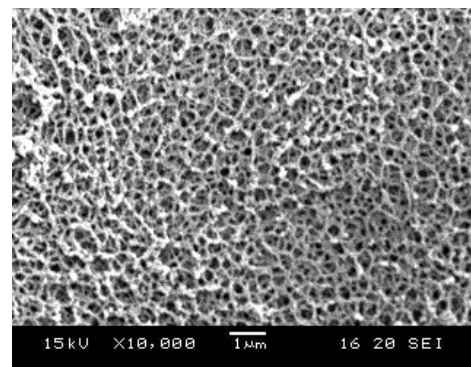
<center>(c): 16%   (d): 18%</center>

Figure 4.4 Effect of CA concentrations in the spinning solutions on the inner surface morphologies of the CS/CA blend hollow fiber membranes

4.3.3   Effect of chitosan (CS) concentrations

CS was added as a functional polymer to provide the CS/CA blend hollow fiber membranes with excellent adsorptive performance. Although it was desirable to fabricate the CS/CA blend hollow fiber membranes with greater amounts of CS, the addition of
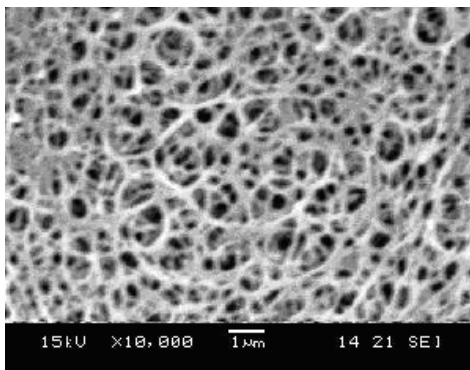
(a): 2%
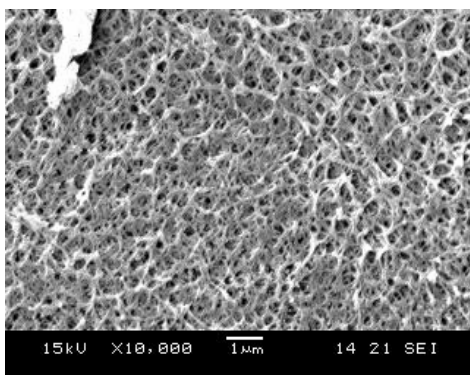
(b): 3%
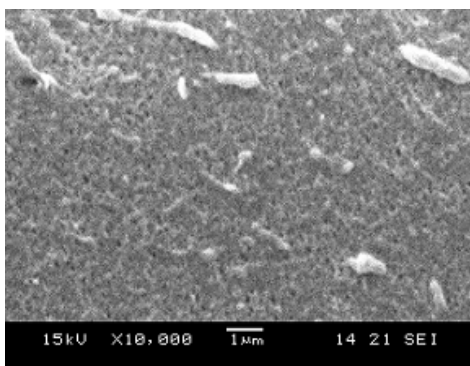
(c): 4%

Figure 4.5 Effect of CS concentrations in the spinning solutions on the outer surface morphologies of the CS/CA blend hollow fiber membranes

CS significantly increased the viscosity of the spinning dope solution and the spinning process became increasingly more difficult. It was found that when CS concentration exceeded 4 wt%, a non-flow behavior of the spinning dope solution was observed. Therefore, the effect of CS concentration on the morphologies and structures of the blend hollow fiber membranes was examined at the CS concentration range from 2 to 4 wt% with the CA concentration being set at a low constant value of 12 wt% in this study. Again, water was used as both the external and internal coagulants in this case.

Again, all the hollow fiber membranes showed the sponge-like and macrovoids-free porous structures. However, the most significant differences in this case is that a small increase in the CS concentration would largely decrease the surface pore sizes of the hollow fiber membranes, as shown by the typical SEM images in Fig. 4.5. This is possibly because that CS enriched at the outer surface of the membranes and formed a dense layer. The effect of CS concentrations on the surface pore sizes, porosity, and specific surface areas of the hollow fiber membranes are shown in Fig. 4.6. The averaged pore sizes of the outer surfaces were found to decrease from 0.54 to 0.22 and to 0.063 μm when CS concentration was increased from 2 to 3 and 4 wt%, respectively. As expected, the porosities of the hollow fiber membranes were not significantly changed but the specific surface areas increased due to the addition of a small amount of CS in the blend. The results support the advantages of entrapping CS in the CA matrix to increase the reactivity of the blend hollow fiber membranes for improved or enhanced adsorptive performance.
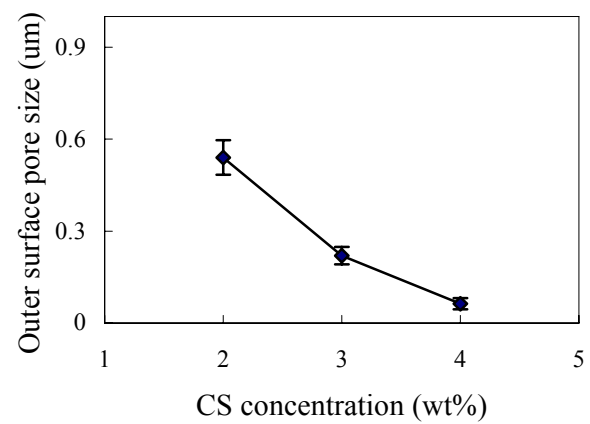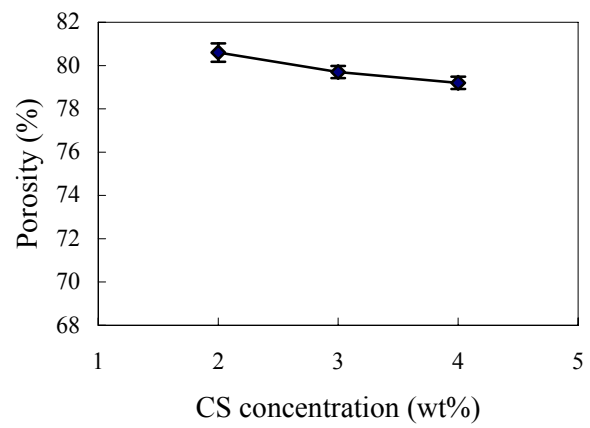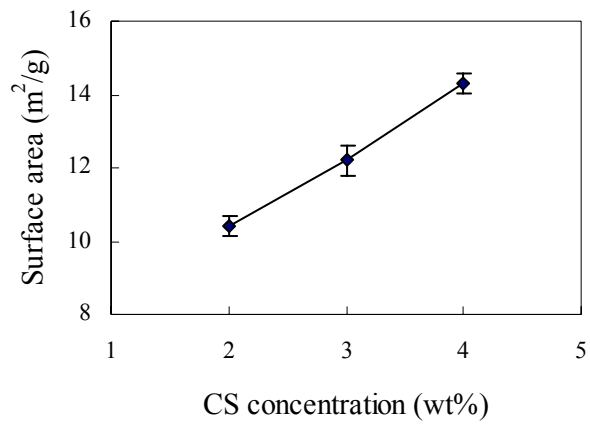
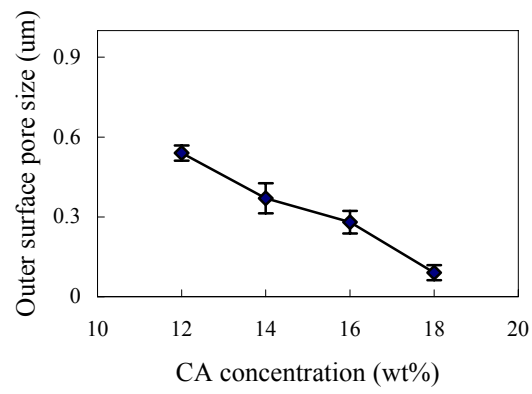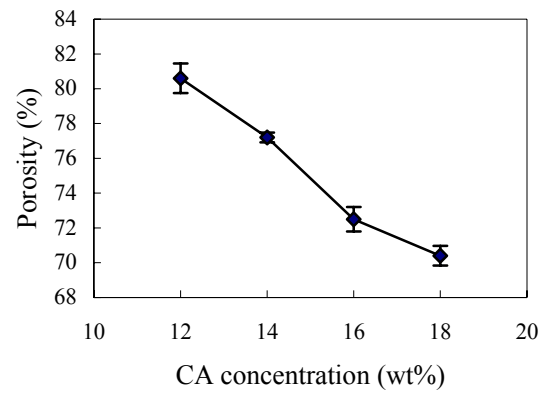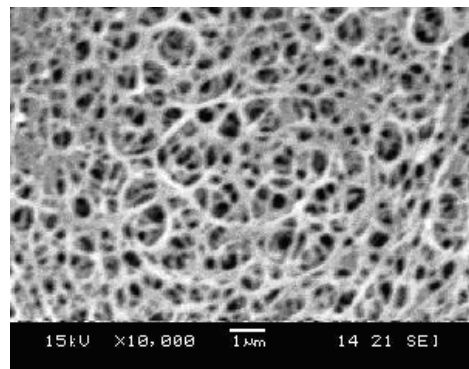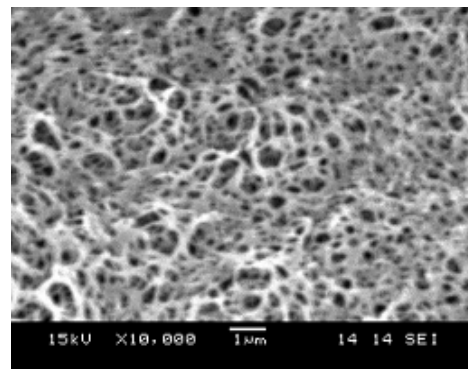Figure 4.6 Effect of CS concentrations in the spinning solutions on the structural characteristics of the CS/CA blend hollow fiber membranes

4.3.4 Effect of coagulant compositions

The hollow fiber membranes mentioned in Sections 4.3.2 and 4.3.3 were fabricated by using water as both the external and internal coagulants. Generally, most polymeric hollow fiber membranes in the literature were prepared through a wet or dry-jet wet spinning process, with water being frequently used as the coagulant, largely due to the fact that water is a good nonsolvent for many polymers, has high mutual affinity with many common polymer solvents, and is inexpensive as a large quantity of the external coagulant is usually needed. However, the conventional method often results in the production of asymmetric membranes, typically with a thin dense top layer (or skin) supported on a porous layer with macrovoids. For the CS/CA blend hollow fiber membranes prepared in this study, the results in Sections 4.3.2 and 4.3.3 clearly illustrate the highly porous, macrovoid-free and relatively uniform porous structures of the hollow fiber membranes, suggesting that delayed demixing of the hollow fiber memrbanes took place during phase separation/inversion and that water was a relatively weak coagulant or nonsolvent for the CS/CA/FA ternary spinning dope solutions. In addition to this, the unconventional solvents used in this research, protic solvents, may also contribute to the unique structures of the blend hollow fiber membranes [136-138].

The possible effect of other weaker or stronger coagulants on the membrane structures is therefore of interest to be studied. Strathmann et al. have reported that one type of polymer dope solution may produce a range of membrane structures (sponge-like to finger-like voids), depending on the choice of nonsolvent [139-140]. In the following part, we present the results for the CS/CA blend hollow fiber membranes fabricated with some alkali or acid added into the water coagulant to change the coagulant compositions. The

interest in examining this was also arising from the cloud point study in Section 4.3.1 where the results show that using water or NaOH solution as coagulant affected the cloud point or phase separation of the CS/CA blend solutions.

4.3.4.1 Effect of external coagulant compositions

Instead of using water as the external coagulant, NaOH solution (3 wt%), NaAc solution (10 wt%) and FA solution (3.6×10^{-2} wt%) were examined as the external coagulant to prepare the CS/CA blend hollow fiber membranes which were spun from the solutions containing 2 wt% CS and 12 wt% CA (see Table 4.1). Water was stilled used as the internal coagulant.

In the case of using the 3 wt% NaOH solution as the coagulant, the hollow fiber membranes were observed to show a faster phase separation/inversion than those using water as the coagulant, supporting that the NaOH solution is a relatively stronger coagulant than water, and agreeing with the results from the cloud point experiments. The resultant hollow fiber membranes were observed to have some sparkly distributed "tear-drop" shaped macrovoids which appeared near the outer surface of the fiber (see Fig. 4.7). With the use of the 10 wt% NaAc and 3.6×10^{-2} % FA solutions, the resultant hollow fiber membranes did not show any macrovoids across the cross-sections of the membranes (images not shown), indicating that the NaAc and dilute FA solutions were relatively weaker coagulants than the NaOH solution for the CS/CA blend hollow fiber membranes.
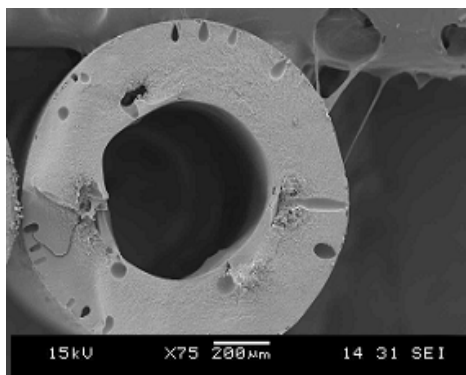
Figure 4.7 Overall view of the CS/CA blend hollow fiber membrane 2-12-OH/w

The SEM images showing the outer surfaces of these hollow fiber membranes are given in Fig. 4.8 and the corresponding outer surface pore sizes, specific surface areas and porosities are given in Table 4.3. It is clear that the hollow fiber membranes generally had smaller surface pore sizes (surface pores from 0.47 to 0.087 to 0.049 μm) when the external coagulant was changed from the FA to NaAc to NaOH solutions (i.e., the solution pH increased). This result may be attributed to the relatively more rapid coagulation rate of the hollow fiber membranes in a more basic coagulation solution. However, the internal surface areas and porosity did not show significant change when external coagulant changed from FA to NaAc to NaOH solutions (see Table 4.3). As internal surface areas and porosity are the structural characteristics of the bulk membranes, they are contributed mainly by the internal micropores in the cross-section. Although outer surface morphologies changed so much with different solution as coagulant, it was possible that the internal membrane structure was similar among these four types of membranes due to same polymer concentration. Therefore, it is possible that internal surface areas and porosity showed no significant change among the four types of membrane.
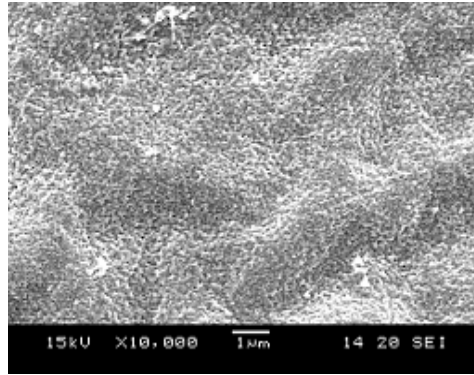
(a): 2-12-OH/w
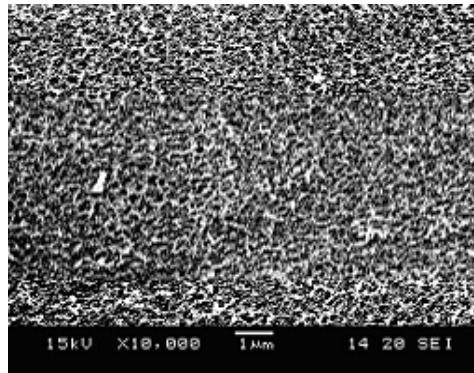
(b): 2-12-NaAc/w
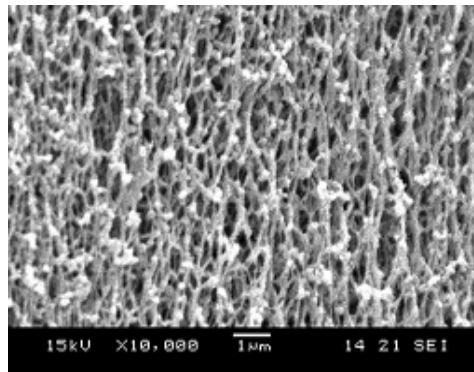
(c): 2-12-FA/w

Figure 4.8 Effect of external coagulant composition on the outer surface morphologies of the CS/CA blend hollow fiber membranes

Table 4.3 Effect of external coagulant composition on the structural characteristics of the CS/CA blend hollow fiber membranes

External coagulant	Hollow fiber membranes	Average pore size of outer surface (μm)	Specific surface area (m^2/g)	Porosity (%)
3 wt% NaOH	2-12-OH/w	0.049±0.01	11.7±0.5	79.0±2.0
10 wt% NaAc	2-12-NaAc/w	0.087±0.01	11.2±0.4	79.2±1.2
3.6×10^{-4} wt% FA	2-12-FA/w	0.470±0.03	10.4±0.6	80.4±1.6
Water	2-12-w	0.540±0.05	10.4±0.5	80.6±1.1

4.3.4.2 Effect of internal coagulant compositions

In this part of the study, NaOH solutions were examined as the internal coagulant. The spinning solutions were prepared with 12 wt% CA, plus 2 or 3 wt% CS. Water was used as the external coagulant and NaOH solutions at the concentration of 2 or 3 wt% were used as the internal coagulant, respectively.

(a): 2-12-w/OH2% (2% NaOH)   (b): 2-12-w/OH (3% NaOH)
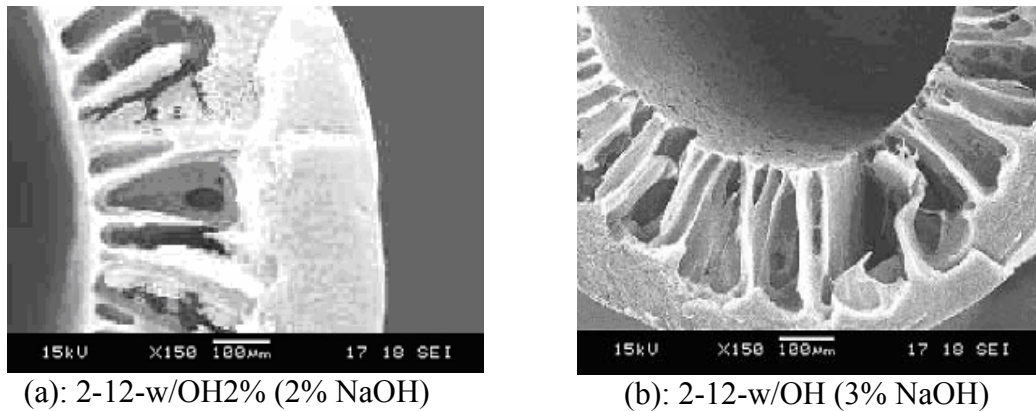
Figure 4.9 Effect of internal coagulant composition on the cross-sectional structures of the CS/CA blend hollow fiber membranes

It was found that for the hollow fiber membranes prepared with 2 wt% CS, large macrovoids were formed near the lumen side in the hollow fiber membranes and more and

larger macrovoids appeared for the NaOH solution with a higher concentration of 3% (see Fig. 4.9). In contrast, the hollow fiber membranes prepared with 3 wt% CS did not show apparent macrovoids in the cross-sections (images not shown) for the NaOH solutions studied, possibly due to the high viscosity of the spinning dope solution at 3 wt% of CS. It is interesting to note that the shape of these macrovoids was different from the typical tear-drop or finger-like shape usually reported in the literature (The macrovoids in this case were very wide). The special shape of the macrovoids in this work may be attributed to the different phase separation behaviors of the CS/CA blends from many others reported in the literature using a single polymer in the spinning dope solution.

The nucleation theory [25] has often been used to explain the formation of macrovoids. After a top surface layer is formed, the nonsolvent will penetrate through the top thin layer into the inner wall. During the period of growth of a droplet of nonsolvent in the sublayer, the influx of solvent from surrounding polymer solutions into the nonsolvent droplet makes the droplet a solvent and nonsolvent mixture. Hence, the surrounding polymer solution remains in the form of liquid and the solidification (or phase inversion) of the polymers could not be possible. Only when more and more solvent was extracted (at the same time the droplet becomes larger and larger in size), the surrounding polymers started to have phase separation. After the surrounding polymers are completely solidified, the spaces occupied by the large droplets of the solvent and nonsolvnet mixture thus form the macrovoids. The formation of macrovoids depends on the ratio of influx of the nonsolvent from the coagulant into the sublayer and the influx of solvent from the surrounding polymer solutions into the nonsolvent droplet. One of the factors dominating the influxes of nonsolvent and solvent is the kinetic hindrance from the polymer solutions which are

dependent on the polymer concentrations and thus on the viscosities of the dope solution. In this work, the blend dope solution at 3 wt% CS showed much higher viscosity than that at 2 wt% CS. At such a high viscosity, the influx of the FA from the surrounding polymer solutions into the nonsolvent droplet was very slow. Under this condition, due to the high concentration nonsolvent in contacting with the surrounding polymers, the surrounding polymers solidified rapidly before a large droplet of solvent and nonsolvent mixture formed, leading to the formation of microporous structures rather than macrovoids structures.

(a): 3-12-w/OH2% (2% NaOH)   (b): 3-12-w/OH (3% NaOH)
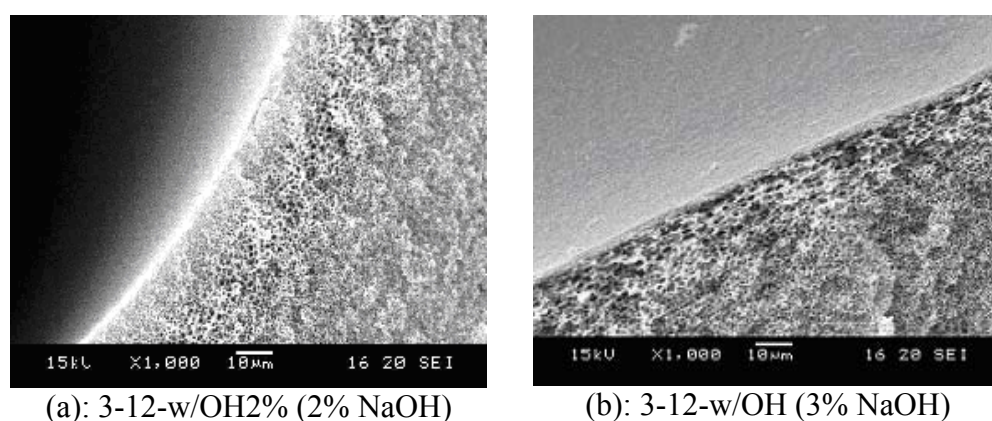
Figure 4.10 Effect of internal coagulant composition on the inner edge structures of the CS/CA blend hollow fiber membranes

Although hollow fiber membranes prepared at 3 wt% CS did not show macrovoids in the cross-sections, a tendency of phase separation into polymer rich and polymer lean phases was also observed when NaOH solution was used as the internal coagulant. The inner edges of the hollow fiber membranes are shown in Fig. 4.10. It can be found that a more porous region existed below the relatively denser inner surfaces. With increasing the NaOH concentration in the bore fluid, the pore size and porosity of this subsurface region obviously increased. Moreover, the starting point of this region was much closer to the

inner surfaces with increasing NaOH concentration in the bore fluid. This was attributed to the stronger coagulation effect of 3 wt% NaOH solutions than 2 wt % NaOH solutions.

(a): 2-12-w/OH2% (2% NaOH)

(b): 2-12-w/OH (3% NaOH)

(c): 3-12-w/OH2% (2% NaOH)

(d): 3-12-w/OH (3% NaOH)
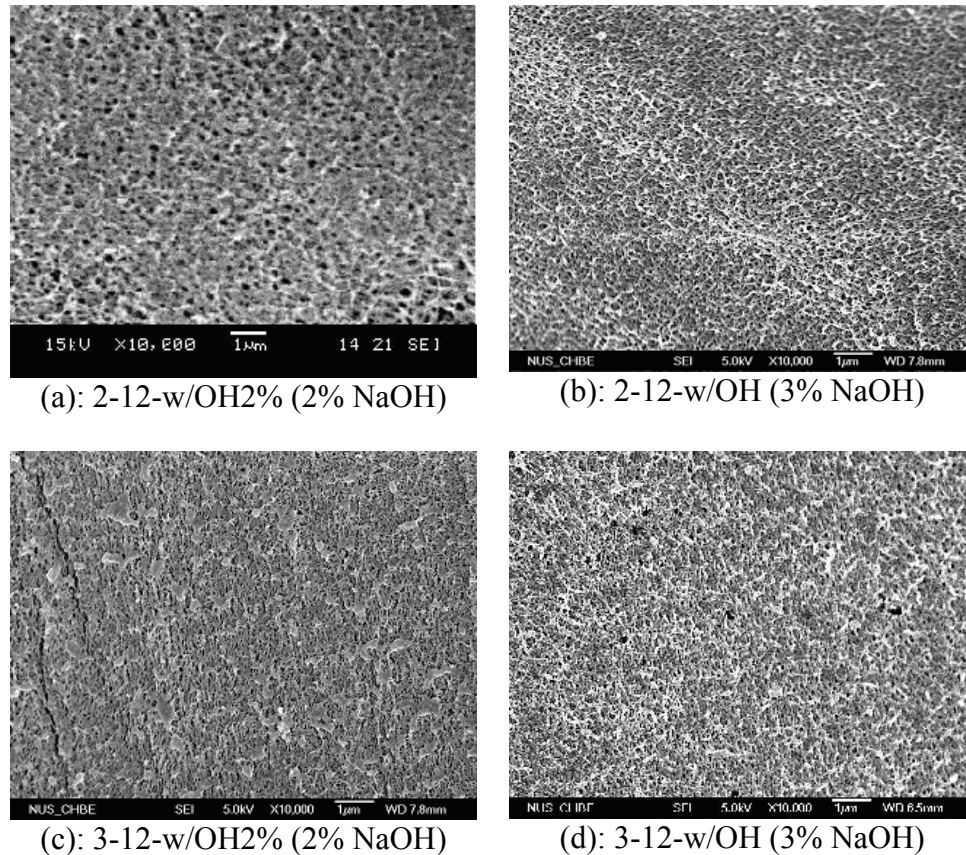
Figure 4.11 Effect of internal coagulant composition and CS concentration on the inner surface morphologies of the CS/CA blend hollow fiber membranes

SEM images showing the inner surfaces of these hollow fiber membranes are given in Fig. 4.11. Clearly, all these membranes had open porous inner surfaces. However, the pore sizes were much smaller than those fibers with water as the internal coagulant. In addition, a slight reduction in the surface pore sizes was observed with the increase of the NaOH concentrations and with the increase of CS concentrations in the spinning solutions. The specific surface areas and porosities of these hollow fiber membranes are given in Table

4.4. At the CS concentration of 2 wt%, the porosity is found to increase to a higher value at a higher NaOH concentration, which may be attributed to the presence of more and larger macrovoids as discussed earlier. The changes in the specific surface areas were not significantly in this case. At the CS concentration of 3 wt%, however, the changes of both the specific surface areas and the porosities did not appear to be significant.

Table 4.4 Effect of internal coagulant composition and CS concentration on the structural characteristics of the CS/CA blend hollow fiber membranes

Dope composition (CS/CA/FA, g/g/g)	Bore fluid composition	Surface area (m^2/g)	Porosity (%)
2.0/12.0/86.0	DI water	10.4±0.2	80.6±1.3
	2 wt% NaOH	10.9±0.4	82.3±1.1
	3 wt% NaOH	11.3±0.2	86.7±1.4
3.0/12.0/85.0	DI water	12.2±0.4	79.7±1.3
	2 wt% NaOH	13.0±0.4	79.0±1.2
	3 wt% NaOH	13.4±0.3	79.2±1.0

4.3.5   Mechanical properties of the blend hollow fiber membranes

As the CA concentration in the spinning solutions was reduced to 12-18 wt% in this study, the mechanical properties of the membranes may be reduced. We examined the tensile stress and elongation ratio at break for these highly porous hollow fiber membranes, and some of the typical results are given in Table 4.5. It can be found that the blend hollow fiber membranes still had sufficiently high tensile stress (7.8-8.3MPa) and break elongations (22.1-25.3%) even for the highly porous membranes prepared at low polymer concentrations (CS/CA=2/12 or 3/12). With the increase of the CA concentration to 18 wt%, the tensile stress is also found to be increased significantly from 7.8 MPa to 18.2

MPa while the elongation ratio increased moderately. The mechanical strength of the

hollow fiber membranes also appears to be strengthened when NaOH solution was used as

the internal coagulant.

Table 4.5 Mechanical test results for some of the CS/CA blend hollow fiber membranes
prepared at CS/CA/FA weight ratio of 2.0/12.0/86.0 and 2.0/13.0/85.0 in the spinning
solutions

Dope composition (CS/CA/FA, g/g/g)	External coagulant	Internal coagulant	Tensile stress (MPa)	Elongation ratio (%)
2.0/12.0/86.0	Tap water	DI water	7.8±0.3	22.1±0.2
2.0/18.0/80.0	Tap water	DI water	18.2±0.2	27.6±0.4
3.0/12.0/85.0	Tap water	DI water	7.6±0.3	23.7±0.3
3.0/12.0/85.0	Tap water	3 wt% NaOH	8.3±0.3	25.3±0.3

4.4 Conclusions

CS/CA blend hollow fiber membranes with different structure and morphologies

were successfully fabricated through a wet spinning process with CA in the concentration

range of 12-18 wt% and CS concentration at up to 4 wt% in the spinning dope solutions.

Depending on the polymer concentrations in the spinning solution and the coagulant

compositions, the outer surface pore sizes, the specific surface areas, and the porosities of

the blend hollow fiber membranes can change from 0.54 to 0.049 μm, 10.4 to 14.5 m^2/g,

and 80.6 to 70.4%, respectively. Water can be used as both the external and internal

coagulants in the fabrication process and the resultant hollow fiber membranes showed

sponge-like, macrovoids-free and relatively uniform porous structures which are desirable

for affinity membranes. The composition of the coagulants affected the structures of the

blend hollow fiber membranes greatly. By increasing the alkalinity of the coagulants, the

coagulation rate of the blend hollow fiber membranes was increased, resulting in relatively denser surfaces with smaller pore sizes. In particular, the membranes with macrovoids could be produced by using NaOH solutions (2-3 wt%) as the internal coagulant and by reducing the polymer concentrations, particularly CS (CS<3%, CA=12%), in the spinning solutions. In conclusion, the present work demonstrates that the CS/CA blend hollow fiber membranes can be made into highly porous adsorptive membranes with large specific surface areas and various desirable pore sizes by properly controlling the CS and CA concentrations in the spinning solutions and by adjusting the compositions of the external and internal coagulants.

Chaper 5 Adsorptive removal of copper ions with CS/CA blend hollow fiber membranes

Summary

In this part of the work, CS contents on highly porous membranes that were prepared in last chapter were investigated. It was found the actual CS content on the membrane was lower than that in spinning solution. This is possibly because neutralization of nonsolvent by out-diffusing protic solvent leads to dissolution of a portion of CS from the nascent membrane. However, it was also found that dissolution of CS could be reduced by using alkali solution as coagulant and by increasing CA concentration in spinning solution. Maximum CS density of 120mg/g was achieved in this work. Very fast adsorption kinetics towards copper ion was observed (<70mins) for these highly porous membranes. Maximum copper ion adsorption amount at batch mode increased to 12.5mg/g, about two times larger than that of membranes prepared in Chapter 3. Elution of Cu^{2+} solution at filtration mode gave saturation capacity of 11.13mg/g at residence time of 3mins. However, due to the highly porous structure of the membranes, HCl solution was not applicable as desorbent solution because CS easily detached from highly porous membranes and dissolved in HCl solution.

5.1 Introduction

Heavy metal contamination of various water resources is of great concern because of the toxic effect to the human beings and animals and plants in the environment [129]. Conventional techniques used to remove heavy metal ions may include chemical precipitation, electrolysis, solvent extraction, ion exchange, adsorption and reverse osmosis (RO). These methods are either costly, or ineffective at low concentrations, or slow in processing. Some of them also generate a large amount of sludge or second wastes that are difficult to handle. Recently, adsorptive microfiltration membranes, which combine the advantages of both the microfiltration technology and the adsorption technology, have emerged as an attracting method for the removal of heavy metal ions by providing high retention ratio, fast processing rate, high selectivity and high efficiency at low concentrations with low energy consumption. With the application of such adsorptive membranes, the function of the MF process can be expanded from filtration separation only (for particle removal) to filtration plus adsorption separation together (for particles and heavy metal removal).

The reports on using adsorptive membranes for heavy metal ion removal have been rather limited. They are mainly prepared by (1) the attachment of dyes (Cibacron blue F3GA, Procion Brown MX 5BR, Procion Green H-4G, etc.) to polyvinylbutyral membranes, polyvinylalcohol membranes, poly(2-hydroxyethyl methacrylate) membranes [141-143], or poly(hydroxyethylmethacrylate/chitosan) composite membranes [73, 144], or (2) the grafting of acrylic acid or maleic acid monomer on polyethylene membranes [145-146], or the grafting of polyamino acids onto cellulose and cellulose acetate membranes [147-148]. Although the modified membranes become adsorptive or have high

adsorption capacities, the polymeric base membranes can be deteriorated due to the harsh physical or chemical treatment needed for the surface modification, or the functional chemicals used to modify the membrane surfaces are usually too costly to be used for practical applications in heavy metal removal.

Due to the high chelating capability of chitosan, chitosn based membranes can be directly used for adsorption of heavy metal ions. Since the membranes need no further surface modifications, it greatly simplifies the preparation of adsorptive membranes, as compared to the conventional approach of surface modification. Alumina/chitosan composite membranes have been fabricated and used to remove copper (II) from polluted water [75]. Chitosan/cellulose acetate blend films were also prepared and used for copper (II) removal and the isotherm study showed a saturation plateau of 123 mg of copper per gram of the hybrid [76]. However, these membranes are flat sheet membranes and have limitation to be used on a large scale.

In this work, the CS/CA blend hollow fiber membranes were prepared and examined in adsorptive removal of copper ions from aqueous solutions. Highly porous membrane having similar structure as that prepared in Chapter 4 was studied for copper ion removal. Firstly, the actual CS content on the blend membranes was investigated. Although the adsorption of copper ions with CS/CA blend hollow fiber membranes had been preliminary tested in the previous study (see Chapter 3), detailed examination on the capacity, kinetics and adsorption mechanisms as well as regenerations/reuse is necessary for actual applications. In addition, the adsorption of copper ions in previous studies was conducted with the CS/CA blend hollow fiber membranes (0.5-26.5-OH and 1-26-OH) with relatively denser surfaces and much lower CS contents (1.7-3.5 wt%). The adsorption

performance with highly porous membranes having much higher CS contents may be very different from that in previous study.

Four types of highly porous CS/CA blend hollow fiber membranes were prepared from two dopes with weight ratio of CS/CA/FA=3/12/85 and 2/18/80 in two different coagulants (water and 3 wt% NaOH solution), and were examined in their adsorptive performance for the removal of copper ions. The copper ion adsorption capacity, kinetics and performances at very low concentrations were investigated. Both batch mode and filtration mode experiments were carried out. The adsorption mechanisms were revealed from the X-ray proton spectroscopic (XPS) studies. The desorption of copper ion and the regeneration of the hollow fiber membranes were examined with both the EDTA and HCl solutions.

5.2 Experimental

5.2.1 Materials

CS with MW of 75,000 g/mol and deacetylation degree of 73.5% was used to prepare the CS/CA blend hollow fiber membranes. CA and formic acid (FA, 98-100%, from Fluka) used were of the same grades as those in previous studies (Chapter 3).

5.2.2 Preparation of CS/CA blend hollow fiber membranes

The general methods to prepare the CS/CA blend hollow fiber membranes have been described in previous studies. In this work, four types of CS/CA blend hollow fiber membranes were prepared by wet spinning two types of blend solutions with CS/CA/FA weight ratio as 3/12/85 or 2/18/80 into two types of coagulants or non-solvents (i.e., water

or 3 wt% NaOH solutions). Other information on the four types of blend hollow fiber membranes are summarized in Table 5.1.

Table 5.1 Information on the CS/CA blend hollow fiber membranes prepared for copper ion adsorptions

Hollow fiber membrane ID	3-12-w	3-12-OH	2-18-w	2-18-OH
Blend dope composition: CS/CA/FA (g/g/g)	3/12/85	3/12/85	2/18/80	2/18/80
Weight ratio of CS/(CS+CA) in the spinning blend dope	20%	20%	10%	10%
External coagulant	Tap water	3 wt% NaOH	Tap water	3 wt% NaOH
Bore fluid (internal coagulants)	DI water	3 wt% NaOH	DI water	3 wt% NaOH
Specific surface area (m^2/g)	12.2	14.1	14.5	15.2
Porosity (%)	79.7	79.1	70.4	70.4
Outer surface pore size (μm)	0.22	0.07	0.09	0.05
CS content in the dry hollow fiber membranes	3.7%	12%	8.5%	9.3%

5.2.3   Characterization of CS/CA blend hollow fiber membranes

The structures and morphologies, specific surface areas and porosities of the hollow fiber membranes were measured with the methods described in previous studies. CS contents in the blend hollow fiber membranes were analyzed with the ninhydrin method [128]. All these information is also given in Table 5.1.

5.2.4   Copper ion adsorption at batch mode

As the primary purpose of the study was to evaluate the adsorptive performance and behaviors of the hollow fiber membranes, the removal of copper ions was therefore conducted in a batch adsorption mode. The hollow fiber membranes were cut into pieces at about 0.5 cm length. To examine the adsorption amounts of the hollow fiber membranes, a 1.1 g amount of the dried hollow fiber membrane pieces from a particular type of the hollow fiber membranes were added, respectively, into a number of flasks, each of which contained 50 mL of a copper ion solution with an initial concentration varying in the range of 10-150 mg/L. The initial pH of the copper ion solutions in the flasks was all adjusted to 5 with dilute HCl and NaOH solutions. The mixture in the flasks was stirred in a water bath shaker at 150 rpm and at 25°C for 2 h (more than the adsorption equilibrium time), and the final copper ion concentrations in the solutions were analyzed. The amounts of copper ions adsorbed on the hollow fiber membranes were then calculated from the concentration difference of the solutions before and after the adsorption.

For isotherm study, a 67 mg amount of hollow fiber membrane pieces was suspended into 50 mL of a copper ion solution, with a concentration varying in the range of 10-150 mg/L. The initial pH of the copper ion solution was adjusted to 5. Other adsorption conditions were totally same as that described in last paragraph.

Adsorption kinetic studies were conducted for two types of the hollow fiber membranes. Again, a 1.1 g amount of the dried hollow fiber membrane pieces from a particular type was added into 50 mL of a copper ion solution in a flask, with an initial solution pH of 5 and an initial copper ion concentration of 50 mg/L. The mixture was

stirred in a water bath shaker at 150 rpm and at 25 ^{o}C and samples were taken from the solution at desired time intervals for the analysis of copper ion concentrations in the solution.

One type of the hollow fiber membranes was also examined for their removal of copper ions at very low copper ion concentrations. In this case, the initial concentrations of copper ions in the solutions were changed in the range of 0.28-6.5 mg/L and other experimental conditions were the same as those in the adsorption capacity study. Copper ion concentrations in all the samples in this study were determined with an inductively coupled plasma mass spectrometer (ICP-MS, Perkin- Elmer Elan 6100).

5.2.5   Copper ion adsorption at filtration mode

Hollow fiber membrane 3-12-OH was packed into a bundle with one end sealed. The filtration was conducted at dead end mode. Cu2+ solution was delivered into the lumen of the membrane and permeated out from the outer side of the membrane. The total volume of the membrane at wet state was 1.29mL. Specifically, 10 pieces of hollow fiber membranes, each with effective length of 15cm, were packed together.

The filtration was conducted at constant flow mode. The flow rate was controlled precisely by a high pressure syringe pump. The residence time of solution in the membrane was kept at 3mins, so the flow rate of permeate was controlled at 0.43mL/min. At desired time, a drop of permeate (weighed exactly using an analytical electrical balance) was collected. 5mL ultrapure water was added into the collected permeate to dilute the solution. The copper ion concentration in the dilute solution was determined with ICP-MS.

The initial concentration of copper ion solution was set at 20mg/L and pH was set at 5. The experiment was lasted until the concentration in the permeate equals to 20mg/L.

5.2.6   Desorption of copper ions and reuse of the hollow fiber membranes

Desorption of copper ions from the hollow fiber membranes was examined in a batch mode with an EDTA (Ethylenedinitrilo tetraacetic acid disodium salt) or HCl solution in the concentration range from 0.01 to 50 mM. The hollow fiber membranes were first equilibrated with copper ions in a solution with an initial concentration of 150 mg/L at pH 5 (1.1 g hollow fiber membranes were added into 50 mL copper solution). Then, the hollow fiber membranes were separated and added into 150 mL of the desorption solution and the mixture was stirred in a water bath shaker at 150 rpm and at 25°C, and samples were taken from the solution to monitor the amount of copper ions desorbed into the solution. After the desorption test, the hollow fiber membranes were regenerated by washing with water followed by neutralization with dilute NaOH solution (for the fibers desorbed with 50 mM HCl) or by washing with DI water directly (for the fibers desorbed with EDTA). The regenerated hollow fiber membranes were reused in the next cycle of adsorption experiment. The adsorption-desorption experiments were conducted for four cycles.

5.2.7   Other analyses

To examine the mechanism of copper ion adsorption on the hollow fiber membranes, X-ray photoelectron spectroscopes (XPS) of the CS/CA blend hollow fiber membranes before and after copper ion adsorption were obtained with a VGESCALAB MKII spectrometer using an Al Kα X-ray source (1486.6 eV of photons). The photoelectron

scanning angle was set as 90° in order to maximize the scanning depth of the sample. The elements of C, O and N on each sample were scanned and the XPSpeak 4.1 software was used to fit the XPS spectra peaks. To eliminate the effect of surface charging on the analysis results, all XPS spectra were referred to the C 1s peak of the aliphatic carbons at 284.6 eV.

5.3 Results and discussion

5.3.1   Characteristics of the CS/CA blend hollow fiber membranes

The four types of CS/CA blend hollow fiber membranes used in this study were prepared from two different CS/CA ratios (1/4 or 1/9) and two different coagulants (water or 3 wt% NaOH solution), as given in Table 5.1. Fig. 5.1 shows the surface morphologies and cross-sectional structures of the hollow fiber membranes obtained from the SEM analysis. In general, the hollow fiber membranes with water as the coagulant (i.e., 3-12-w and 2-18-w) had larger pore sizes than their corresponding ones with the NaOH solution as the coagulant (i.e., 3-12-OH and 2-18-OH). Consequently, the hollow fiber membranes prepared with water as the coagulant showed slightly lower specific surface areas than the hollow fiber membranes with the NaOH solution as the coagulant (see Table 5.1). The two different coagulants however did not seem to affect the porosity of the hollow fiber membranes significantly. With the increasing of the CA contents (or the decrease in the CS/CA ratio) in the spinning blend dope solutions, the surface pore sizes and porosities of the hollow fiber membranes decreased but the specific surface areas increased (see Table 5.1). All the four types of hollow fiber membranes possessed sponge-like and open porous structures across the cross-sections, which is desirable and beneficial for adsorptive

membranes to have high surface areas and hence provide high binding capacities. As can be found in Table 5.1, the specific surface areas of the hollow fiber membranes reached as high as 12.2-15.2 m^2/g and the hollow fiber membranes were highly porous with porosities in the range of 70.4-79.7%. The outer surface pore sizes of the hollow fiber membranes were in the range of 0.05-0.22 μm that is sufficiently large enough to allow free passage of any heavy metal ions into the internal adsorptive sites of the membranes. The structural characteristics of the membranes prepared in this chapter are very similar to that in chapter 4.

It has been found that the CS contents or the weight ratios of CS/(CS+CA) of the blend hollow fiber membranes were always lower than their corresponding ones in the spinning solutions (see Table 5.1). This indicated that partial dissolution of CS occurred during the coagulation and the rinsing process in preparing the highly porous CS/CA blend membranes. When the CS/CA blend solution was spun into the coagulant, the formic acid (solvent) was extracted into the coagulant (water or NaOH solution), which lowered the pH value of the coagulant. This was especially the case in the lumen side of the hollow fiber membranes where the amount of coagulant (or bore fluid) was very small. Hence, before the CS polymers were solidified, the CS polymers on the fiber surfaces can partially dissolve into the coagulant solution at the fiber/coagulant interfaces if the coagulant solution pH was brought down to lower than 4. It also can be found that the coagulant type and the CA content in the spinning solutions significantly affected the CS contents in the resultant hollow fiber membranes. From the results given in Table 5.1, it is clear that the dissolution of CS from the hollow fiber membranes can be reduced by using

	Outer surface	Inner surface	Cross-section
3-12-w			
3-12-OH			
2-18-w			
2-18-OH			
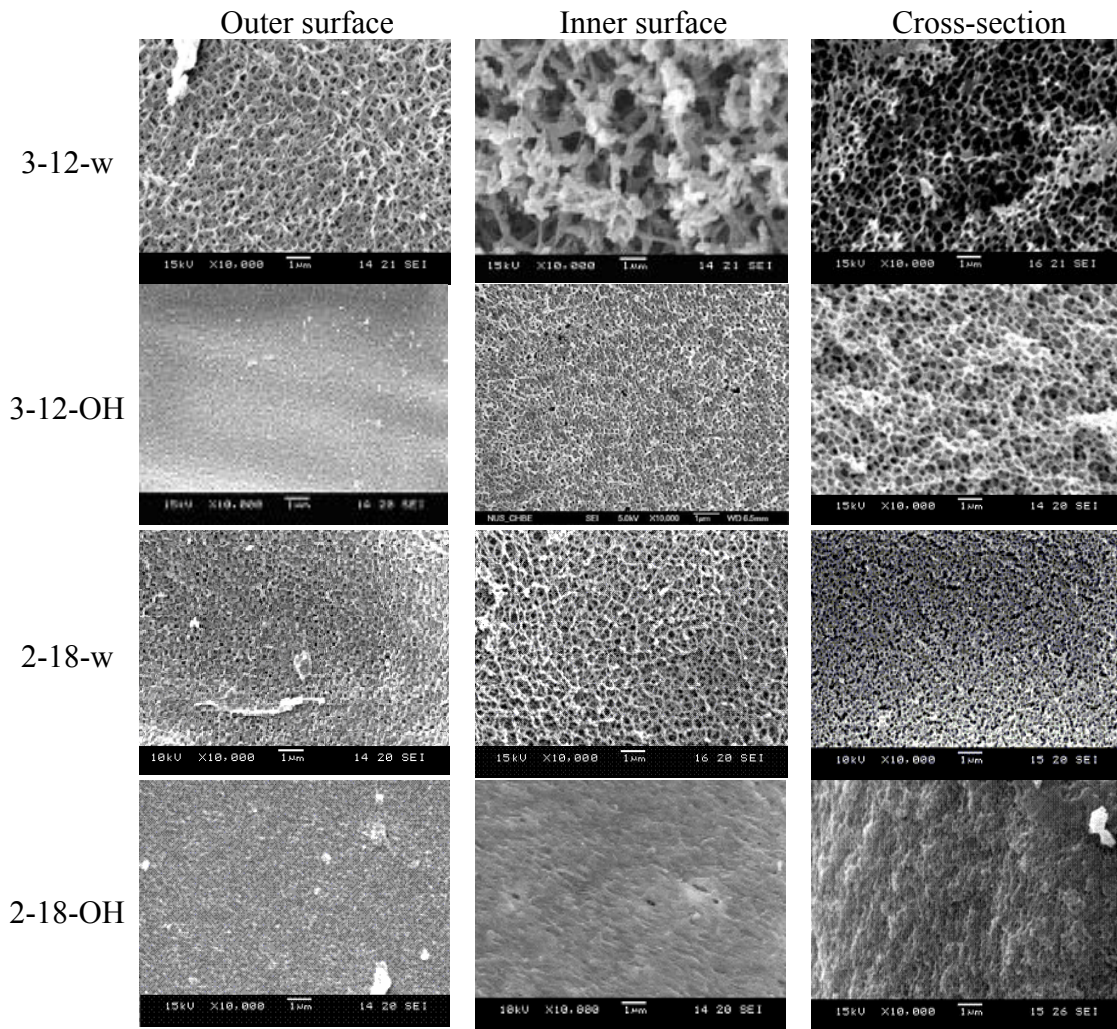
Note: "w": water as the external and internal coagulant, "OH": NaOH (3 wt%) solution as the external and internal coagulant

Figure 5.1 Morphologies of CS/CA hollow fiber membranes for copper ion adsorptions

an alkali solution as the coagulant and/or by spinning the CS/CA blend dope solution at a higher CA content. This is due to the fact that the CS polymers can solidify more rapidly in alkali solutions and the presence of more CA molecules in the blend formed much denser matrix webs that can hinder the diffusion of the CS polymers into the coagulant during the spinning and coagulation process.

5.3.2   Copper ion adsorption amount

Fig. 5.2 shows the amounts of copper ions adsorbed at adsorption equilibrium (q_e, mg/g) on the four types of hollow fiber membranes in an initial copper ion concentration (C_0, mg/L) ranging from 10 to 150 mg/L. In general, the equilibrium adsorption amounts increased with the increase of the copper ion concentrations. It is also clear that the hollow fiber membranes 3-12-OH always had the highest adsorption amounts, and in all cases, the amounts of copper ion uptakes by the hollow fiber membranes followed the order of 3-12-OH>2-18-OH≈2-18-w>3-12-w. This order is closely related to the order of CS contents in the four different types of the hollow fiber membranes (see Table 5.1). The results hence confirm that CS was the main reactive polymer that provides adsorptive sites on the blend hollow fiber membranes for copper ion adsorption.
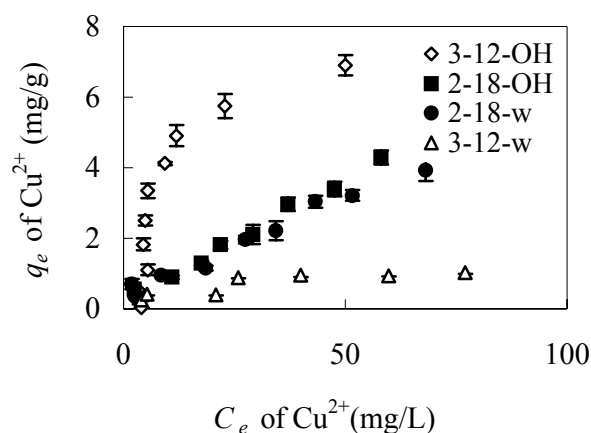
Figure 5.2 Equilibrium copper ion adsorption amounts on the CS/CA blend hollow fiber membranes versus C_e

5.3.3   Copper ion adsorption isotherm

Only 3-12-OH membranes were examined for isotherm study because of the high CS content. The Langmuir and Freundlich isotherm models were used to fit the experimental

results for copper ion adsorption by 3-12-OH hollow fiber membranes in Fig. 5.2. The

fitting using the Langmuir model is shown in Fig. 5.3 and that using the Freundlich model

is shown in Fig. 5.4. A comparison between the predicted and the experimental adsorption

results is shown in Fig. 5.5.

The adsorption amounts on 3-12-OH hollow fiber membranes may be modeled by

both the Langmuir and Freundlich isotherm models, giving the R^2 value of 0.9125 and

0.937 respectively. The maximum amount of copper ions that could be adsorbed (q_m) was

calculated to be 12.5 mg/g (104 mg/gCS). The values of n and K_f in the Freundlich model

were calculated to be 3.4 and 4.2 respectively. This indicates that although the binding

energy on membrane surface show a heterogeneous structure (as confirmed by Freundlich

model), the adsorption may follow a monolayer pattern (as confirmed by Langmuir

model).
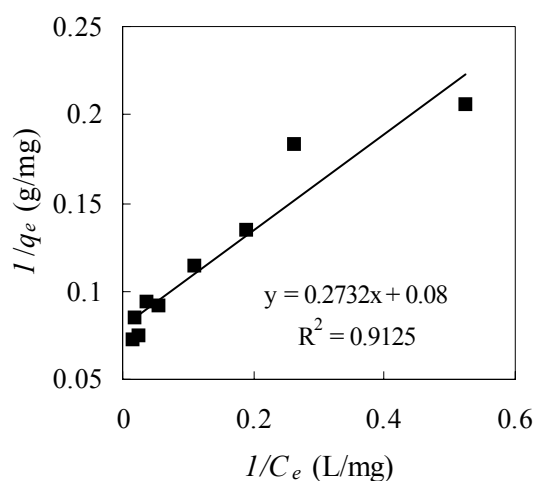
Figure 5.3 Correlating copper ion adsorption on 3-12-OH CS/CA blend hollow fiber
membranes with Langmuir isotherm model
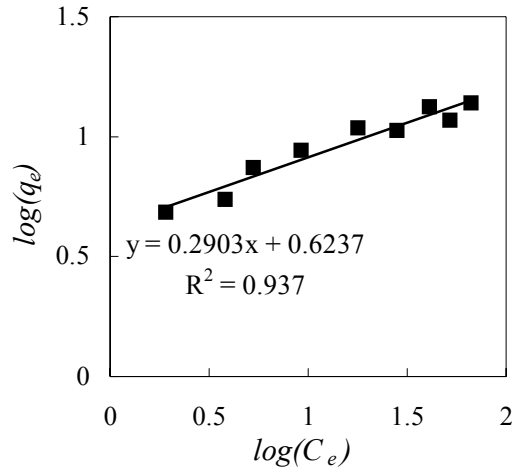
Figure 5.4 Correlating copper ion adsorption on the 3-12-OH CS/CA blend hollow fiber membranes with Freundlich isotherm model
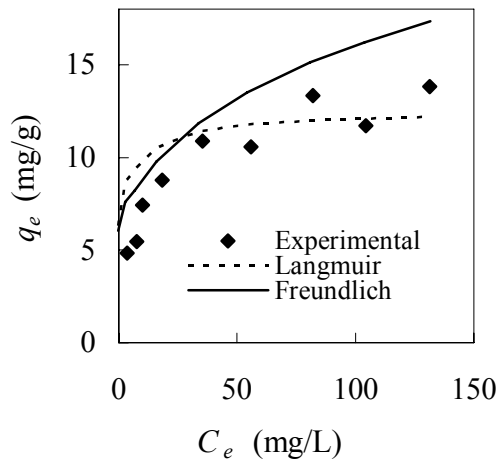
Figure 5.5 Comparison of the experimental adsorption results of copper ion adsorption on 3-12-OH CS/CA blend hollow fiber membranes with the fitted results from the Langmuir and Freundlich models

5.3.4   Adsorption kinetics

Fast adsorption is always desirable in all adsorption separation processes. The typical results from the kinetic adsorption study with the hollow fiber membranes 3-12-w and

3-12-OH are shown in Fig. 5.6. It can be observed in Fig. 5.6a that very high adsorption

rates for copper ions (i.e., rapid change of concentrations with time) on the hollow fiber

membranes occurred in the initial stage of the adsorption process and the adsorption

process finally reached the adsorption equilibrium in about 20 and 70 min respectively for

the hollow fiber membranes 3-12-w and 3-12-OH. The kinetic adsorption equilibrium

time was much shorter than those with chitosan hydrogel beads/resins that were reported

to be at least several hours in the literature [129, 149-152]. The fast adsorption kinetics of

the CS/CA blend hollow fiber membranes may be attributed to the high porosities and the

large pore sizes of the membranes, which facilitated the transport of copper ions to the

external and internal adsorption or binding sites.
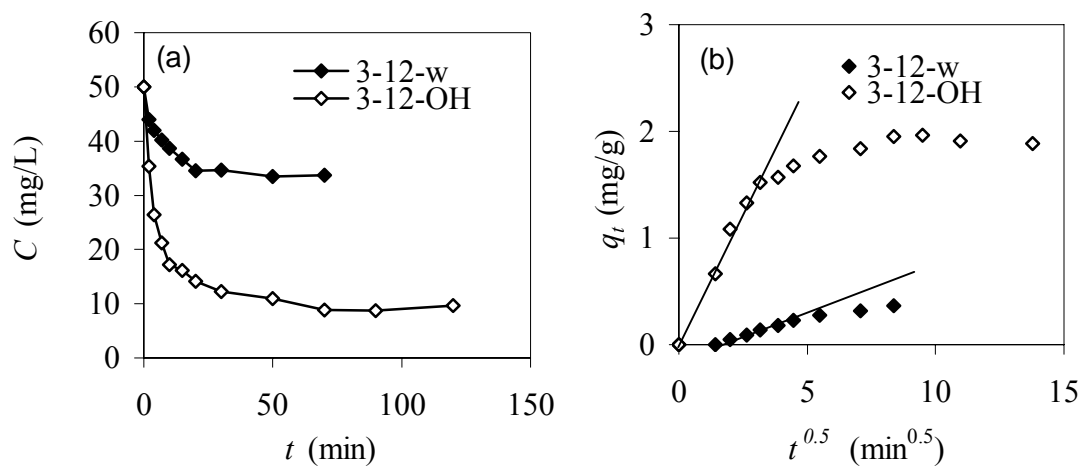
Figure 5.6 Adsorption kinetics of copper ions on the CS/CA blend hollow fiber
membranes 3-12-w and 3-12-OH

The kinetic adsorption results can be analyzed with the various adsorption kinetic

models to reveal the control factors in the adsorption process. For diffusion or transport

controlled adsorption kinetics, the adsorption amount q_t at time t versus $t^{0.5}$ would satisfy

the following equation [153]:

$$q_t = k_d \, t^{0.5} \qquad\qquad\qquad (5.1)$$

where q_t is the amount of copper ions adsorbed (mg/g) at time t (min), and k_d (mg · g^{-1} · min$^{-0.5}$) depicts the intrinsic kinetic rate constant for diffusion-controlled adsorption and is related to the initial concentration of the copper ions in the bulk solution, the specific surface area of the hollow fiber membranes and the diffusion coefficient of the copper ions in this case.

The fitting of Eq. (5.1) to the experimental results in Fig. 5.6a is shown in Fig. 5.6b. The linear relationship of q_t against $t^{0.5}$ is indeed observed for both types of the hollow fiber membranes in the initial stage of the adsorption process. This means that the transport of copper ions from the solution to the adsorption sites on the external and internal surfaces of the hollow fiber membranes was the rate-controlling step in the initial adsorption stage. Since the adsorption was conducted in a batch mode in this study, the diffusion controlled adsorption would be greatly reduced in actual applications where the hollow fiber membranes are usually operated in a filtration mode and the copper ions to be removed can be brought to the binding sites by the convective flow. From the slopes of the straight lines in Fig. 5.6b, the transport-controlled rate constants k_d (mg · g-1 · min$^{-0.5}$) can be calculated to be 0.49 and 0.069 for the hollow fiber membranes 3-12-OH and 3-12-w, respectively. The higher transport-controlled rate constant for the hollow fiber membranes 3-12-OH may be attributed to the much higher CS content or adsorption capacity of the hollow fiber membranes, under which the more rapid adsorption facilitated the transport of copper ions to the adsorption sites on the hollow fiber membranes 3-12-OH than on 3-12-w.

The pseudo first-order and pseudo second-order kinetic models have often been used to fit the experimental adsorption kinetic results to determine whether the overall adsorption rate is dominated by the chemical attachment [154]. The linearized forms of the pseudo first-order and pseudo second-order kinetics models are given in Eq. (5.2) and Eq. (5.3) respectively [154]:

$$\log(q_e - q_t) = \log(q_e) - \frac{K_1}{2.303}t \qquad\qquad (5.2)$$

$$\frac{t}{q_t} = \frac{1}{K_2 q_e^2} + \frac{1}{q_e}t \qquad\qquad (5.3)$$

where q_e is the amount of copper ions adsorbed at adsorption equilibrium (mg/g), q_t (mg/g) is the amount of copper ions adsorbed at time t (min), and K_1 (min^{-1})and K_2 (g · mg^{-1} · min^{-1})) are the rate constants of the pseudo first-order and pseudo second-order kinetics models respectively and the constants are related to the reaction temperatures for a given adsorbent.

Based on Eq. (5.2) and Eq. (5.3), the plots of *log (q_e-q_t)* vs. *t* and *t/q_t* vs. *t* for the two types of hollow fiber membranes for the experimental results in Fig. 5.6 are shown in Fig. 5.7a and Fig. 5.7b, respectively. From Fig. 5.7a, it is found that the pseudo first-order kinetic model could not describe the experimental results. On the contrary, from the linear relationships shown in Fig. 5.7b, it is clear that the adsorption of copper ions on both types of the hollow fiber membranes well followed the pseudo second-order kinetic model (i.e., *t/q_t* vs. *t* gives a straight line), with the linear regression coefficients of $R^2 = 0.999$ for the hollow fiber membranes 3-12-OH and $R^2 = 0.996$ for the hollow fiber membranes 3-12-w.

The results suggest that chemical interaction between the copper ions to be adsorbed in the solution and the functional groups on the hollow fiber membrane surfaces dominated the overall adsorption rate. The pseudo second-order rate constants (K_2) are found to be 0.29 and 0.14 $g \cdot mg^{-1} \cdot min^{-1}$ for the hollow fiber membranes 3-12-w and 3-12-OH respectively. The higher attachment-controlled rate constant for the hollow fiber membranes 3-12-w may be attributed to the larger pore sizes and higher porosities (surface and cross-sections) of the hollow fiber membranes that exposed the adsorption sites to a greater extent for copper ion attachment.
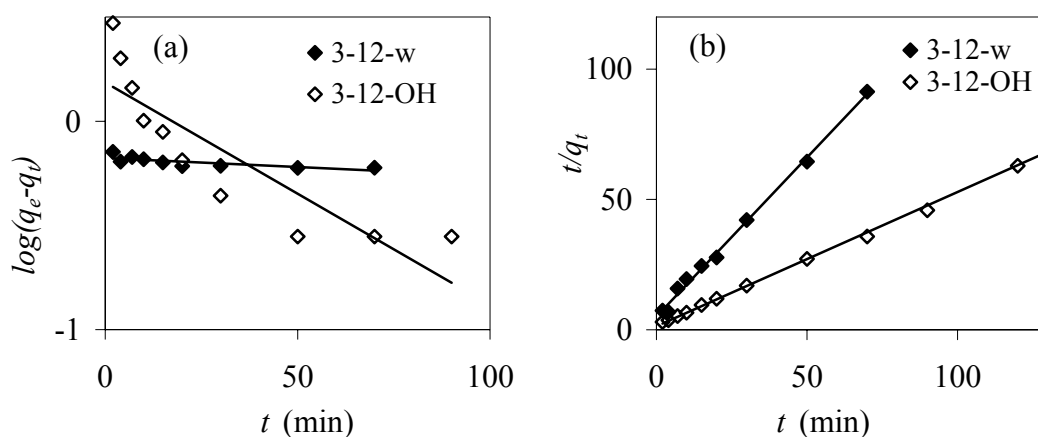
Figure 5.7 Correlating the copper ion adsorption kinetics on CS/CA blend hollow fiber membranes 3-12-OH with pseudo first-order (a) and pseudo second-order (b) kinetics models

5.3.5   Copper ion adsorption at low copper ion concentrations

The adsorption of copper ions at very low initial concentrations (0.28-6.5 mg/L) was investigated with the hollow fiber membranes 3-12-OH. Fig. 5.8 shows the plot of the equilibrium concentration (C_e) versus the initial concentration (C_0) of copper ions in the solution. The results indicate that the CS/CA hollow fiber membranes can effectively reduce copper ion concentrations down to 0.1-0.6 mg/L, a level well below the USEPA

maximum contaminant level for copper ion at 1.3 mg/L for drinking water supply. From the calculation, it was found that the copper ion removal efficiency was higher than 90% in the studied concentration range. The effectiveness of the CS/CA hollow fiber membranes for heavy metal removal at low concentrations has great significance since the traditional methods for metal ion removal, such as chemical coagulation, electrolysis, and adsorption with activated carbon, are usually ineffective or inefficient to remove metal ions to such a low level.
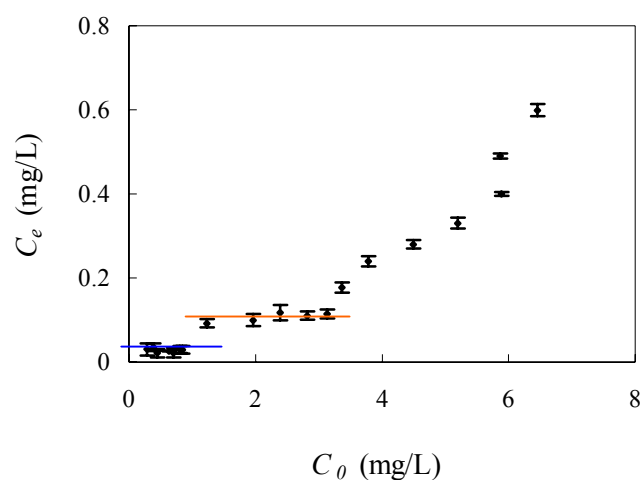
Figure 5.8 Copper ion adsorption at low concentrations (C_0 = 0.28-6.5 mg/L) using the hollow fiber membranes 3-12-OH, showing the equilibrium copper ion concentrations (C_e) versus the initial copper ion concentrations (C_0) in the bulk solution

Particularly, the results in Fig. 5.8 also support the early conclusion in kinetic study that the adsorption of copper ions on the hollow fiber membranes was primarily a chemical adsorption process. If a physical process dominates the adsorption process, the removal is usually reversible and dependent on the equilibrium between the metal concentration in the solution and the metal content on the surface of the adsorbent, and as a result, the process performs poorly at low concentrations in the solution. Thus, the

results were also indirectly confirmed that chemical interaction dominated the adsorption process.

It is interesting to note that there are two plateaus of C_e observed in Fig. 5.8 at the initial concentrations of 0.28-0.84 mg/L and 0.84-3.13 mg/L, respectively. At each plateau, the C_e remained unchanged even though C_0 increased. The presence of the plateaus in the figure is again an indication of the irreversible chemical adsorption phenomenon in the process because the C_e in the solution would increase with C_0 if a reversible physical adsorption process existed as the main adsorption mechanisms. The presence of the two different plateaus may suggest that two different functional groups were possibly involved in the chemical adsorption of copper ions and the first type of functional groups may have slightly higher adsorption energy than the second type of functional groups. From the chemical structures of chitosan and cellulose acetate, it can be possible that the –NH$_2$ and –NH– groups in CS and the –OH groups in CA and CS contributed to these functional groups. It is also observed in Fig. 5.8 that, with the further increase of C_0 at above 3.13 mg/L, C_e increased proportionally as well, suggesting that physical adsorption phenomenon still probably played some roles in copper ion removal in the process.

5.3.6   Adsorption mechanism

To further elucidate the mechanism of copper ion adsorption on the CS/CA blend hollow fiber membranes, XPS analysis was conducted on the hollow fiber membranes before and after copper ion adsorption. From the XPS analysis, the 1s binding energies for the elements of C, O and N at different oxidization states before and after copper ion adsorption are summarized in Table 5.2.

It is clear that all the C 1s and O 1s binding energies did not show significant changes before and after copper ion adsorption because less than 0.5 eV was considered insignificant for nonconductive polymer. Therefore, the results at least indicate that there is no clear evidence to prove that the hydroxyl groups were involved in the chemical adsorption of copper ions on the hollow fiber membranes (unless a noticeable increase in the O 1s binding energy was observed after copper ion adsorption). In contrast, the N 1s binding energy of the CS/CA blend hollow fiber membranes showed significant changes before and after copper ion adsorption.

Table 5.2 XPS C 1s, O 1s and N 1s binding energies of the CS/CA blend hollow fiber membranes before and after copper ion adsorption

Element	Binding Energy (BE), eV		
	Before adsorption	After adsorption	Shift of BE (eV)
C 1s	284.6	284.6	0.00
	286.0	286.3	+0.30
	287.5	287.8	+0.30
O 1s	531.1	531.1	0.00
	532.3	532.4	+0.10
N 1s	399.0	399.7	+0.70
	400.7	401.7	+1.00

Fig. 5.9 shows the N 1s XPS spectra of the hollow fiber membranes before and after copper ion adsorption. Before copper ion adsorption, there are two peaks at the binding energies of 399.0 and 400.7 eV. The peak at the binding energy of 399.0 eV can be attributed to the nitrogen atoms in the $-NH_2$ and/or the $-NH-$ groups of CS and the peak at the binding energy of 400.7 eV to the protonated nitrogen atoms in the $-NH_3^+$ groups of

CS on the surfaces of the hollow fiber membranes [153, 155]. After copper ion adsorption, significant shifts or increases of the binding energies at both peaks are observed (399.0 to 399.7 eV and 400.7 to 401.7 eV, respectively). The increase of the binding energies provide evidence that the N atoms in the $-NH_2$ or $-NH-$ and $-NH_3^+$ were all involved in the adsorption of the copper ions, possibly through forming surface complex in which a pair of lone electrons from the N atoms were shared with the copper ions, which increased the oxidation states and thus binding energies of the nitrogen atoms [153]. It is also noted that the area under the peak at 400.7 eV before copper ion adsorption increased after copper ion adsorption (see the area under the peak at 401.7 eV). The adsorption process seemed to result in some nitrogen atoms in the $-NH_2$ or $-NH-$ groups to form $Cu\cdots NH_3^+-$ complexes when the $Cu\cdots NH_2-$ complexes were formed, which increased the area under the peak at 401.7 eV after copper ion adsorption.
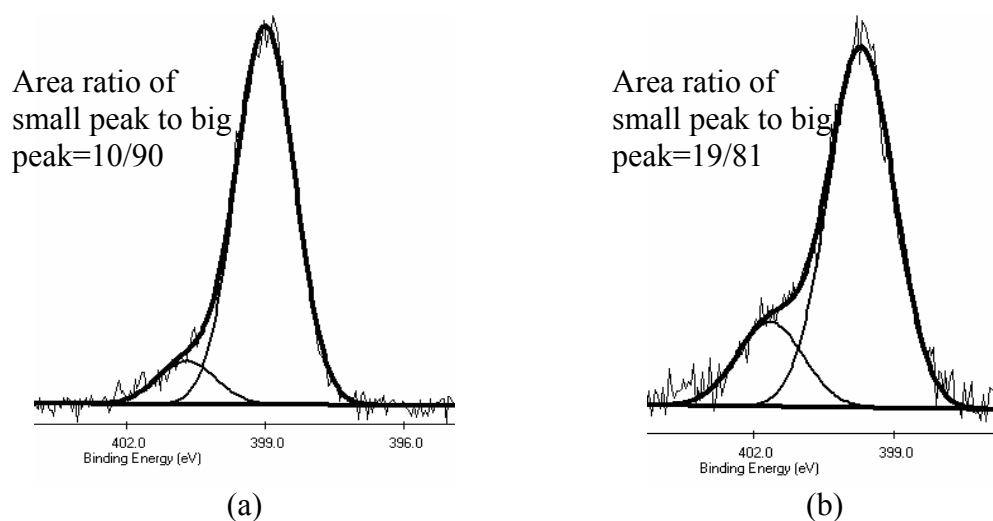
Figure 5.9 Typical N 1s XPS spectra of the CS/CA hollow fiber membranes 3-12-OH before (a) and after (b) copper ion adsorption

5.3.7　Desorption and reuse

For potential practical applications, it is of interest to examine the possibility of desorbing the copper ions adsorbed on the hollow fiber membranes and reusing them. Both EDTA and HCl solutions were examined in the study for hollow fiber membranes 3-12-OH. Table 5.3 shows the results obtained at different concentrations of EDTA and HCl solutions and the corresponding desorption efficiencies. As can be found from the table, the desorption efficiencies increased generally with the concentrations of the EDTA or HCl solutions. Although both EDTA and HCl solutions appeared to be effective for copper ion desorption, the EDTA solution performed much better than the HCl solution and the maximum desorption efficiency reached about 99% with the EDTA solution but only 90% with the HCl solution. In view of the neutral pH value of the EDTA solution, it may be desirable to desorb metal ions from the CS/CA blend hollow fiber membranes with EDTA than HCl solution because CS in the hollow fiber membranes could dissolve in the acid solution.

Table 5.3 Desorption of copper ions from CS/CA blend hollow fiber membranes 3-12-OH
using EDTA and HCl solutions as the desorbents

Desorbent concentration (mM)	EDTA solution		HCl solution	
	pH	Desorption percentage (%)	pH	Desorption percentage (%)
0.01	5.40	2.6	6.09	1.7
0.1	5.38	3.8	4.98	2.2
1	5.34	16.7	3.83	10.9
10	5.21	99.3	2.80	90.2
50	5.13	98.8	2.11	90.5

The desorbed hollow fiber membranes were reused in the next adsorption experiments to examine the effect of the desorption process. Table 5.4 shows the results of adsorption from four adsorption-desorption cycles. It is clear that the adsorptive hollow fiber membranes can be effectively regenerated with 50mM EDTA and reused almost without any significant loss in their adsorption capacity for copper ions. However, for desorption conducted with the 50mM HCl solution, the adsorption capacity reduced significantly after each cycle. This may be attributed to the dissolution of CS from the hollow fiber membranes into the HCl solution (with pH<4) during the desorption tests.

Table 5.4 Reuse of the CS/CA blend hollow fiber membranes 3-12-OH for copper ion adsorption

| Cycle No. | Amounts of copper ions adsorbed (mg/g) | |
	Desorbed with 50 mM EDTA	Desorbed with 50 mM HCl
1	8.74	8.74
2	8.12	4.60
3	8.09	3.57
4	7.96	2.88

As in earlier study, the desorption of copper ions from the blend hollow fiber membranes of 0.5-26.5-OH and 1-26-OH (in Chapter 3) with 50 mM HCl solution was successfully done, and the copper ion adsorption capacity of the regenerated membranes in the following run only showed a maximum reduction of about 25% and no further significant reduction were observed in the subsequent runs. However, the results in the present study showed that the 50 mM HCl solution did not work effectively to regenerate the highly porous hollow fiber membranes 3-12-OH. This may be attributed to the difference in the CA contents in the blend hollow fiber membranes. The CA content in the

fibers 3-12-OH was much lower than that in the fibers 0.5-26.5-OH and 1-26-OH, which resulted in the highly porous structures of the hollow fiber membranes and the porous structures may facilitated the dissolution of CS from the membranes into the HCl solutions in this case.

5.3.8   Elution of copper ion solution using 3-12-OH membrane

Change of copper ion concentration in permeate with filtrated bed volume (bed volume=volume of permeate/volume of membrane) is shown in Fig. 5.10. The breakthrough point occurred at 108 bed volume. The abrupt increasing stage was very short as it lasted only 40 bed volume and this is associated with the fast adsorption kinetics inside the membrane. The saturation capacity was calculated to be 11.13mgCu^{2+}/g. This value is comparable to that of 12.5mg/g at batch mode of adsorption.
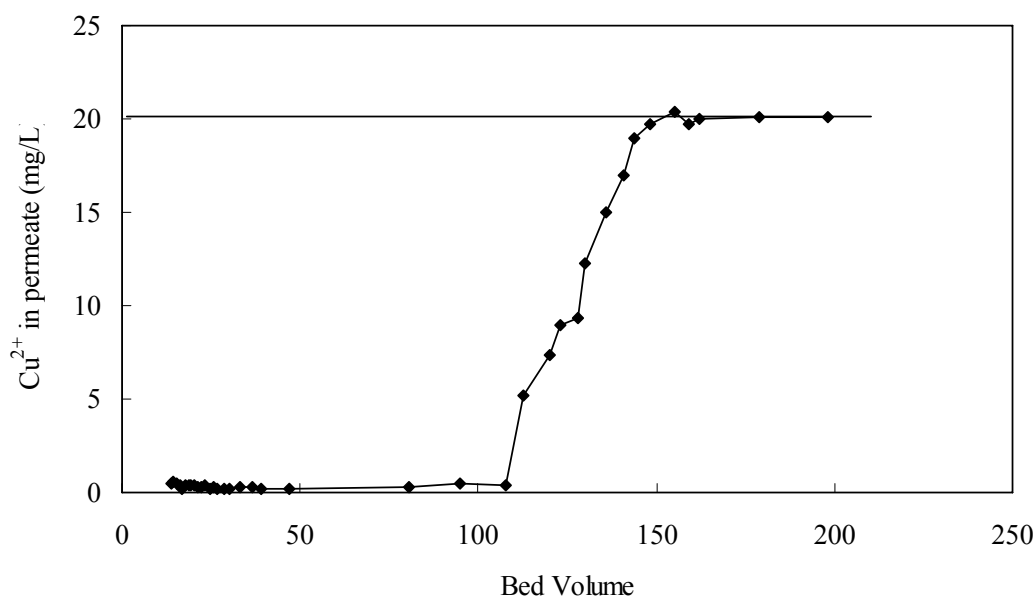
Figure 5.10 Copper ion elution profile using 3-12-OH CS/CA blend hollow fiber membrane

5.4   Conclusions

Highly porous CS/CA blend hollow fiber membranes were examined as adsorptive membranes for removal of copper ions from aqueous solutions. Coagulants with higher alkalinity and higher concentration of CA in the spinning solutions were favorable for preparing CS/CA blend hollow fiber membranes containing higher contents of CS and hence resulting in higher copper ion adsorption capacities. The adsorption study showed that the CS/CA blend hollow fiber membranes had good adsorption capacity (12.5mg/g at batch mode, and 11.13mg/g at filtration mode), fast adsorption rate and short adsorption equilibrium time (<70mins) for copper ions. The CS/CA adsorptive hollow fiber membranes can also work effectively at low copper ion concentrations and were able to reduce the concentration of copper ions in the solution down to a level of 0.1-0.6 mg/L. Copper ion adsorption on the hollow fiber membranes followed the pseudo second-order kinetic model, indicating the importance of chemical adsorption in controlling the adsorption rates. Mechanisms study through the XPS analysis suggested that copper ion adsorption involved forming surface complexes with the nitrogen atoms of CS in the hollow fiber membranes. The copper ions adsorbed on the highly porous hollow fiber membranes can be effectively desorbed in an EDTA solution and the hollow fiber membranes can be reused almost without loss of the adsorption capacity.

Chapter 6 Copper ions coupled CS/CA blend hollow fiber membranes for affinity-based adsorption of bovine serum albumin proteins

Summary

Besides in environmental engineering field, adsorption membrane is also widely used in bioseparation field. This work is therefore to examine the potential of CS/CA blend membrane in bioseparations. To achieve specific separation, membrane must be coupled with a specific ligand. In this work, metal ion ligand (copper ion) was coupled onto membrane through complexation with –NH$_2$ groups on CS polymer. A single component solution containing BSA was studied to investigate the membrane performance. The adsorption experiment was conducted at batch mode. The amount of copper ion ligand tightly coupled on the blend membranes was small (3.9 mg/g or 0.9 mg/ml). However, the maximum binding capacity for BSA was comparable (60 mg/g at pH 7.4 and NaCl concentration 120 mM) to those of other reported adsorptive membranes. Therefore, the copper ion utilization efficiency in this work was very high (15.4mgBSA/mgCu^{2+}). This is possibly due to the more binding arms available for binding proteins on copper ion ligand in this work than in other works. The BSA binding was favored under neutral or slightly basic condition and at low salt concentration. The leakage of metal ion ligand from the membrane during adsorption process was <12.8% in the initial BSA concentration range of 0-4.0 mg/mL.

6.1 Introduction

Immobilized metal ion affinity chromatography (IMAC), introduced by Porath et al. in 1975 [156], has become a popular and powerful chromatographic tool for the separation/purification of proteins and enzymes. The membrane based IMAC, i.e., immobilized metal ion affinity membranes (IMAMs) chromatography, is of particular research interest, due to its higher processing rate than that of the column-based chromatography separation. The current method to prepare the IMAMs normally consist of at least four steps: (1) preparation of base membranes, (2) activation and functionalization of the base membranes, (3) coupling of spacer arms (metal ion chelators such as IDA, NTA) and (4) immobilization of metal ion ligands onto the membranes. The process is therefore complex, time consuming and costly. Moreover, the second step (activation and functionalization of the base membranes) is usually conducted under harsh physical and chemical conditions that can often cause significant damage to the base membrane structures [135]. It is therefore of great research and practical interest to be able to prepare IMAMs in a simpler way and under mild reaction conditions for surface functionalization.

Progress has been made by using cellulose and its derivatives [157-159] and ethylene vinylalcohol copolymer [135] etc, that contain –OH groups on the polymer backbones as the base membrane materials. Although the second stage, i.e., activation and functionalization of the base membranes, in the preparation of IMAMs may be skipped, the reactivity of the –OH groups in these polymers is limited and the coupling of metal ion chelators or spacer arms on –OH groups is still necessary for protein separation. To further

simplify the preparation process, polymers with more reactive functional groups such as -NH$_2$ and –COOH that can bind metal ions ligands directly would be more desirable in the preparation of IMAMs. Chitosan is one of such polymers with abundant free amino groups that can form complexes with various metal ions. Thus, the preparation of IMAMs from chitosan only needs two steps and hence it greatly simplifies the preparation of IMAMs. Recently, a few researches using chitosan as the IMAC support were also reported [60-61]. These studies used chitosan in the bead form that usually has low processing rate.

The objective of this part of study is therefore to evaluate the performance and examine the behavior of the IMAM prepared by complexing a metal ion ligand onto the CS/CA blend hollow fiber membranes for binding proteins. In contrast to commonly used metal ion chelators such as IDA and NTA, which form strong chelate with metal ion ligands, the interaction between CS and metal ion ligand is a weak complexation because it involves only 1-2 binding arms between NH$_2$ and metal ion ligand in the interaction. Therefore, we use word "couple" to replace "immobilization" to indicate the interaction difference. The highly porous CS/CA blend hollow fiber membranes 3-12-OH, prepared in Chapter 5 was used as the base membranes. A typical metal ion ligand, Cu^{2+}, was coupled on the CS/CA blend hollow fiber membranes. The resulting IMAMs (i.e., CS/CA-Cu) were used to adsorb a model protein, bovine serum albumin (BSA), from single species solution in a batch mode. The amount of metal ion ligand coupled, the binding capacity and binding kinetics of BSA were examined. The effect of solution chemistry (pH and ionic strength) on the adsorption behavior was investigated. The possible release of the copper ion ligand from the membranes was also studied.

6.2 Experimental

6.2.1 Materials

The CS/CA blend hollow fiber membranes 3-12-OH were used as the base membranes for preparing the IMAMs. BSA was provided by Sigma and had a MW of 67 KDa. The BSA solutions used in the experiments were prepared by dissolving the solid BSA powder in an acetate or phosphate buffer solution (10 mM), depending on the pH to be controlled.

6.2.2 Coupling with copper ion ligand

1.1 g dry hollow fiber membrane pieces were added into 50 mL of a copper ion solution with an initial concentration of 1g/L and an initial pH of 5. The suspension was shaken at 150 rpm and 25ºC for 2 hours. The high concentration of copper ion in solution was aimed to improve the copper ion coupling amount.

6.2.3 Washing the membrane coupled with copper ion ligand

The blue hollow fiber membranes (referred to as CS/CA-Cu) were washed thoroughly with DI water. This is to wash off the copper ions adsorbed through physical adsorption, which will strip off during BSA adsorption. Then the membrane was washed with 10mM phosphate and acetate buffer solutions and 2M NaCl solutions. This is because BSA adsorption was carried out in buffer solutions with different NaCl concentration. The amount of the copper ions on the fibers was determined by stripping the copper ions with 50 mM EDTA solution and then analyzing their concentration with ICP-OES.

6.2.4   BSA adsorption

BSA adsorptions with CS/CA-Cu were conducted in a batch mode. The BSA adsorption capacity was investigated by suspending 1.1 g of CS/CA-Cu in 50 mL of a BSA solution with an initial concentration in the range of 0.2 to 4.0 mg/mL at an initial pH and NaCl concentration of 7.4 (NaH_2PO_4 /Na_2HPO_4 buffer: 10mM) and 120 mM, respectively. The suspensions were shaken at 25ºC and 150 rpm for 24 hours and the concentrations of BSA in the solutions were determined with a UV-Vis spectrometer at 278 nm.

The adsorption kinetic study was conducted by suspending 1.1 g CS/CA-Cu in 150 mL BSA solution with an initial concentration of 2.5 mg/mL. Other experimental conditions were the same as those in the adsorption capacity study. At desired time intervals, a small amount of solutions was taken out respectively for concentration analyses.

The effects of solution pH and ionic strength on the capacities of BSA adsorption were investigated. The solution pH was adjusted to a level in the range of 4.9-8.0 with different buffer solutions (NaAc/HAc for pH 4-6 and NaH_2PO_4 /Na_2HPO_4 for pH 6-8, both have concentration of 10mM) or the ionic strength was varied in the range of 0-1.8 M by the addition of NaCl into the solution (pH at constant). The initial BSA concentration was 2.5 mg/mL and the other adsorption conditions were the same as those in the capacity study.

6.2.5 Leakage of copper ions during BSA adsorption

It was of interest to examine the possible leakage of the copper ion ligands on the membranes during BSA adsorption. The BSA solutions after the adsorption experiments in the capacity study were analyzed with the ICP to determine the amount of copper ions released into the solutions.

6.3 Results and discussion

6.3.1 Amount of copper ion ligands coupled

The amount of metal ions coupled on the membrane is crucial in determining the capacity of protein adsorption on the IMAMs. In this work, the amount of copper ions coupled on the CS/CA blend hollow fiber membranes was measured to be 3.9 mg/g or (0.9 mg/ml) dry hollow fiber membranes. The value of 3.9mg/g was lower than the amount of copper ions adsorbed on CS/CA-Cu found in Chapter 5 where the adsorption amount was 5.8 mg/g even at a lower copper initial concentration (only 150 mg/L). The difference may be caused by the method used to post-treat the copper ion adsorbed membranes in this work. For IMAMs, the loosely attached copper ions have to be washed off with water and buffers to avoid the contamination of the treated BSA solutions. Therefore, only a portion of the copper ions that had been adsorbed through forming complex remained on the IMAMs. However, for adsorption study in last chapter, the adsorption capacity was calculated from the concentration difference before and after adsorption. Therefore, both loosely and tightly adsorbed copper ions accounted for the adsorption capacity. The presence of loosely adsorbed copper ions may indicate the presence of physical adsorptions. A comparison of the amount of copper ions coupled in this work with those

immobilized on other membranes is shown in Table 6.1. As can be seen, the immobilized amount of copper ions in the literature varies significantly, but most are much larger than that in this study.

Table 6.1 Comparison of copper ions immobilized in literatures

	membrane material	chelate agent	Cu^{2+} capacity	protein	adsorption capacity	metal ion utilization	Ref.
1	glycidyl methacrylate-grafted PE hollow fibers	IDA	70-77 mg/g or 11.5mg/mL	BSA	0.26μM/mL	0.02 μM/mg	[160]
2	epoxidized PSF membrane	IDA	2.6mg/g				[161]
3	hydrophilic copolymer membranes (Sartorius)	IDA	221-248 mg/mL	HSA	60-67mg/mL	0.24-0.30 mg/mg	[162]
4	glycidy-4-oxoheptyllether modified PSF membrane	IDA	0.5-0.8mg/mL				[162]
5	PSF membrane(Sartorius)	IDA	0.9mg/mL				[162]
6	hydroxyethyl-cellulose coated nylon membrane	IDA	0.7mg/mL	lysozyme	21.4mg/mL	30mg/mg	[163]
7	surface modified PE hollow fiber	IDA	96mg/mL	lysozyme	1-8.5 μmol/mL	0.01-0.09 μM/mg	[164]

8	microporus sheets with NH$_2$ groups (Arbor Tech.)	IDA	51.2mg/g				[165]
9	polyglycidyl methacrylate-grafted cellulose membranes	IDA	1.0-7.3 mg/g				[166]
10	PVDF based membranes	IDA	1.9-2.4 mg/mL	lysozyme	3.9-6.1 µM/mL	1.6-3.2 µM/mg	[167]
11	regenerated cellulose membranes	IDA TED	4.88(IDA) 2.48(TED)mg/mL	BSA	0.094(IDA) 0.1(TED) µM/mL	0.02(IDA) 0.02(TED) µM/mg	[157]
12	regenerated cellulose membranes	IDA	7.7mg/mL				[158]
13	poly(2-hydroxyethyl-methacrylate) membranes	CB-F3GA	0.36mg/mL	lysozyme	2.8mg/mL	7.6mg/mg	[168]
14	poly(2-hydroxyethyl-methacrylate)/chitosan networks	PBMX5BR	15mg/mL	lysozyme	128mg/mL	8.5mg/mg	[169]
15	regenerated cellulose membranes	CB3GA CR3BA	1.0(CB3GA) 2.8(CR3BA) mg/mL	lysozyme	0.64(CB3GA), 1.03 (CR3BA) µM/mL	0.59(CB3GA),0.37(CR3BA)µM/mg	[157]
16	cellulose membranes	imidazole	38.8mg/mL	HAS	9.25mg/mL	0.24mg/mg	[170]
17	chitosan/cellulose acetate blend hollow fibers	chitosan	3.9mg/g	BSA	60mg/g or 13.8mg/mL	15.4mg (0.24µM)/ mgCu^{2+}	This work

6.3.2   Nonspecific and specific binding of BSA

Nonspecific binding is always present in the chromatography technology, particularly on the hydrophobic surfaces, and is undesired for selective separation. The nonspecific and specific bindings of BSA on CS/CA and CS/CA-Cu blend hollow fiber membranes are shown in Fig. 6.1. As can be observed, the nonspecific adsorption on the CS/CA blend hollow fiber membranes was less than 9 mg/g under the conditions studied. The nonspecific binding may be resulted from the electrostatic and hydrophobic interactions between the BSA and CS/CA membrane surfaces.
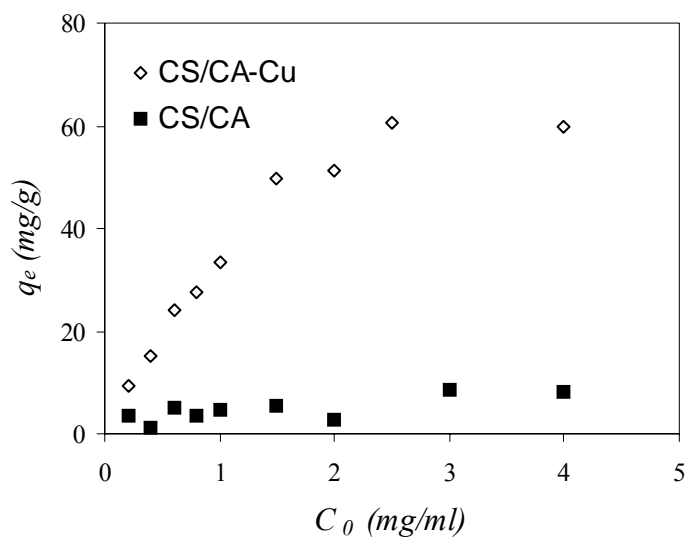
Figure 6.1 Adsorption of BSA on CS/CA and CS/CA-Cu blend hollow fiber membranes

After coupling with Cu^{2+}, the binding capacity of BSA on CS/CA-Cu was much greater than that on CS/CA. The amounts of BSA on CS/CA-Cu increased almost linearly with the increase of the initial BSA concentration in the range from 0.2 to 2.5 mg/mL, and then approached a plateau with further increases in the BSA concentration. The saturation

capacity reached about 60 mg/g or 13.8 mg/mL in this case (see Fig. 6.1). This is comparable to that of many other reported affinity membranes.

The binding of BSA on CS/CA-Cu not only involves specific binding that took place between Cu^{2+} and BSA, but also involves nonspecific binding that took place between CS and BSA. However, as BSA binding by CS/CA was very small in amount (<9mg/g), we can say that specific binding between Cu^{2+} and BSA dominated the BSA binding on CS/CA-Cu.

The binding of BSA on CS/CA-Cu is mainly associated with copper ion coupled on the membranes. The binding mechanism between copper ion ligand and BSA is described as followings. Usually, one copper ion ligand has six binding arms and several of them may form complex with metal ion chelator (NH_2 in this case). The remained binding arms are therefore available for binding proteins. The number of remained binding arms determines the protein binding capacities. After calculation, it was found in this work that averagely 68 Cu^{2+} bond to every one BSA molecule. This is possible because one BSA molecule contains numerous binding sites (imidazole groups) along the molecular chain.

6.3.3 Copper ion ligand utilization

Although the amount of metal ion ligands (copper ion) coupled on the CS/CA blend hollow fiber membranes was lower than many others reported in the literature (see Table 6.1), the BSA adsorption capacity of CS/CA-Cu was comparable or even higher than those of IMAMs in the literature. Therefore, the utilization of copper ions in this work appears to be high. The utilization of metal ion ligands is defined as the amount of protein bond on

per unit mass (or molar) of metal ion ligands [157]. In this study, the copper ion utilization was calculated to be 15.4mgBSA/mgCu^{2+} (or 0.24μMBSA/mgCu^{2+}) which is indeed obviously higher than many of the reported values for metal utilization in the literature (see Table 6.1). This may be due to the reduced effect of the steric hindrance on protein adsorption (large molecules) at lower metal ion ligand densities. Another contributing factor may be the copper ions bonded on –NH$_2$ can provide higher number of binding sites for proteins than the copper ions bonded on strong chelators such as IDA and TED. This will be further discussed in the latter part of this chapter.

6.3.4   Adsorption isotherms

Two commonly used adsorption isotherm models, the Langmuir (Eq. (3.2)) and Freundlich isotherm (Eq. (3.3)) models were used to fit the experimental results of BSA adsorption on the CS/CA-Cu hollow fiber membranes. The plots of $1/q_e$ against $1/C_e$ and $logq_e$ against $logC_e$ are shown in Fig. 6.2. It is found that the Langmuir model can fit the experimental data reasonably well, giving the R^2 value of 0.9846. The experimental data, however, could not be correlated well with the Freundlich model as the R^2 value was only 0.8632. This may be due to the fact that the copper ions were the main binding sites for BSA and hence a homogeneous binding energy may be present on the membranes surfaces. This also suggests that the adsorption of BSA on CS/CA-Cu fibers may be a monolayer adsorption rather than multi-layer adsorptions. The values of the maximum adsorption capacity (q_m) and the adsorption equilibrium constant b are calculated to be 66.2 mg/g and 4.44×10^{-3} L/mg, respectively. The calculated maximum adsorption capacity is very close to the experimental saturation value of 60 mg/g in Fig. 6.1. The maximum capacity is also comparable to most of other IMAMs reported.
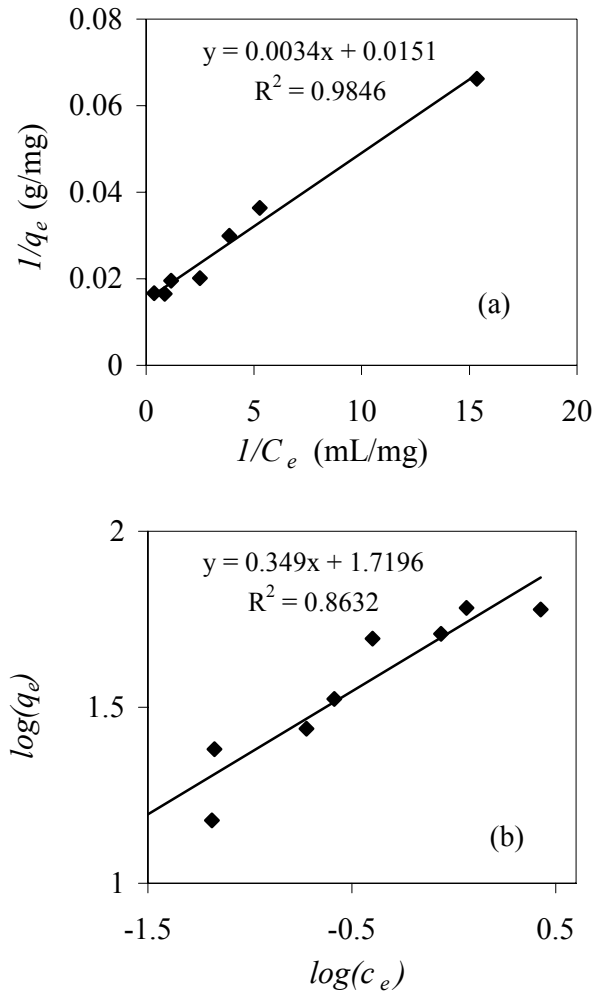
Figure 6.2 Correlation of BSA adsorption on the CS/CA-Cu blend hollow fiber membranes with the Langmuir isotherm model (a) and the Freundlich isotherm model (b)

6.3.5 Effect of solution pH on BSA binding

In general, the adsorption of protein on the IMAC (Immobilized Metal ion Affinity Chromatography) is governed by the coordination of metal ions with electron-donor atoms or groups exposed on the surface of the proteins [171-172]. Hence, the liquid phase pH would have an important effect on the protein binding capacity. Fig. 6.3 shows the effects of solution pH values on the BSA amounts adsorbed on the CS/CA-Cu hollow fiber membranes from the experiments. The ionic strength (i.e., NaCl concentration) was kept

constant at 120 mM for all the experiments in this part. It was observed in Fig. 6.3 that the binding amount increased remarkably from 35mg/g to 58mg/g with the increase of solution pH from 4.9 to 6.6 and then approached a plateau level with further increase of pH from 6.6 to 8.0. Therefore, the adsorption was favored under neutral or slightly basic conditions.
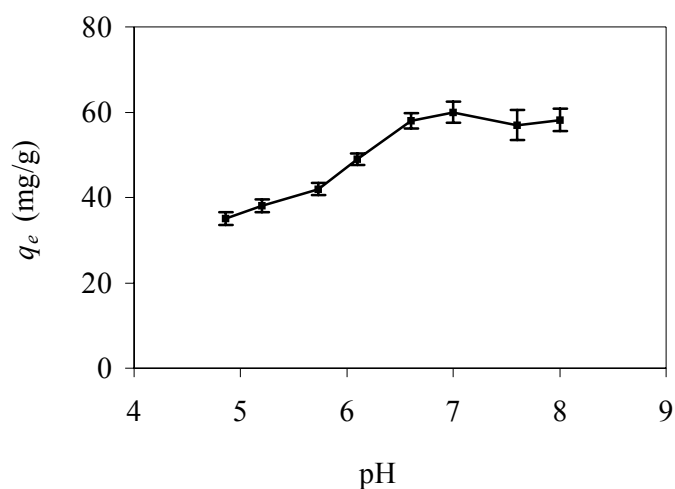
Figure 6.3 Effect of solution pH on BSA binding amounts on the CS/CA-Cu blend hollow fiber membranes. NaCl concentration was 120 mM

The dependency of binding amount on pH can be explained by the interaction between copper ions and BSA molecules. The affinity interaction between copper ions (electron acceptors) and imidazole nitrogens (electron donors) on BSA surfaces dominates the binding. With increasing pH from 4.9 to 6.6, the imidazole nitrogen (pKa=6.95 [173]) on BSA surface became less protonated and therefore the affinity interaction with copper ions was favored. However, with further increasing solution pH, the affinity interaction was no longer changed as imidazole nitrogens were already fully deprotonated under the basic conditions, leading to unchanged binding amount.

The trend of BSA binding amount with solution pH in this work is similar to that reported in [157] where the maximum adsorption capacity was found to occur at 7.4-8.4 for BSA adsorption on Cu-IDA modified cellulose membranes. However, the result in this work is a bit different from other reports. In references [60-61], BSA was adsorbed onto chitosan coated silica gels which were immobilized with copper ions. The optimum pH for maximum binding amount in these two references was at pH 5 or 6 respectively, and with further increasing the solution pH the binding capacities decreased significantly. The result in this work is also different from that reported in [174] where the BSA binding capacity increased almost linearly with solution pH from 5.5 to 9 and then decreased with pH. In general, it seems that there always is an optimum pH or pH range at which the adsorption capacity is the highest. However, the optimum pH is different for one report to another, possibly due to the different buffer solutions (acetate or phosphate or others) or ionic strengths or support materials used in various studies.

6.3.6   Effect of ionic strength on BSA binding

The dependency of BSA binding on the ionic strength of the solution for CS/CA and CS/CA-Cu was examined at pH of 7.4 and initial BSA concentration of 2.5 mg/mL. The results are shown in Fig. 6.4. Clearly, the specific binding amounts of BSA on the CS/CA-Cu fibers decreased with the increase of the ionic strength. For the ionic strength from 0 to 1.2 M, the adsorption amounts of BSA on CS/CA-Cu decreased from about 60mg/g to only 28 mg/g. With the further increase of ionic strength to 1.8 M, the adsorption amount decreased slowly and seemed to reach a minimum of 24.5mg/g.
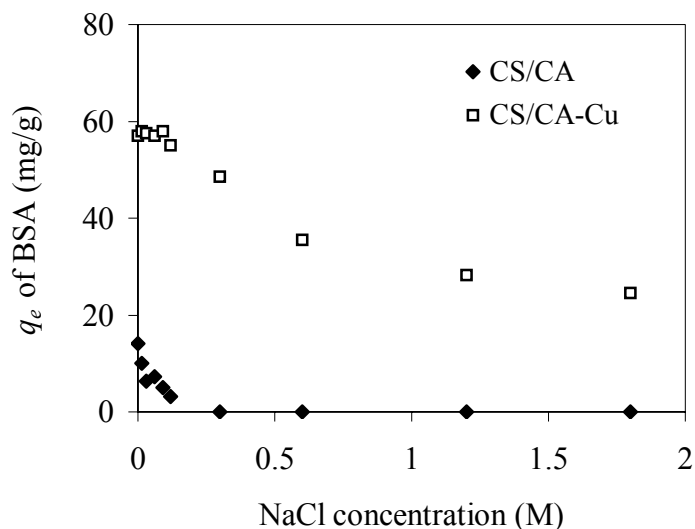
Figure 6.4 Effect of ionic strength (NaCl concentration) on the BSA bindings on the CS/CA and CS/CA-Cu blend hollow fiber membranes. Solution pH was 7.4

The nonspecific binding amount of BSA on CS/CA hollow fiber membranes also decreased with the increase of the ionic strength. When NaCl concentration was 0.3 M or above, the nonspecific adsorption amount was reduced to zero. Hence, increasing the ionic strength of the solution can be an effective way to suppress or eliminate the nonspecific bindings of BSA on CS/CA hollow fiber membranes.

At pH 7.4, donor–acceptor interaction is the primary force of adsorbing BSA on CS/CA-Cu. However, addition of NaCl at a high concentration would cause the free coordination sites to be pre-occupied by anions, leading to the reduced adsorption amount. [173]. The decrease of nonspecific binding, which is always present, also leads to the decrease of binding on CS/CA-Cu. The decrease of nonspecific binding on CS/CA may be caused by the reduction of the attraction force between negatively charged BSA and

positively charged groups on CS/CA (PI=8.5, determined by Z-potential) with increasing

salt concentration.

6.3.7   BSA binding kinetics

The change of BSA concentration in the bulk solution with adsorption time is shown

in Fig. 6.5. The adsorption equilibrium was achieved in about 10 hours. In comparison

with copper ion adsorption on similar type of fibers (see Chapter 5), the BSA adsorption

was much slower. This may be due to the larger size of BSA molecules than copper ions,

which resulted in lower molecular diffusion rates for BSA adsorption on CS/CA-Cu. In

comparison with the adsorption of BSA on commercialized chitosan resins [45], the

adsorption kinetics in this work is much faster because the chitosan resins need several

days to reach adsorption equilibrium.
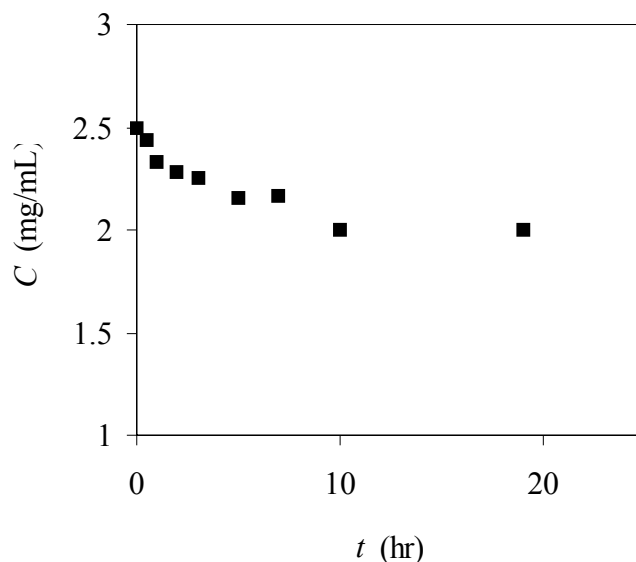
Figure 6.5 Change of BSA concentrations (*C*) in the bulk solution with adsorption time (*t*)
with the CS/CA-Cu hollow fiber membranes as the adsorbent

The pseudo first-order and pseudo second-order kinetic models were applied to analyze the adsorption kinetics (See Eq. (5.2) and Eq. (5.3)). The plots of $log(q_e-q_t)$ agaisnt t and t/q_t against t are shown in Fig. 6.6. The linear regression coefficients (R^2) for these two models were 0.9049 and 0.9657, respectively. Therefore, the adsorption of BSA on the CS/CA-Cu blend hollow fiber membranes can be better correlated with the pseudo second-order kinetics model. This indicated that the chemical interaction between BSA and the CS/CA-Cu surface played an important role in the adsorption kinetics. The adsorption rate constant, K_2, was calculated to be 3.8×10^{-3} g/mg·hr. The constant value is much lower than that (0.14 g/mg·min or 8.4 g/mg·hr) for copper ion adsorption on the same hollow fiber membranes in last chapter.
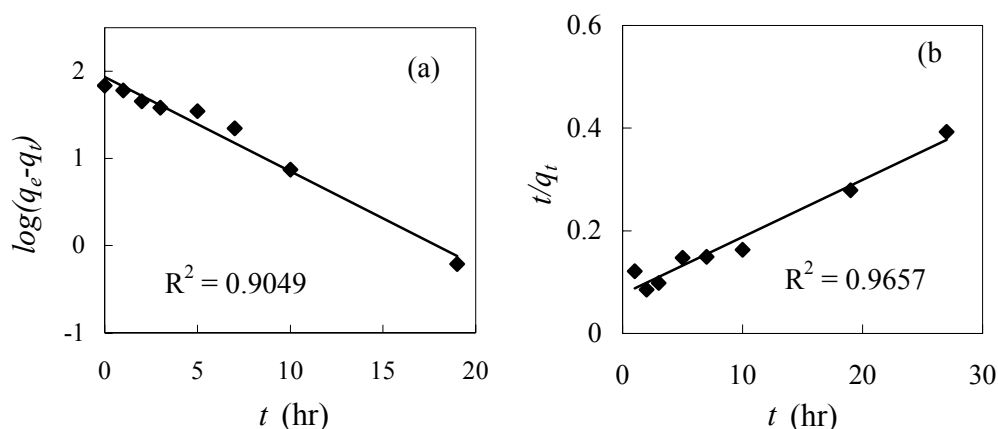
Figure 6.6 Correlating the BSA adsorption kinetic data on the CS/CA-Cu blend hollow fiber membranes with the pseudo first-order (a) and pseudo second-order (b) kinetics models

6.3.8   Copper ion leakage

Leakage of metal ion ligands is often observed in IMAC due to the affinity interactions among the immobilized metal ions and the protein in the solution. The leakage of metal ion ligands is undesired because it causes the loss of the capacity of

IMAC for a long-term use, even though the released metal ions can be removed from the treated solution by post-treatment with a column packed with strong chelating adsorbent such as tris-carboxymethyl ethylene diamine (TED) [175].

The amount of leaked metal ions is affected by both the affinity strength between the metal ions and the chelators and the affinity strength between the metal ions and proteins. Multidentates (tridentate, tetradentate, and pentadentate) are the most frequently used chelators, which can provide 3, 4 and 5 binding sites to the metal ions respectively. Due to the strong binding strength, they could induce high stability of metal ion ligands and hence low metal ion leakage. However, the number of available coordination sites on the metal ions left for the binding of proteins (the total binding sites on each metal ion is usually 6) will be small and hence a low protein binding capacity would be resulted in [172]. In contrast to these strong chelators, the weak metal ion chelators (for example, -NH$_2$ in this case) may provide less number of binding sites to metal ions and, therefore, more binding sites would be available on the metal ions for the binding of more proteins. However, the metal ions could be subject to leakage from the weak chelators due to the weak binding strength between them. In the case of CS/CA-Cu hollow fiber membranes, the weak chelator, –NH$_2$ groups may only function as a mono-dentate or di-dentate for copper ions as proposed by other researcher [176]. Therefore, it is reasonable that high metal ion utilization is achieved with Cu^{2+} as shown in earlier study. However, the study of leakage behavior of the copper ions from the CS/CA blend hollow fiber membranes has practical importance for the actual application of the IMAMs.
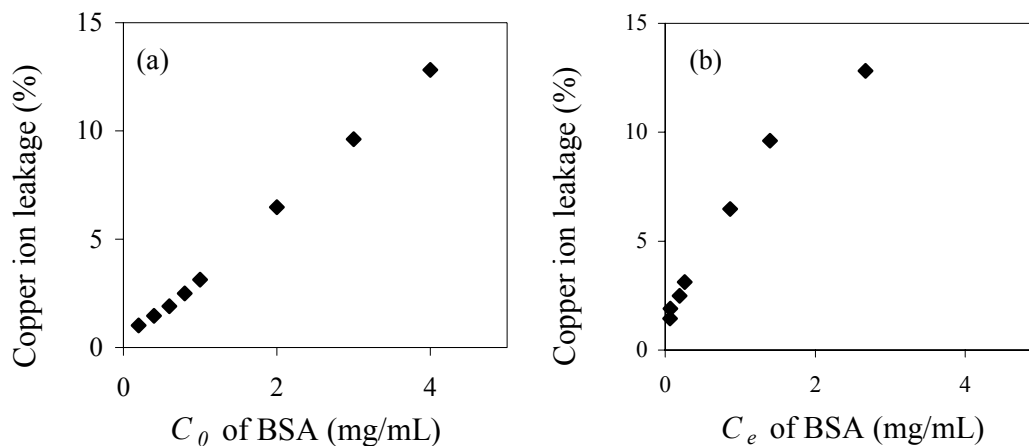
Figure 6.7 Copper ion leakages from CS/CA-Cu hollow fiber membranes during BSA adsorption

The percentage of copper ions released from the CS/CA-Cu hollow fiber membranes during adsorption is shown in Fig. 6.7. The leakage was found to be 12.8% at an initial BSA concentration up to 4 mg/mL. It appears that the released amount of copper ions was dependent on the BSA concentrations, with an almost linear relationship with C_0 in the concentration range studied (see Fig. 6.7a). The amount also appeared to increase with the equilibrium BSA concentrations C_e (see Fig. 6.7b). However, a comparison of the 12.8% leakage with other cases has not been possible due to no such data being reported. Ideally, leakage of immobilized metal ions from the column in the chromatographic operation should be minimized. This has been emphasized by Porath et al. [156] who advocate either charging the chelate column to about 2/3 of its capacity for the metal ion in question or using a capture column to scavenge any metal ion that may leak from the separation column.
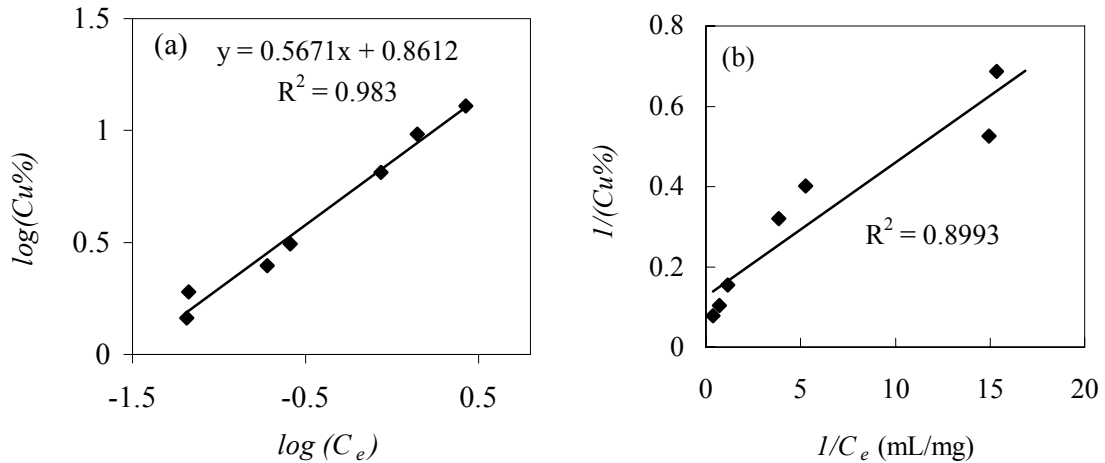
Figure 6.8 Correlation of the copper ion leakages from the CS/CA-Cu blend hollow fiber membranes with the Freundlich (a) and Langmuir (b) isotherm models

Since the copper ion leakage from the CS/CA-Cu blend hollow fiber membranes was dependent on the BSA concentration, models were used to correlate the copper ion leakage with the BSA concentration. It is interesting to find that the adsorption isotherm model, i.e., the Freundlich model, can fit the experimental results quite well, giving the linear regression coefficient of R^2=0.983 (see Fig. 6.8a). The Langmuir isotherm model is however not able to correlate the experimental data with the BSA concentrations well (see Fig. 6.8b) as the linear regression coefficient R^2 was only 0.8993. The fitness with Freundlich model could be attributed to the competition between the stripping of copper ions by BSA in solution and the binding of the copper ions on the membrane surfaces by forming complex or chelates with –NH$_2$. The n value in the Freundlich model was 1.8 and greater than 1 ($1/n<1$), indicating the leakage of copper ions will reach a saturation value when the BSA concentrations are further increased. The K_f was calculated to be 7.26 (mg/mL)$^{1.8}$.

6.4 Conclusions

This work evaluated the adsorption performance of BSA on a new and low cost IMAMs prepared by directly coupling of copper ion ligands onto the CS/CA blend hollow fiber membranes. The amount of tightly coupled copper ion ligands forming complex with $-NH_2$ on the hollow fiber membranes was found to be 3.9 mg/g. The BSA binding amount was 60 mgBSA/g at a pH of 7.4 and a NaCl concentration of 120mM, and is comparable with those in the literature. The nonspecific binding amount of BSA on CS/CA under the same reaction conditions was generally lower and at less than 9 mg/g and it can be totally suppressed or eliminated by increasing the ionic strength of the solution to a certain level. The study also showed that the IMAMs had much higher binding capacity under neutral or slightly basic conditions (pH 6.6-8) and at low NaCl concentration. The adsorption isotherm at pH 7.4 and 25°C followed the Langmuir isotherm model reasonably well and the adsorption capacity was calculated to be 66.2 mg/mL. The kinetic study showed that the adsorption reached equilibrium in 10 hours under the studied conditions and the adsorption rate could be correlated satisfactorily with the pseudo second-order kinetic model. The leakage of copper ions from the hollow fiber membranes was found to increase with the BSA concentrations but would reach a limit. It is found that the leakage of copper ions with BSA concentrations can be described by the Freundlich isotherm model. The results demonstrated the potential to use copper ions immobilized CS/CA hollow fiber membranes as an economical IMAM for practical application in protein separation/concentration.

Chapter 7 Surface modification of CS/CA blend hollow fiber membranes with Cibacron Blue F3GA dye for improved adsorption performance in heavy metal ion removal

Summary

As copper ion adsorption in Chapter 5 by highly porous CS/CA blend membranes still had drawbacks of low capacity and poor reusability with HCl as desorbent, the membrane was modified with other chemical to overcome these problems in this part of the work. The chemical adopted as modifying reagent in this work was Cibacron Blue F3GA (CB) dye, which is cheap and abundant in $-SO_3^-$ groups. CB dye was covalently coupled onto membrane via nucleophilic reaction. The maximum coupling amount of CB dye was 89mg/g. Zeta-potential analysis showed the dyed membranes had negative Zeta potential values in both acidic and basic solutions, which favors cationic metal ion adsorption. It was found dyed membrane possessed higher adsorption amount than unmodified membrane at low copper ion concentration (<150mg/L) as well as at low solution pH. After modification, HCl can successfully desorb copper ion without causing significant loss of adsorption capacity in subsequent runs. Another significant improvement after modification was the much higher adsorption rate observed for modified membrane. It was proposed that most of the improvement observed for copper ion adsorption was associated with the introducing $-SO_3^-$ groups onto membrane.

7.1 Introduction

In the case of heavy metal ion removal, it is often desirable to enhance the CS/CA blend hollow fiber membranes with high adsorption capacity, good chemical stability for use in acid solution, and regeneration with acid solution. Moreover, the CS/CA blend hollow fiber membranes can be easily chemically modified to improve the properties and performances due to the presence of reactive functional groups of $-NH_2$ and $-OH$. Therefore, surface modification of the membrane was conducted in this research.

Coupling of dyes has been one of the common methods for surface modification because dyes are usually cheap, versatile, easy for coupling, and highly durable [177]. In the separation and purification field, dyes are usually coupled on the chromatographic support and function as specific ligands for selective separation of proteins. In recent years, dye-modified supports are also used in the field of water treatment as cheap and stable adsorbents to adsorb or selectively separate heavy metal ions. Dye coupling using Cibacron Blue F3GA (CB) is one of the most widely studied methods because of the high number of reactive functional groups on the dye molecules. CB dye is a monochlorotriazine dye (see Fig. 7.1), and each molecule contains 3 sulfonic acid groups and 4 primary and secondary amino groups. These functional groups can function as ion exchangers (sulfonic acid groups) or metal ion chelators (amino groups). CB dye coupling usually results from the nucleophilic reaction between the chloride of the triazine ring and the hydroxyl and amine groups on the support. CB dye has been coated on support with surfaces bearing $-OH$ groups, such as, poly(ethylene glycol dimethacrylate-hydroxyl-ethyl methacrylate) microbeads [178], polyethylene glycol methacrylate gel beads [1798],

polyvinylbutyral microbeads [180], polyhydroxyethylmethacrlate microbeads [181], microporous polyvinylbutyral based affinity membrane [141], poly(2-hydroxyethyl methacrylate) sheets [182], polyvinylalcohol sheets [142], polyvinylalcohol coated polypropylene hollow fiber membranes [183], via the nucleophilic reaction. These beads or membranes before dye coupling have no metal ion binding capacity. Surface modification with CB dye has been found to improve the adsorption capabilities greatly. Fast kinetics was also usually observed for these adsorbents.
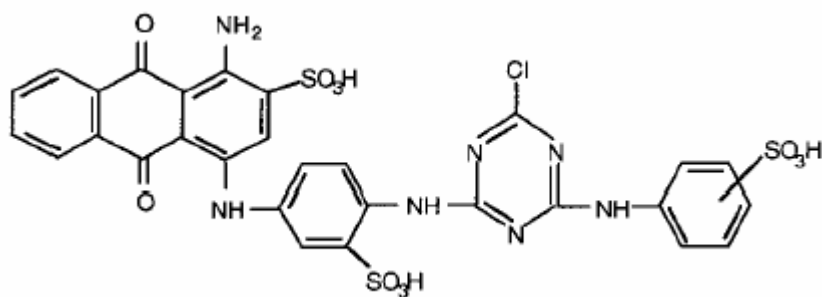
Figure 7.1 Schematic chemical structure of Cibacron Blue F3GA

In this study, CB dye was used as modifying reagent for CS/CA blend membrane to improve the performance of the membranes in heavy metal ion removal. A typical metal ion, copper ion, was again examined in this study. The highly porous CS/CA blend hollow fiber membranes 3-12-OH was employed as the base membranes. The adsorption amount, kinetics, effect of pH on adsorption and reuse of the membrane for membranes before and after dye modification were in detail studied and the results were compared.

7.2　Experimental

7.2.1　Materials

The CS/CA blend hollow fiber membranes 3-12-OH was used as the base membranes. Cibacron Blue F3GA was purchased from Sigma-Aldrich and the molecular weight was 774.2 g/mol.

7.2.2　Coupling of CB dye onto CS/CA blend hollow fiber membrane

CB dye was covalently coupled onto the membrane surface through nucleophilic reaction involving –Cl atoms on CB dye and –OH/NH$_2$ groups on membrane. The reaction scheme is shown in Fig. 7.2. To facilitate the reaction, the reaction was conducted at high temperature (80ºC) and under basic condition (0.2M Na$_2$CO$_3$).

Specifically, the dye solution with a concentration of 10mg/mL was first prepared. Then a 1 g amount of CA/CS hollow fiber membrane pieces were added in 88 mL of the dye solution and the mixture was shaken at 60ºC for 1 hour. Then, sodium chloride (NaCl) was added (1M) to salt out the dye. The dye deposited as a solid layer on the membrane surfaces. The solid dye layer has high concentration and hence can increase the amount of dye to be loaded on the membrane [51], although the reaction may be slowed down due to the solid state of both dye and substrate. After 2 hours, the solution temperature was increased to 80ºC and sodium carbonate (Na$_2$CO$_3$) was added into the suspensions (0.2M) to increase the pH and accelerate the covalent coupling of dye. The coupling reaction was allowed for 1 hour.
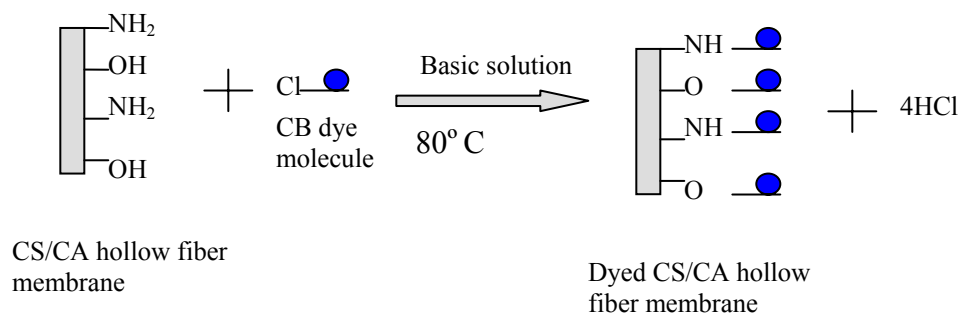
Figure 7.2 Schematic illustration of reaction between CB dye and CS/CA hollow fiber membrane

After the reaction, the suspension was cooled down to room temperature. The dyed hollow fiber membranes were separated and washed extensively with DI water until no dye was detected by the UV spectrometer at 610 nm. The water on the dyed hollow fiber membranes was exchanged with 1-propanol and 1-heptane successively. Then the membranes were dried in the air.

7.2.3   Characterization of the hollow fiber membranes

FTIR and XPS analysis were conducted for CB dye and CS/CA blend hollow fiber membranes before and after dye coupling. The analysis methods have been described in Chapter 2 and Chapter 5, respectively.

The amount of CB dye loaded was determined through analysis with UV spectrometer [51]. The standard curve was prepared from solutions with 0, 1.4, 1.8, 2.2, 2.6, and 3.0 mg of dye added into 5 mL of 12 M hydrochloric acid (HCl), respectively. The suspensions were shaken at 60°C for 15mins. The dye solutions became red, indicating reaction between the blue dye and HCl occurred. The clear and red solutions were allowed to cool

down at room temperature. 5 mL of DI water was then added into each solution to dilute the HCl solution to 6 M. The absorbance at 505 nm for each solution was measured using the UV spectrometer and a graph of absorbance against the dye concentration was plotted. Then, 3mg of the sample, i.e., dyed hollow fiber membranes, was added to 5 ml of 12M HCl at 60°C for 15 mins. Both the CS/CA hollow fiber membranes and the dye on the membranes were dissolved and red clear solutions were formed. The absorbance of the sample solution and blank solution at 505nm was noted and checked against the calibration curve to determine the amount of dye loaded on the hollow fiber sample.

Zeta potential measurements were made to quantify the magnitudes of the zeta potentials of the fibers in aqueous solutions with different pH values. Both the dyed and undyed CS/CA blend hollow fiber membranes were embrittled in liquid nitrogen and subsequently grounded into powder. Then, the fiber powders were added into DI water and the mixtures was sonicated for 4 hours. Finally, the suspensions were filtered through a buchner funnel to remove the large (>11μm) fragments, and the filtrates were used for zeta potential analysis. Prior to analysis, the pH of the filtrate samples was adjusted to the required value, by the addition of dilute HCl and NaOH. The zeta potentials were determined by a Brookhaven Zeta Plus4 Instrument.

7.2.4 Adsorption studies

Both dyed and undyed hollow fiber membranes were tested for their adsorption capacities for copper ions. A 67 mg amount of hollow fiber membrane pieces was suspended into 50 mL of a copper ion solution, with a concentration varying in the range of 10-150 mg/L. The initial pH of the copper ion solution was adjusted to 5 using 0.01M HCl or NaOH solutions. The fiber-loaded suspensions were then shaken in a water bath

shaker at 150 rpm and 25ºC for 2 hrs for the adsorption equilibrium to be reached. The final copper ion concentrations in the solutions were determined by ICP-OES. The adsorption amount was calculated from the concentration difference before and after copper ion adsorption.

Both dyed and undyed hollow fiber membranes were examined for their kinetic adsorption performances. A 150 mg amount of dried hollow fiber membrane pieces were suspended into 50 mL copper ion solution with the initial concentration of 150 mg/L. The initial pH of the copper ion solution was also adjusted to 5. The fiber-loaded suspensions were then shaken in a water bath shaker at 150 rpm and 25ºC. At desired time intervals, a small amount of sample was taken out for determining copper ion concentration through ICP-OES analyses.

To examine the effect of pH on the adsorption amount, the pH of the copper ion solutions were adjusted to a value in the range of 2-5 with the addition of 0.01M HCl and NaOH solutions. The initial concentrations of all the copper ion solutions was 150 mg/L. A 150 mg amount of dried hollow fiber membrane pieces was suspended into 50 mL of a copper solution. The suspensions were shaken at 150 rpm and 25ºC for 2 hours to ensure full adsorption equilibrium. The final copper ion concentrations in the solutions were determined by ICP-OES.

7.2.5   Regeneration and reuse of the hollow fiber membranes

The dyed CS/CA blend hollow fiber membranes after copper ion adsorption were regenerated with 50mM EDTA or 50mM HCl solutions. 150 mg hollow fiber membranes from the kinetics studies were suspended in 50 mL of the solution and shaken at 150 rpm

and 25ºC for 30mins. After desorption, the fibers were separated and first neutralized with NaOH solution, and then extensively washed with DI water. The regenerated hollow fiber membranes were reused to adsorb copper ions again. The cycle of adsorption-desorption was repeated for 4 times.

7.2.6   Competitive adsorption

A solution containing Cu^{2+}, Pb^{2+}, Cd^{2+}, and Hg^{2+} ions, each having a concentration of 1mM, was prepared and the initial pH of the solution was adjusted to 5. A 50mg amount of dried hollow fiber membrane pieces were suspended in 50 mL of the metal ions mixture solutions in a flask and the content of the flask was shaken at 150 rpm and 25ºC for 2 hours. The concentration of each metal ions in the solution was determined by ICP-OES.

7.3   Results and discussion

7.3.1   FTIR and XPS analysis

FTIR and XPS analyses were conducted to verify the expected covalent coupling of CB dye on the hollow fiber membranes and the actual functional groups on membranes involved in the coupling reactions. The FTIR spectra of CB dye and CS/CA blend hollow fiber membranes before and after dye coupling are shown in Fig. 7.3. The spectrum for the dyed hollow fiber membranes, as compared to those of the undyed hollow fiber membranes, shows two new peaks at 1504.4 cm^{-1} and 1566.1 cm^{-1} which are characteristic peaks of CB dye [184], indicating the presence of CB dye on the hollow fiber membranes. After dye coupling, the peak at 1164.9 cm^{-1} for the C-O-C groups on the undyed hollow fiber membranes was shifted to 1157.2 cm^{-1} which is attributed to the asymmetric

stretching of S=O on CB dye [179], suggesting the introducing of CB dyes to the hollow fiber membranes and the coupling reaction affected the C-O-C groups on the hollow fiber membranes and the –SO₃H groups of CB dye.
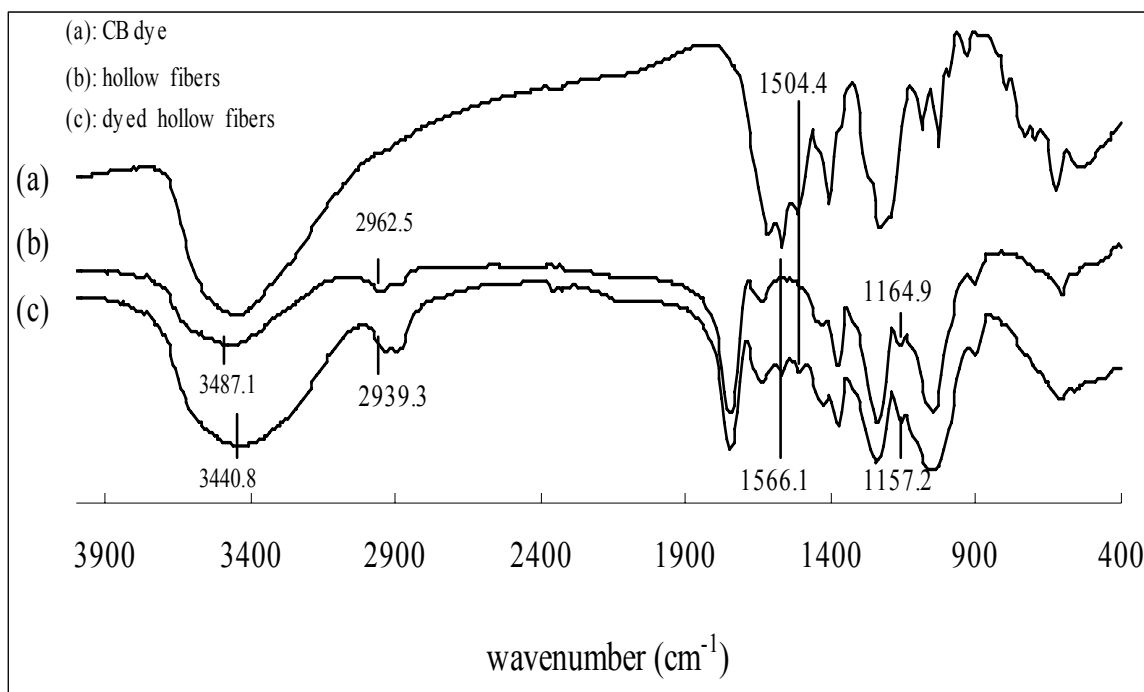
Figure 7.3 FTIR spectra for CB F3GA dye and CS/CA blend hollow fiber membranes before and after CB F3GA dye coupling

In addition, the peak at 2962.5 and 3487.1 cm^{-1} for the stretching vibration of –CH$_2$– and the stretching vibration of O-H and N-H, respectively, were shifted to 2939.3 and 3440.8 cm^{-1} after dye coupling, indicating hydroxyl group at C-6 position (-CH$_2$OH) or/and the amino groups (C-NH$_2$) on CS polymer chains were involved in the interaction (See Fig. 7.4).
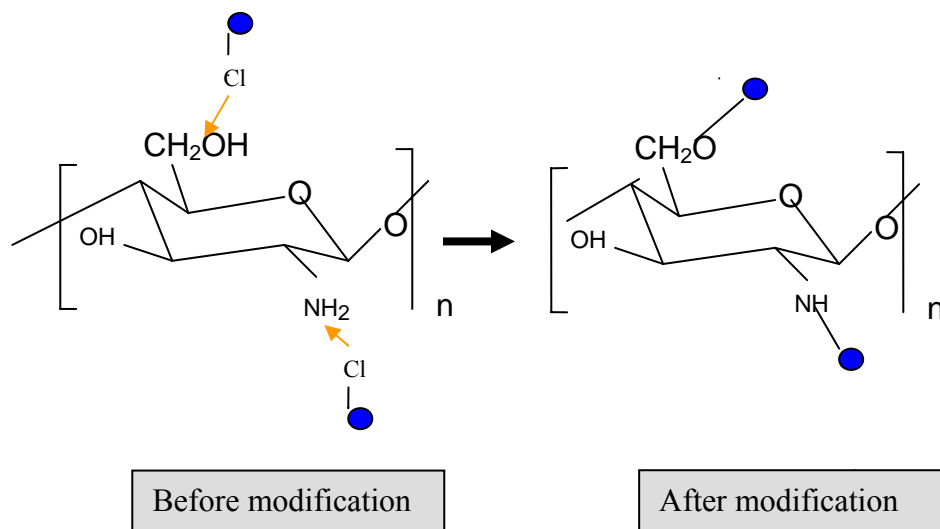
Figure 7.4 Nuleophilic reaction mechanisms between CS/CA membrane and CB dye

XPS spectras for the blend hollow fiber membranes before and after dye coupling are shown in Fig. 7.5. Clearly, a new peak at 168 ev was observed for the dyed hollow fiber membranes. This peak was attributed to the S atoms of $-SO_3^-$ groups of CB dye [184], indicating the successful introduction of CB dyes onto the hollow fiber membranes. The Cl atom on CB dye molecules cannot be observed on the dyed attached hollow fiber membranes, indicating the attachment of CB dye was through the nucleophilic reaction involved the Cl atoms on CB dye.
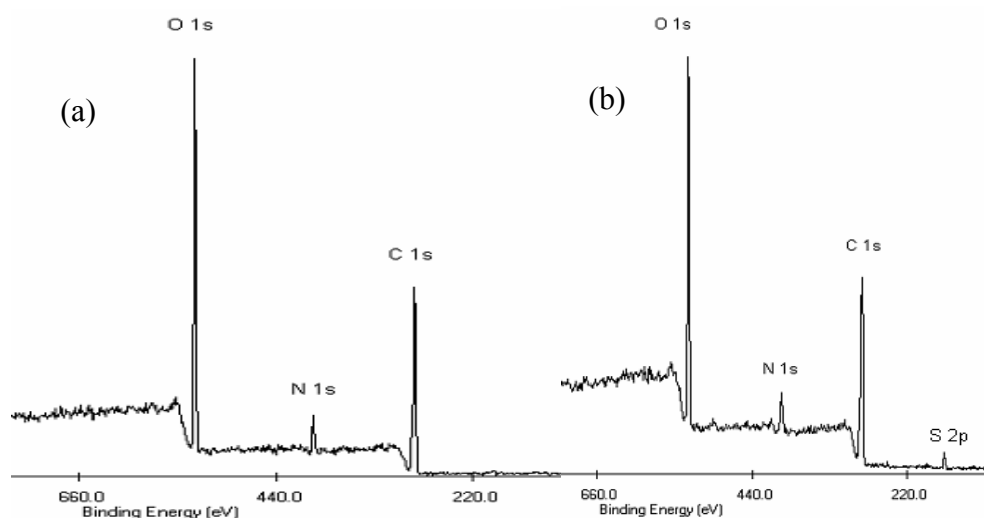
Figure 7.5 XPS spectra for CB F3GA dye and CS/CA blend hollow fiber membranes before (a) and after (b) CB F3GA dye coupling

7.3.2 Dye coupling amount

The amount of dye is crucial in improving the heavy metal ion binding performance. The amount of dye coupled on the membrane was determined to be 89 mg/g in this work. In comparison with those using other support (see Table 7.1), the coupled amount was high in this work. The reason may be due to the fact highly porous membranes containing high content of –OH and -NH$_2$ groups were used. The amount of –SO$_3^-$ groups coupled on the hollow fiber membranes was calculated to be 0.34mM/g. However, this value is much lower than that of commercial ion exchange resins (4-5 mM/g). The amount of effective –NH$_2$ groups on the membrane that came from both CS and CB dye could not be accurately calculated since some –NH$_2$ groups on CS were involved in the reaction with dye and the amount of that portion is difficult to be determined. The amount of –NH$_2$ groups introduced by CB dye was calculated to be 0.038mM/g.

Table 7.1 CB F3GA dye coupling amounts for different materials attempted by various researchers

Material	Dye loading amount (mg/g)	Ref.
Polyvinylbutyral microbeads	9.6	[180]
Polyhydroxyethylmethacrylate (PHEMA) microbeads	17.3	[181]
Polyethylene glycol methacrylate(PEG-MA) microbeads	33.0	[179]
Chitosan coated polyethersulfone flat sheets	29.8	[50]
Poly(ethylene glycol dimethacrylate-hydroxyl methacrylate)(poly EGDMA-HEMA) flat sheets	12.8	[185]
Polyvinyl alcohol coated polypropylene hollow fibers	68.1	[183]
Chitosan/cellulose acetate (CS/CA) blend hollow fibers	89.0	This work

7.3.3   Zeta potentials

The zeta potentials of CS/CA blend hollow fiber membranes before and after CB dye coupling are shown in Fig. 7.6. The hollow fiber membranes before dye coupling had positive zeta potential values at pH < 8.5 and negative values at pH > 8.5. The positive zeta potentials at pH <8.5 may be attributed to the protonation of the $-NH_2$ groups (from NH_2 to $-NH_3^+$) of the hollow fiber membranes. The negative zeta potentials may be caused by the dissociation of the $-OH$ groups on CS and CA molecules and/or the adsorption of OH^- from the alkali solutions. The zero point of zeta potential occurred at pH 8.5, which is higher than that of pure chitosan usually at pH 6.3-6.6 [153].
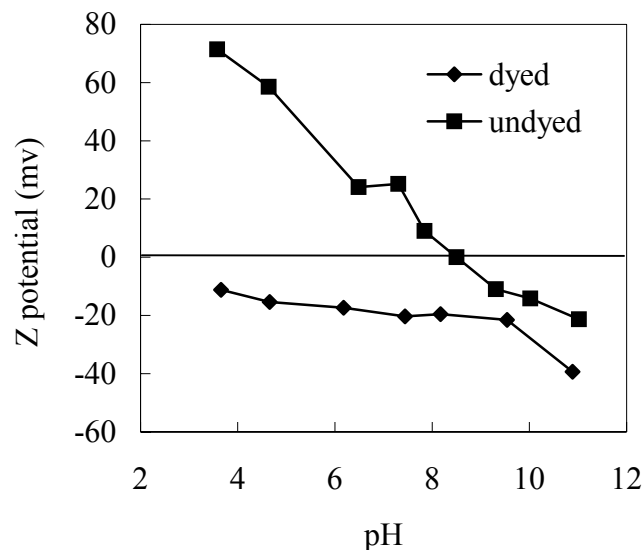
Figure 7.6 Zeta potentials for undyed and dyed CS/CA blend hollow fiber membranes

After dye coupling, the surface electrical property of the hollow fiber membranes changed significantly. The zeta potentials of the hollow fiber membranes became negative for the whole pH range examined, (i.e., 3.7-10.9). The negative zeta potentials may be attributed to the introduction of the $-SO_3^-$ groups to the fibers. The sulfonic group ($-SO_3^-$) moiety is a strong acid group and has a pKa in the vicinity of 0 [186]. Thus, at a pH>4, the sulfonic acid groups will dissociate completely. The negative zeta potentials of the hollow fiber membrane surfaces at low solution pH indicate that the $-SO_3^-$ groups introduced had a greater effect than the $-NH_2$ groups introduced from CB dye on the zeta potentials of the dyed hollow fiber membrane. From an electrostatic interaction point of view, the negative zeta potentials of the dyed hollow fiber membrane would favor the adsorption of cationic metal ions.

7.3.4   Copper ion adsorption capacity

The plots of equilibrium adsorption amounts against initial copper concentrations, for both dyed and undyed hollow fiber membranes, are shown in Fig. 7.7. As can be seen, the dyed hollow fiber membranes had higher adsorption amounts than the undyed fibers in the copper ion concentration range examined (i.e., 10-150mg/L). This proves that the adsorption amounts for heavy metal ions by the CS/CA blend hollow fiber membranes can be improved by surface coupling of CB dye.
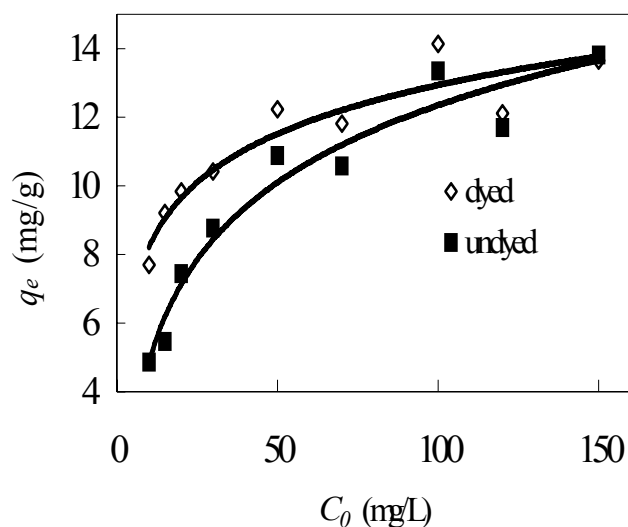
Figure 7.7 Equilibrium copper ion adsorption amount for undyed and dyed CS/CA blend hollow fiber membranes

More importantly, the improvement in the adsorption amount after dye coupling was more significant at lower copper ion concentrations. Although the adsorption amount at the initial copper ion concentration of 150 mg/L was about the same for two types of hollow fiber membranes, the adsorption amount at copper ion concentration of 10 mg/L

was only 4.85 mg/g for the undyed hollow fiber membranes and increased to 7.70 mg/g for the dyed hollow fiber membranes. This can be a very important feature because many adsorbents do not have good adsorption performance at low metal ion concentrations.

7.3.5   Adsorption isotherms

The Langmuir and Freundlich isotherm models were used to fit Cu^{2+} adsorption by dyed hollow fiber membranes. The adsorption isotherm for unmodified membranes has been studied in Chapter 5 and this was not repeated here. The fitting of adsorption of Cu^{2+} by dyed membrane using the Langmuir model is shown in Fig. 7.8 and that using the Freundlich model is shown in Fig. 7.9. A comparison between the predicted and the experimental adsorption results is shown in Fig. 7.10.

As can be observed, the adsorption amounts on the dyed blend hollow fiber membranes can be modeled by the Freundlich model (see Fig. 7.9) reasonably well, giving R^2 values of 0.9291. However, the results can not be adequately modeled using the Langmuir isotherm model, with the R^2 values being only 0.6798. The parameters in the Freundlich model, n and Kf, were calculated to be 9.7 and 8.7 respectively for the dyed hollow fiber membranes. A value of n greater than 1 (1/n<1) suggests that the amount of adsorption will reach a saturation limit.
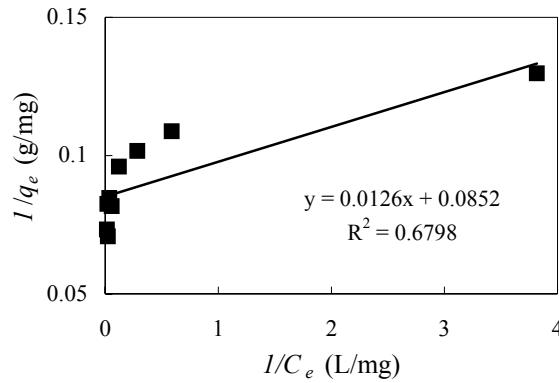
Figure 7.8 Correlating copper ion adsorption on dyed CS/CA blend hollow fiber
membrane with Langmuir isotherm model
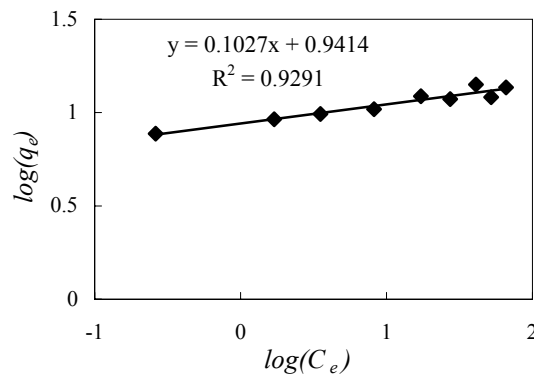
Figure 7.9 Correlating copper ion adsorption on dyed CS/CA blend hollow fiber
membrane with Freundlich isotherm model
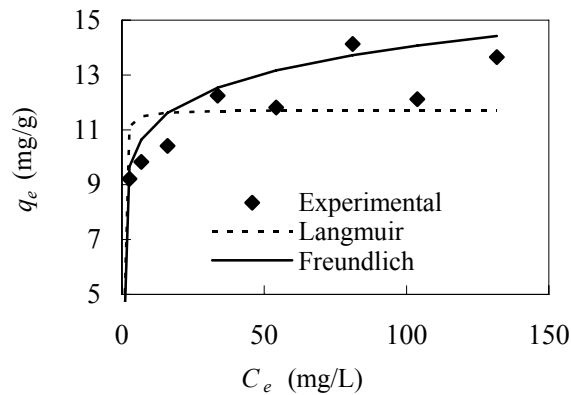
Figure 7.10 Comparison of the experimental adsorption results of copper ion adsorption
on dyed CS/CA blend hollow fiber membranes with the fitted results from the Langmuir
and Freundlich models

The fact that adsorption isotherm on dyed hollow fiber membranes can only be modeled by the Freundlich isotherm model is possibly attributed to the different types of functional groups ($-SO_3^-$, $-NH_2$, $-NH-$) coupled onto the membrane surface which show different binding energies for Cu^{2+}. In contrast, the adsorption on undyed hollow fiber membranes in previous study can be modeled by both the Langmuir and Freundlich isotherm models. This was possibly due to the relatively more homogeneous surface structure for unmodified membranes.

7.3.6   Adsorption kinetics

Fig. 7.11 shows the plot of copper adsorption amount against the elapsed time for both types of the hollow fiber membranes. Clearly, surface modification with CB dye improved the adsorption kinetics greatly as the equilibrium time for the dyed hollow fiber membranes was only around 6 mins, as compared to 30 mins for the undyed hollow fiber membranes. The fast adsorption rate is certainly a favorable feature for the dyed hollow fiber membranes for practical applications because of shorter process time and hence more economy. The adsorption capacity at the adsorption equilibrium however appeared to be the same for both types of the hollow fiber membranes in this case (see Fig. 7.7 where the two types of hollow fiber membranes showed similar adsorption amount at initial copper ion concentration of 150 mg/L).

The improvement of kinetics after modification may be associated with $-SO_3^-$ that is coupled on membrane. The interaction between $-SO_3^-$ and Cu^{2+} is an ion exchange which usually shows faster kinetics than complexation (or chelation) that occurs between $-NH_2$ and Cu^{2+}.
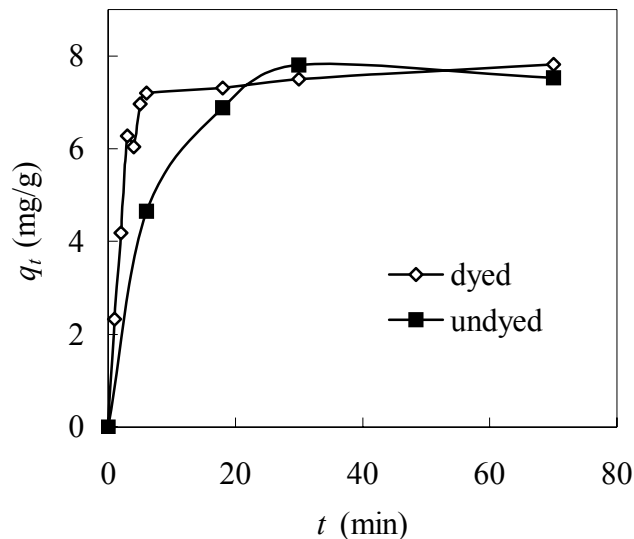
Figure 7.11 Copper ion adsorption kinetics on the dyed and undyed CS/CA blend hollow fiber membranes

7.3.7 Effect of pH on adsorption capacity

The effect of pH on the equilibrium adsorption amounts of copper ion on the two types of hollow fiber membranes is shown in Fig. 7.12. It is clear that the adsorption was pH dependant for both types of the hollow fiber membranes and the adsorption amounts generally increased with the increase of the solution pH.

The dyed hollow fiber membranes appeared to be more effective than the undyed hollow fiber membranes for copper ion adsorption at very low solution pH. For instance, the adsorption amount of the dyed fibers at pH 2 was 8.5 mg/g and that of the undyed fibers was only 5.2 mg/g. Moreover, no release of dye at pH 2 was detected from UV analysis during the adsorption process, indicating the stability of the coupled dyes on the hollow fiber membranes under such highly acidic conditions. This is another important

feature of the dyed hollow fiber membranes as many other adsorbents usually do not perform well at such low solution pH values for heavy metal adsorption.

The improvement might be associated with the $-SO_3$ groups introduced onto the membrane. Before modification, $-NH_2$ is the major group accounting for the adsorption. However $-NH_2$ performs poorly at low pH due to protonation by absorbing H^+ from surrounding solution. After modification, $-SO_3^-$ was introduced. Sulfonic groups are strong acid and take the form of ionized state even in a wide pH range of 1-14. Hence, this group shows good binding capability with Cu^{2+} in wide pH range. Therefore, it improved the membrane's binding capacity at low pH.
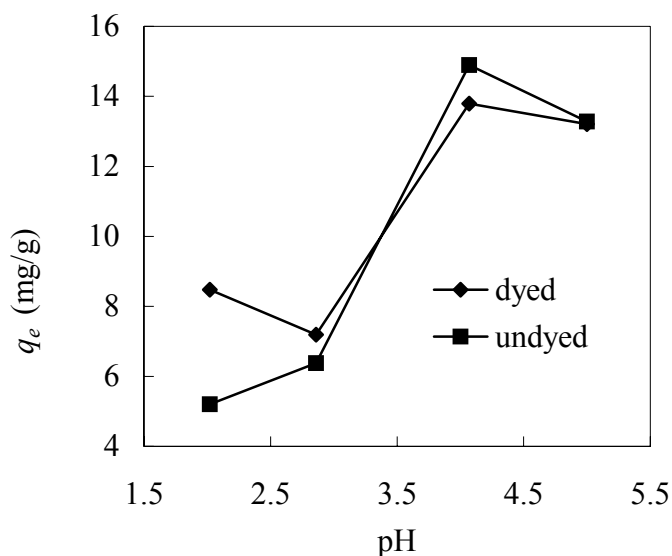
Figure 7.12 Effect of solution pH on copper ion adsorption on the dyed and undyed
CS/CA blend hollow fiber membranes

7.3.8   Regeneration and reuse of the dyed hollow fiber membranes

The dyed hollow fiber membranes with adsorbed copper ions were regenerated and reused in the next adsorption experiments. The results from four cycles are tabulated in Table 7.2. Both EDTA and HCl solutions were found to effectively desorb copper ions and regenerate the hollow fiber membranes. In previous study (Chapter 5), the highly porous CS/CA blend hollow fiber membranes 3-12-OH without surface modifications was found to have poor regeneration behaviour with the 50mM HCl solutions. The present study showed that the surface modifications with CB dye improved the regeneration performance of the hollow fiber membranes.

Table 7.2 Amount of copper ions adsorbed on dyed hollow fiber membranes for different cycles using 50mM HCl and 50mM EDTA as the desorbents

Cycle no.	Copper ion adsorption amount (mg/g)	
	50mM EDTA as desorbent	50mM HCl as dedorbent
1	7.81	7.81
2	7.10	7.10
3	7.06	7.09
4	6.97	6.99

7.3.9   Competitive adsorption

Batch adsorption was conducted for other persistent heavy metals commonly found in industrial wastewaters to examine the efficiencies of our membrane system. Selective adsorption of metal ions from mixture solutions was investigated, and the results are shown in Table 7.3. Hg(II) ions were the most efficiently removed species for both types of the hollow fiber membranes. The selectivity of the CS/CA blend hollow fiber membranes seemed to be varied by the dye coupling. The efficiency of removal (in terms

of μM/g) for the heavy metal ions by the unmodified fibers was in the order of Hg(II) >

Cu(II) > Pb(II) > Cd(II), but after dye coupling the order changed to Hg(II) > Pb(II) >

Cu(II) > Cd(II). The preliminary results indicate that the adsorptive hollow fiber

membranes developed in this study can be used for other heavy metal ions as well, not just

copper ions that were used as an example throughout this thesis.

Table 7.3 Competitive adsorption capacities of different metal ions for dyed and undyed
hollow fiber membranes

Metal ion	Dyed hollow fiber membranes	Undyed hollow fiber membranes
	(μM/g)	(μM/g)
Hg(II)	177.2	156.2
Cu(II)	40.4	59.1
Pb(II)	79.2	23.2
Cd(II)	21.0	10.7

7.4   Conclusions

Cibacron Blue F3GA was covalently coupled onto the CS/CA blend hollow fiber

membranes. It was found that the dye was effective in improving the adsorption properties

of the hollow fiber membranes. The adsorption capacity was improved after dye coupling,

particularly at low levels of metal ion concentration and at low solution pH values. The

adsorption rate was also greatly increased due to the dye coupling. The adsorbed copper

ions on the dyed hollow fiber membranes can be effectively desorbed with an HCl or

EDTA solution. Competitive adsorption also showed that adsorptive hollow fiber

membrane may be used for other heavy metal ions and an order of removal followed Hg(II)

> Cu(II) > Pb(II) > Cd(II) before dye coupling to Hg(II) > Pb(II) > Cu(II) > Cd(II) after

dye coupling. In conclusion, surface modification, such as the CB dye being used as a functional chemical in this part, has been demonstrated as an effective method to modify the CS/CA blend hollow fiber membranes to achieve improved performance in adsorption if necessary.

Chapter 8 Conclusions and recommendations for future work

8.1 Conclusions

In this research, novel CS/CA blend hollow fiber membrane was successfully prepared. Their material properties and adsorptive performance in heavy metal ion removal and protein separation were examined.

The following conclusions can be drawn from this research:

1.   Mixture of formic acid/acetic acid with water or with organic solvents with minimum concentration of 60v/v% is able to dissolve CS and CA polymers together to produce a transparent and homogeneous blending solution.

2.   The polymers are miscible in the blends and specific interaction exists between them. The specific interaction may be a hydrogen bonding involving $-NH_2$ and $-OH$ groups.

3.   For all the membranes prepared in this project, the content of CS in the blend hollow fiber membrane is less than that in spinning solution. This is because a portion of CS dissolves in coagulant solution during spinning process. However, with strong coagulant and adding more CA in the spinning solution, the loss of CS can be reduced.

4.   Water is a cheap and weak coagulant to the spinning solution. With it as coagulant, spongy-like and microporous membranes desirable for adsorptive filtration are produced. Moreover, membranes surfaces are highly porous with pore size in the micron range.

However, loss of CS during spinning process is severe due to the weak coagulation capability.

5. 2-3wt% NaOH solution is a relatively stronger coagulant than water. With NaOH solution as coagulant, membrane containing more CS can be produced. However, membranes with macrovoids in the cross-section may be produced if NaOH concentration is high and dope viscosity is low. Macrovoids can be eliminated by slightly increasing CS concentration for example from 2%wt. to 3%wt. in the spinning solution.

6. To make more CS be blended in the membrane, one can spin hollow fiber membrane from solution containing more CS. However, due to the high viscosity of CS/FA system, the spinning solution has to have lower concentration of CA. This resulted in low mechanical strength (8-18MPa) of the membrane. Therefore, sometimes we have to sacrifice either the mechanical strength or the high CS density of the membrane, as we cannot get both of them at the same time.

7. The maximum CS content in the blend membrane achieved in this project was 120mg/g, about 3 times larger than that on chitosan composite hollow fiber membranes reported in literature [121]. The maximum Cu^{2+} adsorption capacity was 12.5mg/g in batch mode and 11.13mg/g in dynamic mode (residence time=3mins). This value is about two times lower than that for commercial adsorptive/ion exchange resins (about 40mg/g).

8. The BSA binding by the blend hollow fiber membrane after coupling with copper ion ligand is satisfactory as binding amount (14mg/mL or 60mg/g) is comparable to those of reported adsorptive membranes in literature. However, the binding capacity is lower than that of commercial products for example adsorptive membranes from Pall and

Sartorius (40-50mg/mL). High utilization of metal ion ligand was observed in this work. Another problem with the membrane could be the leakage of metal ion ligand, which could restrict its commercilization.

9. Adsorption kinetics at batch mode is very fast for both Cu^{2+} (<70mins) and BSA (<10hrs) as the adsorption equilibrium time is significantly lower than that in adsorptive/ion exchange resins.

10. Surface modification with CB F3GA dye can improve the kinetics, adsorption amount at low concentration and low pH as well as regeneration by using HCl as desorbent of the blend hollow fiber membranes for copper ion adsorption. Most of these improvements are related to the introduction of $-SO_3^-$ groups onto membrane surface.

8.2 Recommendations for future work

Many aspects on CS/CA blend hollow fiber membranes can be further studied. These include the improvement of the hollow fiber membrane by using other co-solvents or coagulants, to increase the amount of CS in the blend hollow fiber membrane, exploring other polymers that can be blended with CS for improved mechanical or chemical properties, grafting of other functional polymers for improved adsorption capacity, adsorption rate and selectivity, evaluating the blend hollow fiber membranes under dynamic flow, and exploiting the application of the blend hollow fiber membranes in other processes such as RO, dialysis and pervaporation etc. Specifically they are listed in the followings:

a)   Use other co-solvents to prepare the dope and spin the hollow fiber membranes. Besides formic acid used in this work, other similar co-solvents were also found to be effective in dissolving both CS and CA. They include pure acetic acid, mixtures of formic acid/acetic acid with water and mixtures of formic acid/acetic acid with common organic solvents such as acetone, DMF, DMSO etc. These studies may have a great theoretical importance. The change of co-solvents may change the phase separation behavior of the spun dope and hence influence the membrane structures. Moreover, the mixture of acids with water may be a more economical co-solvent than pure acids, reducing the cost for production of CS/CA blend hollow fiber membranes.

b)   Use other types of coagulants to solidify the hollow fiber membranes. Besides water and alkali solution, many other solutions can be used as the coagulants and they may include sodium tripolyphosphate, surfactant, and crosslinkers etc. The study may not only have theoretical importance as the new coagulants may change the phase separation behavior but also have practical importance to prevent or avoid the dissolution of CS in the coagulants during the spinning process. The coagulants that could prevent dissolution of CS may be solutions containing crosslinkers. CS in the polymer solution may be effectively crosslinked when in contact with the coagulants containing crosslinkers and hence minimizing the dissolution. However, crossliking may take place at $-NH_2$ position of CS that is responsible for the adsorption of heavy metal ions for the blend hollow fiber membranes. Therefore, optimizing the amount of crosslinkers added into the spinning solution or coagulants may be the focus of the study so that highest adsorption capacities can be achieved.

c)   Modify the membrane surface with other functional polymers to improve the binding capacities of the membranes for heavy metal ions. The major problem with the CS/CA hollow fiber membranes in this work is the limited adsorption amount for heavy metal ions, which hinders the applications of the membranes on larger scales. Although increasing CS content in the hollow fiber membranes is an effective method, the prospect is greatly limited by the high viscosity of CS in the solvent used in the present work. Chemical modification of the hollow fiber membranes may provide an alternative. Grafting long chain polymers with numerous functional groups will be an effective way to enhance the adsorptive capacity. The modification of CS has been extensively studied and reviews on this can be found in references [38, 187-189]. Representative work to modify CS in our lab is the grafting of polyacrylamide or poly(acrylic acid) onto CS [190-191].

d)   Carry out dynamic filtration experiments with the hollow fiber membranes. All the adsorption experiments in this work have been conducted in batch mode. It does not reflect actual adsorption performance in a dynamic mode in actual applications. Therefore, the performances of the hollow fiber membranes in dynamic operation modes, particularly the kinetics properties, need to be studied and compared with that of packed beds and conventional membrane separation processes such as RO and NF. Two dynamic flow modes may be adopted as schematically shown in Fig. 9.1. One mode is the same as that of membrane chromatography, or called as "flow through" (Fig. 9.1a). The feed is forced into the membrane and permeated through the hollow fiber wall and out from the other side of the membrane. The wall thickness is all the pathway the feed will pass through. In each run, a constant permeate flow rate is maintained throughout the process to allow the adsorption to fully take place. The feed flow rate may be varied in a wide range to test the

kinetics efficiencies of the adsorptive membranes. Another mode is "flow along" (Fig. 9.1b), like that of fiber adsorbent cartridge which contains a twisted bundle of flexible fiber adsorbents. In such process, the membranes behave like an adsorbents but not a membrane. The feed will flow along both the external and internal surfaces of the adsorptive membranes. Due to the two-fold surface areas and the high porosity of the membranes, the adsorption will be much faster than the conventional solid fiber adsorbents. This type of membrane module is also proposed by Baurmeister Ulrich and (Wuppertal, DE) Wollbeck, Rudolf (Erlenbach, DE) in 1993 [192].
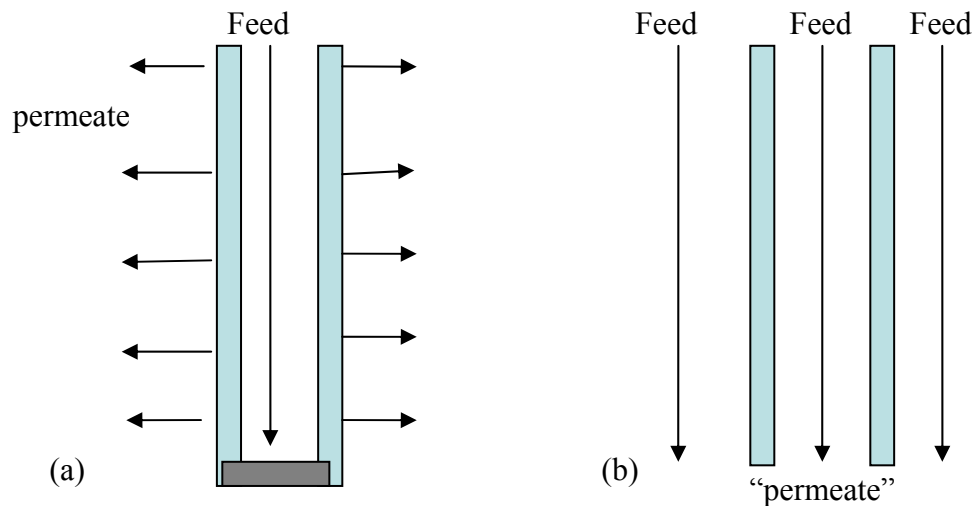
Figure 8.1 Schematic illustrations of two filtration modes for the adsorptive membranes

e)   Broaden the application field of the CS/CA hollow fiber membranes. Besides the adsorptive/affinity separation, the CS/CA hollow fiber membranes may also be useful in other separation processes such as RO, dialysis, and pervaporation etc. The membranes may be used as RO membranes for desalination of seawater. The membranes may reject sodium (Na^+) and potassium (K^+) ions in seawater because the membrane surfaces is

usually positively charged under neutral and acid conditions. Therefore, the efficiency with CS/CA membranes may be much higher than that of conventional RO membranes that is usually neutral in electrical property. For this purpose, the membranes should be prepared to be asymmetric in structures having macrovoids in the sublayer and to be dense in the top layer. For dialysis, the membrane can not only adsorb endotoxins from the dialysis solutions but also reduce the glomeration of proteins in the blood or urine [43, 193]. The biocompatibility of CS and CA polymers also make the membrane a suitable candidate for blood or urine dialysis. Membranes for this purpose should have symmetric and microporous structures. The CS based membranes may also be useful in pervaporation for separation of water and alcohols. A numerous references can be found on this. For this purpose, nonporous membranes or asymmetric membranes can be adopted.

References

1. A.W. Zularisam, A.F. Ismail and R. Salim. Behaviors of natural organic matter in membrane filtration for surface water treatment — a review, Desalination, *194*, pp.211-2313, 2006.

2. E. Klein. Affinity membranes: a 10-year review, J. Membr. Sci., *179*, pp. 1-27, 2000.

3. R. Ghosh. Protein separation using membrane chromatography: opportunities and challenges, J Chromatgra. A., *952,* pp.13-27, 2002.

4. N. Sprang, D. Theirich and J. Engemann, Plasma and ion beam surface treatment of polyethylene, Surf. Coat. Technol., *74–75,* pp.689-695, 1995.

5. M.A. Golub. Concerning apparent similarity of structures of fluoropolymer surfaces exposed to an argon plasma or argon ion beam, Langmuir, *12,* pp.3360-3361, 1996.

6. A. Fozza, J. Roch, J.E. Klemberg-Sapieha, A. Kruse, A. Hollander and M.R. Wertheimer. Oxidation and ablation of polymers by vacuum-UV radiation from low pressure plasmas, Polym. Prepr., *38,* pp.1097-1098, 1997.

7. H. Suhr. Application of Nonequilibrium Plasmas to Organic Chemistry. In Techniques and Applications of Plasma Chemistry, Vol. 2, ed. by J. Hollahan and A.T. Bell, pp. 57-112. New York: John Wiley & Sons, 1974.

8. M.B.O. Riekerink, J.G.A. Terlingen, G.H.M. Engbers and J. Feijen. Selective etching of semicrystalline polymers: CF4 gas plasma treatment of poly(ethylene), Langmuir, *15,* pp.4847-4856, 1999.

9. H. Matsuyama, S. Berghmans and D.R. Loyd. Formation of hydrophilic microporous membranes via thermally induced phase separation, J. Membr. Sci., *142,* pp.213-224, 1998.

10. Z. Chen, M. Deng, Y. Chen, G. He, M. Wu and J. Wang. Preparation and performance of cellulose acetate/polyethyleneimine blend microfiltration membranes and their applications, J. Membr. Sci., *235*, pp.73-86, 2004.

11. K. Scott and R. Hughes. Industrial membrane separation technology, Blackie academic & Profesional, UK. 1996.

12. M. Mulder. Basic principals of membrane technology, 2nd Edi. Kluwer Academic publishers, the Netherlands. 1996.

13. M.A.M. Beerlage. Ultrafiltration membranes for non-aqueous systems, PhD Thesis, The Netherlands: Twente University, 1994.

14. K. Gotoh, Y. Nakata, M. Tagawa and M. Tagawa. Wettability of ultraviolet excimer-exposed PE, PI and PTFE films determined by the contact angle measurements, Colloids Surf., A, *224,* pp.165-173, 2003.

15. Y. Lu, S.L. Yu, B.X. Chai and X. Shun. Effect of nano-sized Al_2O_3-particle addition on PVDF ultrafiltration membrane performance, J. Membr. Sci., *276,* pp.162-167, 2006.

16. W. Zhang, P.K. Chu, J. Ji, Y. Zhang and Z. Jiang. Effects of O_2 and H_2O plasma immersion ion implantation on surface chemical composition and surface energy of poly vinyl chloride, Appl. Surf. Sci., *22,* pp.7884-7889, 2006.

17. M.L. Steen, A.C. Jordan and E.R. Fisher. Hydrophilic modification of polymeric membranes by low temperature H_2O plasma treatment, J. Membr. Sci., *204,* pp. 341-357, 2002.

18. T.Y. Liu, W.C. Lin, L.Y. Huang, S.Y. Chen and M.C. Yang. Hemocompatibility and anaphylatoxin formation of protein-immobilizing polyacrylonitrile hemodialysis membrane, Biomaterials, *26*, pp.1437-1444, 2005.

19. M.A. Aboudzadeh, S.M. Mirabedini and M. Atai, Effect of silane-based treatment on the adhesion strength of acrylic lacquers on the PP surfaces, Int. J. Adhes. Adhes., I*n Press, Available online 21 November 2006.*

20. Y.N. Kwon and J.O. Leckie. Hypochlorite degradation of crosslinked polyamide membranes: I. Changes in chemical/morphological properties, J. Membr. Sci., *283,* pp.21-26, 2006.

21. M. Wang, L.G. Wu, J.X. Mo and C.J. Gao. The preparation and characterization of novel charged polyacrylonitrile/PES-C blend membranes used for ultrafiltration, J. Membr. Sci., *274,* pp.200-208, 2006.

22. T. Białopiotrowicz and B. Jańczuk. The wettability of a cellulose acetate membrane in the presence of bovine serum albumin, Appl. Surf. Sci., *201,* pp.146-153, 2002.

23. W.F.C. Kools. Membrane formation by phase inversion in multicomponent polymer systems: mechanisms and morphologies, PhD Thesis, The Netherlands: Twente University, 1998.

24. A.J. Reuvers. Membrane formation diffusion induced demixing processes in ternary polymeric systems, PhD Thesis, Twente University, 1987.

25. C.A. Smolders, A.J. Reuvers, R.M. Boom and I.M. Wienk. Microstructures in phase-inversion membranes. Part 1. Formation of macrovoids, J. Membr. Sci., *73,* pp.259-275, 1992.

26. H.K. Lonsdale. The growth of membrane technology, J. Membr. Sci., *10,* pp.81-181, 1982.

27. M.H.V. Mulder. Basic principles of membrane technology, Kluwer Academic publishers, Dordrecht, 1991.

28. J.E. Cadotte, F. Forester, M. Kim, R.J. Petersen and T. Stocker; Nanofiltration

membranes broaden the use of membrane separation technology, Desalination, *70,* pp.77-88, 1988.

29. P. Eriksson. Nanofiltration extends the range of membrane filtration, Environ. Prog., *7,* pp.58-62, 1988.

30. R.J. Petersen. Composite reverse osmosis and nanofiltration membranes, J. Membr. Sci., *83,* pp.81-150, 1993.

31. D. Roper and E. Lightfoot. Separation of biomolecules using adsorptive membranes, J. Chromatogr. A, *702,* pp.3-26, 1995.

32. C. Charcosset. Purification of proteins by membrane chromatography, J. Chem. Technol. Biotechnol, *71,* pp.95-110, 1998.

33. X. Zeng and E. Ruckenstein. Macroporous chitin affinity membranes for wheat germ agglutinin purification from wheat germ, J. Membr. Sci., *156*, pp.97-107, 1999.

34. H. Zou, Q. Luo and D. Zhou. Affinity membrane chromatography for the analysis and purification of proteins, J. Biochem. Biophys. Methods., *49*, pp.199-240, 2001.

35. G.A.F. Roberts. Chitin Chemistry, The Macmillan Press. London, 1992.

36. G. Crini. Non-conventional low-cost adsorbents for dye removal: A review, Bioresource Technol., *97,* pp.1061-1085, 2006.

37. T. Yui, K. Imada, K. Okuyama, Y. Obata, K. Suzuki and K. Ogawa. Molecular and crystal structure of the anhydrous form of chitosan, Macromol., *27,* pp.7601-7605, 1994.

38. M.N.V.R. Kumar. A review of chitin and chitosan applications, React. Funct. Polym., *46,* pp.1-27, 2000.

39. B. Krajewska. Membrane-based processes performed with use of chitin/chitosan materials, Sep. Purif. Technol., *41*, pp.305-312, 2005.

40. B. Sandhya and K.T. Agustiono. Low-cost adsorbents for heavy metals uptake from contaminated water: a review, J. Hazard. Mater., *97,* pp.219-243, 2003.

41. S.E. Bailey, T.J. Olin, R.M. Bricka and D.D. Adrian. A review of potentially low-cost sorbents for heavy metals, Water Res., *33,* pp.2469-2479, 1999.

42. M.G. Peter. Applications and environmental aspects of chitin and chitosan, J. Macromol. Sci.: Pure and Appl. Chem., *A32,* pp.629-640, 1995.

43. B. Krajewska, Diffusion of metal ions through gel chitosan membranes, React. Funct. Polym., *47,* pp.37-47, 2001.

44. I.B. Rae and S.W. Gibb. Removal of metals from aqueous solutions using natural chitinous materials, Water Sci. Technol., *47,* pp.189-196, 2003.

45. H. Yoshida and T. Kataoka. Adsorption of BSA on cross-linked chitosan: The equilibrium isotherm, Chem. Eng. J., *41,* pp.B11-B15, 1989.

46. R. Agarwal and M.N. Gupta. Evaluation of gluteraldehyde-modified chitosan as a matrix for hydrophobic interaction chromatography, Anal. Chim. Acta, *313,* pp.253-257, 1995.

47. V. Tangpasuthadol, N. Pongchaisirikul and V.P. Hoven. Surface modification of chitosan films: Effects of hydrophobicity on protein adsorption, Carbohydr. Res., *338,* pp.937-942, 2003.

48. S.S. Freitas, R.L. Machado, E.J. Arruda, C.C. Santana and S.M.A. Bueno. Endotoxin removal from solutions of $F(ab')_2$ fragments of equine antibodies against snake venom using macroporous chitosan membrane, J. Membr. Sci., *234,* pp.67-73, 2004.

49. X. Zeng and E. Ruckenstein, Cross-linked macroporous chitosan anion-exchange membranes for protein separations, J. Membr. Sci., *148,* pp.195-205, 1998.

50. N. Takuo, I. Noriaki and O. Lech. Use of epichlorohydrin-treated chitosan resin as an

adsorbent to isolate kappa-casein glycomacropeptide from sweet whey, J. Agric. Food. Chem., 52, pp.7555-7560, 2004.

51. X. Zeng and E. Ruckenstein. Supported chitosan-dye affinity membranes and their protein adsorption, J. Membr. Sci., *117,* pp.271-278, 1996.

52. E. Ruckenstein and X. Zeng. Albumin separation with Cibacron Blue carrying macroporous chitin/chitosan membranes, J. Membr. Sci., *142,* pp.13-26, 1998.

53. G. Bayramoğlu, M. Yilmaz and M.Y. Arica. Affinity dye–ligand poly(hydroxyethyl methacrylate)/chitosan composite membrane for adsorption lysozyme and kinetic properties, Biochem. Eng. J., *13,* pp.35-42, 2003.

54. M.Y. Arıca, M. Yılmaz, E. Yalçın and G. Bayramolu. Surface properties of Reactive Yellow 2 immobilised pHEMA and HEMA/chitosan membranes: characterisation of their selectivity to different proteins, J. Membr. Sci., *240,* pp.167-178, 2004.

55. J. Shentu, J.Wu, W. Song and Z. Jia. Chitosan microspheres as immobilized dye affinity support for catalase adsorption, Int. J. Biol. Macromol., *37,* pp.42-46, 2005.

56. J. Zhang, Z. Zhang, Y. Song and H. Cai. Bovine serum albumin (BSA) adsorption with Cibacron Blue F3GA attached chitosan microspheres, React. Funct. Polym., In Press, Corrected Proof, Available online 19 January 2006

57. Y.C. Shi, Y.M. Jiang, D.X. Sui, Y.L. Li, T. Chen, L. Ma and Z.T. Ding. Affinity chromatography of trypsin using chitosan as ligand support, J. Chromatogr. A, *742,* pp.107-112, 1996.

58. X.F. Zeng and E. Ruckenstein. Trypsin purification by p-aminobenzamidine immobilized on macroporous chitosan membrane, Ind. Eng. Chem. Res., *37,* pp.159-165, 1998.

59. L. Yang, W.W. Hsiao and P. Chen. Chitosan–cellulose composite membrane for

affinity purification of biopolymers and immunoadsorption, J. Membr. Sci., *197,* pp.185-197, 2002.

60. Q.H. Shi, Y. Tian, X.Y. Dong, S. Bai and Y. Sun. Chitosan-coated silica beads as immobilized metal affinity support for protein adsorption, Biochem. Eng. J., *16,* pp.317-322, 2003.

61. F. Xi and J. Wu. Macroporous chitosan layer coated on non-porous silica gel as a support for metal chelate affinity chromatographic adsorbent, J. Chromatogr. A, *1057,* pp.41-47, 2004.

62. Z.P. Zhao, Z. Wang and S.C. Wang. Formation, charged characteristic and BSA adsorption of carboxymethyl chitosan/PES composite MF membrane, J. Membr. Sci., *217,* pp.151-158, 2003.

63. V.T. Fávere, R. Laus, M.C.M. Laranjeira, A.O. Martins and R.C. Pedrosa, Use of chitosan microspheres as remedial material for acidity and iron (III) contents of coal mining wastewaters, Environ. Technol., *25,* pp.861-866, 2004.

64. Y.K. Twu, H.I. Huang, S.Y. Chang and S.L. Wang. Preparation and sorption activity of chitosan/cellulose blend beads, Carbohydr. Polym., *54,* pp.425-430, 2003.

65. D.A. Musale, A. Kumar and G. Pleizier. Formation and characterization of poly(acrylonitrile)/chitosan composite ultrafiltration membranes, J. Membr. Sci., *154,* pp.163-173, 1999.

66. D.A. Musale and A. Kumar. Effects of surface crosslinking on sieving characteristics of chitosan/poly(acrylonitrile) composite nanofiltration membranes, Sep. Purif. Technol., *21,* pp.27-37, 2000.

67. C.K. Yeom, C.U. Kim, B.S. Kim, K.J. Kim and M.J. Lee, Recovery of anionic surfactant by RO process. Part I. Preparation of polyelectrolyte-complex anionic

membrane, J. Membr. Sci., *143*, pp.207-218, 1998.

68. B. Krajewska. Diffusional properties of chitosan hydrogel membranes, J. Chem. Technol. Biotechnol., *76*, pp.636-642, 2001.

69. N. Kubota, Y. Kikuchi, Y. Mizuhara, T. Ishihara and Y. Takita, Solid-phase modification of chitosan hydrogel membranes and permeability properties of modified chitosan membranes, J. Appl. Polym. Sci. *50,* pp.1665-1670, 1993.

70. M.M. Amiji. Surface modification of chitosan membranes by complexation-interpenetration of anionic polysaccharides for improved blood compatibility in hemodialysis, J. Biomater. Sci. Polym. Ed., *8,* pp.281-298, 1996.

71. S.Y. Nam and Y.M. Lee. Pervaporation separation of methanol/methyl t-butyl ether through chitosan composite membrane modified with surfactants, J. Membr. Sci., *157,* pp.63-71, 1999.

72. W. Won, X. Feng and D. Lawless, Pervaporation with chitosan membranes: separation of dimethyl carbonate/methanol/water mixtures, J. Membr. Sci., *209,* pp.493-508, 2002.

73. Ö. Genç, Ç. Arpa, G. Bayramoğlu, M.Y. Arica and S. Bektaş. Selective recovery of mercury by Procion Brown MX 5BR immobilized poly(hydroxyethylmethacrylate/chitosan) composite membranes, Hydrometallurgy, *67,* pp.53-62, 2002.

74. A.R. Cestari, E.F.S. Vieira and C.R.S. Mattos. Thermodynamics of the Cu(II) adsorption on thin vanillin-modified chitosan membranes, J. Chem. Thermodyn., In Press, Corrected Proof, Available online 19 January 2006

75. G.C. Steenkamp, K. Keizer, H.W.J.P. Neomagus and H.M. Krieg. Copper(II) removal from polluted water with alumina/chitosan composite membranes, J. Membr. Sci.,

197, pp.147-156, 2002.

76. I.S. Lima, A.M. Lazarin and C. Airoldi. Favorable chitosan/cellulose film combinations for copper removal from aqueous solutions, Int. J. Biol. Macromol., *36,* pp.79-83, 2005.

77. X. Zeng and E. Ruckenstein. Control of pore sizes in macroporous chitosan and chitin membranes, Ind. Eng. Chem. Res., *35,* pp.4169-4175, 1996.

78. E. Ruckenstein and X. Zeng. Microporous or macroporous filtration membranes, method of preparation and use, US Patent, 5993661, 1999.

79. E. Ruckenstein and X. Zeng, Macroporous chitin affinity membranes for lysozyme separation. Biotechnol. Bioeng., *56,* pp.610-617, 1997.

80. L. Yang and P. Chen. Chitosan/coarse filter paper composite membrane for fast purification of IgG from human serum, J. Membr. Sci., *205,* pp.141-153, 2002.

81. R. Jiraratananon, A. Chanachai, R.Y.M. Huang and D. Uttapap. Pervaporation dehydration of ethanol–water mixtures with chitosan/hydroxyethylcellulose (CS/HEC) composite membranes: I. Effect of operating conditions, J. Membr. Sci., *195,* pp.143-151, 2002.

82. J. Miao, G.H. Chen and C.J. Gao. A novel kind of amphoteric composite nanofiltration membrane prepared from sulfated chitosan (SCS), Desalination, *181,* pp.173-183, 2005.

83. M. Ghazali, M. Nawawi and R.Y.M. Huang. Pervaporation dehydration of isopropanol with chitosan membranes, J. Membr. Sci., *124,* pp. 53-62, 1997.

84. W. Edwards, W.D. Leukes, P.D. Rose and S.G. Burton. Immobilization of polyphenol oxidase on chitosan-coated polysulphone capillary membranes for improved phenolic effluent bioremediation, Enzyme Microb. Technol., *25,* pp. 769-773, 1999.

85. R.Y.M. Huang, R. Pal and G.Y. Moon. Crosslinked chitosan composite membrane for the pervaporation dehydration of alcohol mixtures and enhancement of structural stability of chitosan/polysulfone composite membranes, J. Membr. Sci., *160,* pp.17-30, 1999.

86. G.C. Steenkamp, H.W.J.P. Neomagus, H.M. Krieg and K. Keizer. Centrifugal casting of ceramic membrane tubes and the coating with chitosan, Sep. Purif. Technol., *25,* pp.407-413, 2001.

87. C.G.L. Khoo, S. Frantzich, A. Rosinski, M. Sjöström and J. Hoogstraate. Oral gingival delivery systems from chitosan blends with hydrophilic polymers, Eur. J. Pharmaceut. Biopharmaceut., *55,* pp.47-56, 2003.

88. M.N. Taravel and A. Domard. Collagen and its interactions with chitosan: III. Some biological and mechanical properties, Biomaterials, *17,* pp.451-455, 1996.

89. S.Y. Nam and Y.M. Lee. Pervaporation and properties of chitosan-poly(acrylic acid) complex membranes, J. Membr. Sci., *135,* pp.161-171, 1997.

90. G. Dhanuja, B. Smitha and S. Sridhar. Pervaporation of isopropanol–water mixtures through polyion complex membranes, Sep. Purif. Technol., *44,* pp.130-138, 2005.

91. P.C. Srinivasa, M.N. Ramesh, K.R. Kumar and R.N. Tharanathan. Properties and sorption studies of chitosan–polyvinyl alcohol blend films, Carbohydr. Polym., *53,* pp.431-438, 2003.

92. N. Minoura, T. Koyano, N. Koshizaki, H. Umehara, M. Nagura and K. Kobayashi. Preparation, properties, and cell attachment/growth behavior of PVA/chitosan-blended hydrogels, Mater. Sci. Eng., C, *6,* pp.275-280, 1998.

93. W.Y. Chuang, T.H. Young, C.H. Yao and W.Y. Chiu. Properties of the poly(vinyl alcohol)/chitosan blend and its effect on the culture of fibroblast in vitro**,** Biomaterials,

20, pp.1479-1487, 1999.

94. T.H.M. Abou-Aiad, K.N. Abd-El-Nour, I.K. Hakim and M.Z. Elsabee. Dielectric and interaction behavior of chitosan/polyvinyl alcohol and chitosan/polyvinyl pyrrolidone blends with some antimicrobial activities, Polymer, *47,* pp.379-389, 2006.

95. B. Smitha, S. Sridhar and A.A. Khan. Chitosan–poly(vinyl pyrrolidone) blends as membranes for direct methanol fuel cell applications, J. Power Sources, In Press, Corrected Proof, Available online 24 January 2006

96. A. Sionkowska, M. Wisniewski, J. Skopinska, C.J. Kennedy and T.J. Wess**.** Molecular interactions in collagen and chitosan blends, Biomaterials, *25,* pp.795-801, 2004.

97. Y. Huang, S. Onyeri, M. Siewe, A. Moshfeghian and S. V. Madihally. In vitro characterization of chitosan–gelatin scaffolds for tissue engineering, Biomaterials, *26,* pp.7616-7627, 2005.

98. X. Ye, J.F. Kennedy, B. Li and B.J. Xie. Condensed state structure and biocompatibility of the konjac glucomannan/chitosan blend films, Carbohydr. Polym., In Press, Corrected Proof, Available online 5 December 2005

99. P. Kanti, K. Srigowri, J. Madhuri, B. Smitha and S. Sridhar. Dehydration of ethanol through blend membranes of chitosan and sodium alginate by pervaporation, Sep. Purif. Technol., *40,* pp.259-266, 2004.

100. B. Smitha, S. Sridhar and A.A. Khan. Chitosan–sodium alginate polyion complexes as fuel cell membranes, Eur. Polym. J., *41,* pp.1859-1866, 2005.

101. J. Yin, K. Luo, X. Chen and V. V. Khutoryanskiy. Miscibility studies of the blends of chitosan with some cellulose ethers, Carbohydr. Polym., *63,* pp.238-244, 2006.

102. A. Dufresne, J.Y. Cavaillé, D. Dupeyre, M.G. Ramirez and J. Romero. Morphology,

phase continuity and mechanical behaviour of polyamide 6/chitosan blends, Polymer, *40,* pp.1657-1666, 1999.

103. Y.B. Wu, S.H. Yu, F.L. Mi, C.W. Wu, S.S. Shyu, C.K. Peng and A. C. Chao. Preparation and characterization on mechanical and antibacterial properties of chitsoan/cellulose blends, Carbohydr. Polym., *57,* pp.435-440, 2004.

104. A. Isogai and R.H. Atalla. Preparation of cellulose-chitosan polymer blends, Carbohydr. Polym., *19,* pp.25-28, 1992.

105. C. Chen, L. Dong, and M.K. Cheung. Preparation and characterization of biodegradable poly(l-lactide)/chitosan blends, Eur. Polym. J., *41,* pp.958-966, 2005.

106. J.J. Shieh and R.Y.M. Huang. Chitosan/N-methylol nylon 6 blend membranes for the pervaporation separation of ethanol–water mixtures, J. Membr. Sci., *148,* pp.243-255, 1998.

107. T. Suzuki and Y. Mizushima. Characteristics of silica-chitosan complex membrane and their relationships to the characteristics of growth and adhesiveness of L-929 cells cultured on the biomembrane, Ferment Bioeng., *84,* pp.128-132, 1997.

108. S.B. Park, J.O. You, H.Y. Park, S.J. Haam and W.S. Kim. A novel pH-sensitive membrane from chitosan-TEOS IPN: preparation and its drug permeation characteristics, Biomaterials, *22,* pp.323-330, 2001.

109. Y.L. Liu, Y.H. Su and J.Y. Lai. In situ crosslinking of chitosan and formation of chitosan–silica hybrid membranes with using γ-glycidoxypropyltrimethoxysilane as a crosslinking agent, Polymer, *45,* pp.6831-6837, 2004.

110. M. Zeng and Z. Fang. Preparation of sub-micrometer porous membrane from chitosan/polyethylene glycol semi-IPN, J. Membr. Sci., *245,* pp.95-102, 2004.

111. M, Zeng, Z. Fang and C. Xu. Effect of compatibility on the structure of the

microporous membrane prepared by selective dissolution of chitosan/synthetic polymer blend membrane, J. Membr. Sci., *230,* pp.175-181, 2004.

112. Y. Liu, J. Tang, X. Chen and J.H. Xin. A templating route to nanoporous chitosan materials, Carbohydr. Res., *340,* pp.2816-2820, 2005.

113. F. Pittalis, F. Bartoli and G. Giovannoni. Process for the preparation of chitosan fibers, US Patent, 4464321, 1984.

114. T. Vincent and E. Guibal. Non-dispersive liquid extraction of Cr(VI) by TBP/Aliquat 336 using chitosan-made hollow fiber, Solvent Extr. Ion Exch., *18,* pp.1241-1260, 2000.

115. Z. Modrzejewska and W. Eckstein. Chitosan hollow fiber membranes, Biopolymers, *73,* pp.61-68, 2004.

116. S. Kuniyasu, H. Yoshio, Y. Shinichi, W. Tetsuo, U. Tadahiro and K. Masaru, Composite membrane, US patent, 5259950, 1993.

117. C.Y. Gong and J.Y. Su. Preparation of chitosan charged microporous filtering film by dip-coating method, Chinese patent, 1119553, 1996.

118. S. Tomonari. Dehumidifying membrane and production of dehumidifying membrane, Japanese patent, 2001038173, 2001.

119. B. Xia, G. Zhang and F. Zhang. Bilirubin removal by Cibacron Blue F3GA attached nylon-based hydrophilic affinity membrane, J. Membr. Sci., *226,* pp. 9-20, 2003.

120. W. Shi and F.B. Zhang. Preparation method of affinity polysulfone-chitosan compound asymmetrical ultrafiltration film, Chinese patent, 1413761, 2003.

121. P. Ye, Z.K. Xu, A.F. Che, J. Wu and P. Seta. Chitosan-tethered poly(acrylonitrile-co-maleic acid) hollow fiber membrane for lipase immobilization, Biomaterials, *26,* pp.6394-6403, 2005.

122. J.H. Wang, C.W. Wei, H.C. Liu and T.H. Young. Behavior of MG-63 cells on nylon/chitosan-blended membranes, J. Biomed. Mater. Res., A, *64*, pp.606-615, 2003.

123. W. Wang, S. Bo, S. Li and W. Qin. Determination of the Mark-Houwink equation for chitosans with different degrees of deacetylation, Int. J. Biol. Macromol., *13,* pp.281-285, 1991.

124. X. Jiang, L. Chen and W. Zhong. A new linear potentiometric titration method for the determination of deacetylation degree of chitosan, Carbohydr. Polym., *54,* pp.457-463, 2003.

125. J.J. Shieh and T.S. Chung. Effect of liquid-liquid demixing on the membrane morphology, gas permeation, thermal and mechanical properties of cellulose acetate hollow fibers, J. Membr. Sci., *140,* pp.67-79, 1998.

126. A. Z. Gollan. Anisotropic membranes for gas separation, U.S.Patent, 4681605, 1987.

127. K. Vasarhelyi, J.A. Ronner, M.H.V. Mulder and C.A. Smolders. Development of wet-dry reverse osmosis membrane with high performance from cellulose acetate and cellulose triacetate blends, Desalination, *61,* pp.211-235, 1987.

128. K. Kugel, A. Moseley, B.H. George and E. Klein. Microporous poly(caprolactam) hollow fibers for therapeutic affinity adsorption, J. Membr. Sci., *74,* pp.115-129, 1992.

129. N. Li and R.B. Bai. Copper adsorption on chitosan–cellulose hydrogel beads: behaviors and mechanisms, Sep. Purif. Technol., *42,* pp.237-247, 2005.

130. C.X. Liu and R.B. Bai. Recovery of Bovine Serum Albumin (BSA) by Tripolyphosphate (TPP) Crosslinked Chitosan Membrane, In Recent Advances in Separation & Purification Techniques for Biological & Pharmaceutical Products Development, 21-23 Feb. 2005, Singapore.

131. S. Puttipipatkhachorn, J. Nunthanid, K. Yamamoto and G.E. Peck. Drug physical state and drug–polymer interaction on drug release from chitosan matrix films, J. Control. Release, *75,* pp.143-153, 2001.

132. R.E. Kesting and A.K. Fritzsche. Polymeric Gas Separation Membranes. New York: John Wiley & Sons. 1993.

133. Y. Liu, G.H. Koops and H. Strathmann. Characterization of morphology controlled polyethersulfone hollow fiber membranes by the addition of polyethylene glycol to the dope and bore liquid solution, J. Membr. Sci., *223,* pp.187-199, 2003.

134. J.H. Kim, B.R. Min, J. Won, H.C. Park and Y.S. Kang. Phase behavior and mechanism of membrane formation for polyimide/DMSO/water system, J. Membr. Sci., *187,* pp.47-55, 2001.

135. M.E. Avramescu, W.F.C. Sager, M.H.V. Mulder and M. Wessling. Preparation of ethylene vinylalcohol copolymer membranes suitable for ligand coupling in affinity separation, J. Membr. Sci., *210,* pp.155-173, 2002.

136. Pall. Process for preparing hydrophilic polyamide membrane filter media and prodict, US Patent, 4340479, 1982.

137. R.M. Macdonogh, C.J.D. Fell and A.G. Fane. Characteristics of membranes formed by acid dissolution of polyamides, J. Membr. Sci., *31,* pp.321-336, 1987.

138. C.W. Yao, R.P. Burford, A.G. Fane, C.J.D. Fell and R.M. Macdonogh. Effect of coagulation conditions on structure and properties of membranes from aliphatic polyamides, J. Membr. Sci., *38,* pp.113-125, 1988.

139. H. Strathmann, K. Kaock, P. Amar and R.W. Baker. The formation mechanism of asymmetric membranes, Desalination, *16,* pp.179-203, 1975.

140. H. Strathmann. Production of microporous media by phase inversion process. In Materail Science of Synthetic Membranes, ed. by D.R. Lloyd, pp. 165-195. American Chemical Society ACS symposium Series 269, Washington, DC, 1985.

141. A. Denizli, D. Tanyolac, B. Salih, E. Aydinlar, A. Özdural and E. Pişkin, Adsorption of heavy-metal ions on Cibacron Blue F3GA-immobilized microporous polyvinylbutyral-based affinity membranes, J. Membr. Sci., *137*, pp. 1-8, 1997.

142. A. Denizli, R. Say and M.Y. Arica. Removal of heavy metal ions from aquatic solutions by membrane chromatography, Sep. Purif. Technol., *21*, pp. 181-190, 2000.

143. A. Denizli, B. Salih, M.Y. Arica, K. Kesenci, V. Hasirci and E. Pişkin, Cibacron blue F3GA-incorporated macroporous poly(2-hydroxyethyl methacrylate) affinity membranes for heavy metal removal, J. Chromatogr. A, *758*, pp.217-226, 1997.

144. Ö. Genç, Ç. Arpa, G. Bayramoğlu, M.Y. Arıca and S. Bektaş. Selective recovery of mercury by Procion Brown MX 5BR immobilized poly(hydroxyethylmethacrylate/chitosan) composite membranes, Hydrometallurgy, *67,* pp.53-62, 2002.

145. E.A. Hegazy, H. Kamal, N. Maziad and A.M. Dessouki, Membranes prepared by radiation grafting of binary monomers for adsorption of heavy metals from industrial wastes, Nucl. Instrum. Meth. B, *151,* pp.386-392, 1999.

146. H.A. Abd El-Rehim, E.A. Hegazy and A. El-Hag Ali. Selective removal of some heavy metal ions from aqueous solution using treated polyethylene-g-styrene/maleic anhydride membranes, React. Funct. Polym., *43,* pp.105-116, 2000.

147. D. Bhattacharyya, J.A. Hestekin, P. Brushaber, L. Cullen, L.G. Bachas and S.K. Sikdar. Novel poly-glutamic acid functionalized microfiltration membranes for sorption of heavy metals at high capacity, J. Membr. Sci., *141*, pp. 121-135, 1998.

148. D. Bhattacharyya, J.A. Hestekin, S.M.C. Ritchie and L.G. Bachas. Functionalized membranes remove and recover dissolved heavy metals, Membr. Technol., *1999,* pp. 8-11, 1999.

149. L. Dambies, E. Guibal and A. Roze. Arsenic(V) sorption on molybdate-impregnated chitosan beads, Colloids. Surf. A, *170,* pp.19-31, 2000.

150. S.T. Lee, F.L. Mi, Y.J. Shen and S.S. Shyu. Equilibrium and kinetic studies of copper(II) ion uptake by chitosan-tripolyphosphate chelating resin, Polymer, *42,* pp.1879-1892, 2001.

151. K. Oshita, M. Oshima, Y. Gao, K.H. Lee and S. Motomizu. Synthesis of novel chitosan resin derivatized with serine moiety for the column collection/concentration of uranium and the determination of uranium by ICP-MS, Anal. Chim. Acta, *480,* pp.239-249, 2003.

152. J.D. Merrifield, G.D. William, D.M. Jean and A. Amirbahman. Uptake of mercury by thiol-grafted chitosan gel beads, Water Res., *38,* pp.3132-3138, 2004.

153. X. Zhang and R.B. Bai. Mechanisms and kinetics of humic acid adsorption onto chitosan-coated granules, J. Colloid Interface Sci., *264,* pp.30-38, 2003.

154. C. Tien. Adsorption Calculations and Modeling. Butterworth-Heinemann Series in Chemical Engineering, Newton, MA. 1994.

155. L. Dambies, C. Guimon, S. Yiacoumi and E. Guibal. Characterization of metal ion interactions with chitosan by X-ray photoelectron spectroscopy, Colloids. Surf. A, *177,* pp.203-214, 2000.

156. J. Porath, J. Carlsson, I. Olsson and G. Belfrage. Metal chelate affinity chromatography, a new approach to protein fractionation, Nature, *258,* pp.598-599, 1975.

157. C.Y. Wu, S.Y. Suen, S.C. Chen and J.H. Tzeng. Analysis of protein adsorption on regenerated cellulose-based immobilized copper ion affinity membranes, J. Chromatogr. A, *996,* pp.53-70, 2003.

158. Y.C. Liu, C.C. ChangChien and S.Y. Suen. Purification of penicillin G acylase using immobilized metal affinity membranes, J. Chromatogr. B, *794,* pp.67-76, 2003.

159. Y.C. Liu, S.Y. Suen, C.W. Huang and C.C. ChangChien. Effects of spacer arm on penicillin G acylase purification using immobilized metal affinity membranes**,** J. Membr. Sci., *251,* pp.201-207, 2005.

160. C.H. Kenneth and R. Zaniewski. Purification of urokinase by combined cation exchanger and affinity chromatographic cartridges, J. Chromatogr. B, *525,* pp.297-306, 1990.

161. K. Rodemann and E. Staude. Synthesis and characterization of affinity membranes made from polysulfone, J. Membr. Sci., *88,* pp.271-278, 1994.

162. Reif, V. Nier, U. Bahr and R. Freitag. Immobilized metal affinity membrane adsorbers as stationary phases for metal interaction protein separation J. Chromatogr. A, *664,* pp.13-25, 1994.

163. K. Rodemann and E. Staude. Polysulfone affinity membranes for the treatment of amino acid mixtures, Biotechnol. Bioeng., *46,* pp.503-509, 1995.

164. S.A. Camperi, M. Grasselli, A.A. Navarro del Canizo, E.E. Smolko and O. Cascone. Chromatographic characterization of immobilized metal ion hollow-fiber affinity membranes obtained by direct grafting, J. Liq. Chromatogr. Rel. Technol., *21,* pp.1283-1294, 1998.

165. J. Crawford, S. Ramakrishnan, P. Periera, S. Gardner, M. Coleman and R. Beitle. Immobilized metal affinity membrane separation: Characteristics of two materials of differing preparation chemistries, Sep. Sci. Tech., *34,* pp.2793-2802, 1999.

166. L. Yang, L. Jia, H. Zou and Y. Zhang. Immobilized iminodiacetic acid (IDA)-type Cu^{2+}-chelating membrane affinity chromatography for purification of bovine liver catalase, Biomed. Chromatogr., *13,* pp.229-234, 1999.

167. Y.H. Tsai, M.Y. Wang and S.Y. Suen. Purification of hepatocyte growth factor using polyvinyldiene fluoride-based immobilized metal affinity membranes: equilibrium adsorption study, J. Chromatogr. B, *766,* pp.133-143, 2002.

168. M.Y. Arica, H.N. Testereci and A. Denizli. Dye–ligand and metal chelate poly(2-hydroxyethylmethacrylate) membranes for affinity separation of proteins, J. Chromatogr. A, *799,* pp.83-91, 1998.

169. G. Bayramoǧlu, B. Kaya and M.Y. Arica. Procion Brown MX-5BR attached and Lewis metals ion-immobilized poly(hydroxyethyl methacrylate)/chitosan IPNs membranes: Their lysozyme adsorption equilibria and kinetics characterization, Chem. Eng. Sci., *57,* pp.2323-2334, 2002.

170. P.R. Hari, W. Paul and C.P. Sharma, Adsorption of human IgG on Cu^{2+}-immobilized cellulose affinity membrane: Preliminary study, J. Biomed. Mater. Res., *50,* pp.110-113, 2000.

171. R.S. Pasquinelli, R.E. Shepherd, R.R. Koepsel, A. Zhao and M.M. Ataai. Design of affinity tags for one-step protein purification from immobilized zinc columns**,** Biotechnol. Progr., *16,* pp.86-91, 2000.

172. E.K.M. Ueda, P.W. Gout and L. Morganti. Current and prospective applications of metal ion–protein binding, J. Chromatogr. A, *988,* pp.1-23, 2003.

173. W.Y. Chen, C.F. Wu and C.C. Liu. Interactions of Imidazole and Proteins with Immobilized Cu(II) Ions: Effects of Structure, Salt Concentration, and pH in Affinity and Binding Capacity, J. Colloid Interface Sci., *180*, pp.135-143, 1996.

174. N. Kubota, Y. Nakagawa and Y. Eguchi. Recovery of serum proteins using cellulosic affinity membrane modified by immobilization of Cu^{2+} ion, J. Appl. Polym. Sci., *62*, pp.1153-1160, 1996.

175. S.C. Grigoriy. Twenty-five years of immobilized metal ion affinity chromatography: past, present, and future, J. Biochem. Biophys. Methods, *49,* pp.313-334, 2001.

176. M. Rhazia, J. Desbrières, A. Tolaimate, M. Rinaudob, P. Votterod and A. Alagui. Contribution to the study of the complexation of copper by chitosan and oligomers, Polymer, *43*, pp. 1267-1276, 2002.

177. Ö. Saatçilar, N. Satiroǧlu, S. Bektaş, Ö. Genç and A. Denizli. Packed-bed columns with dye-affinity microbeads for removal of heavy metal ions from aquatic systems, React. Funct. Polym., *50,* pp.41-48, 2002.

178. A. Denizli, K. Kesenci, B. Salih, S. Senel and E. Piskin. Metal Chelating Properties of Cibacrcon Blue F3GA-derived Poly(EGDMA-HEMA) Microbeads. J. Appl. Polym. Sci., *71,* pp.1397-1403, 1999.

179. E. Büyüktuncel, A. Tuncel, Ö. Genç and A. Denizli. Selective Removal of Lead Ions by Polyethylene Glycol Methacrlate Gel beads carrying Cibacron Blue F3GA, Sep. Sci. Technol., *36,* pp.3427-3438, 2001.

180. A. Denizli, D. Tanyolaç, B. Salih and A. Özdural. Cibacron Blue F3GA-attached Polyvinylbutyral Microbeads as Novel Magnetic Sorbents for Removal of Cu(II), Cd(II) and Pb(II) Ions, J. Chromatogr. A., *793,* pp.47-56, 1998.

181. Ç. Arpa, C. Alim, S. Bekta$\mathbf{5}$, Ö. Genç and A. Denizli. Adsorption of Heavy Metal Ions on Polyhydroxylethylmethacrylate Microbeads Carrying Cibacron Blue F3GA, Colloids Surf. A, *176,* pp. 225-232, 2001.

182. A. Denizli, R. Say, S. Patir and M.Y. Arica. Adsorption of Heavy Metal Ions onto Ethylene Diamine-derived and Cibacron Blue F3GA-incorporated Microporous Poly(2-hydroxyethyl methacrylate) Membranes, React. Funct. Polym., *43,* pp.17-24, 2000.

183. E. Büyüktuncel, S. Bekta$\mathbf{5}$, Ö. Genç and A. Denizli. Poly(vinylalcohol) Coated/Cibacron Blue F3GA-attached Polypropylene Hollow Fiber Membranes for Removal of Cadmium Ions from Aquatic Systems. React. Funct. Polym., *47,* pp.1-10, 2001.

184. M.C.L. Martins, D. Wang, J. Ji, L. Feng and M.A. Barbosa. Albumin and fibrinogen adsorption on Cibacron blue F3G-A immobilised onto PU-PHEMA (polyurethane-poly(hydroxyethylmethacrylate)) surfaces, J. Biomater. Sci., Polym. Ed., *14,* pp.439-455, 2003.

185. A. Denizli, B. Salih and E. Piskin. Comparison of Metal Chelate Affinity Sorption of BSA onto Dye/Zn(II)-derived Poly(ethylene glycol dimethacrylatehydroxyethyl methacrylate) Microbeads, J. Appl. Polym. Sci., *65,* pp.2085-2093, 1997.

186. P.J. Neyman, MGuzy, S. Shah, H. Wang, H.W. Gibson, K.E. Van Cott, R.M. Davis, C. Brands and J.R. Heflin. Enhanced second order nonlinear optical susceptibilities in ionically self-assembled films incorporating dianionic molecules, Mater. Res. Soc. Symp. Proc., *660,* JJ8.30.1-6, 2001.

187. H. Sashiwa and S. Aiba. Chemically modified chitin and chitosan as biomaterials, Prog. Polym. Sci., *29,* pp.887-908, 2004.

188. K. Kurita. Controlled functionalization of the polysaccharide chitin. Prog. Polym. Sci., *26*, pp.1921–1971, 2001.

189. K.C. Gupta and M.N.V.R. Kumar. An overview on chitin and chitosan applications with an emphasis on controlled drug release formulations. J. Macromol. Chem. Phys., *C40*, pp.273–308, 2000.

190. N. Li, R.B. Bai and C.K. Liu. Enhanced and selective adsorption of mercury ions on chitosan beads grafted with polyacrylamide via surface-initiated atomic transfer radical polymerization, Langmuir, *21*, pp.11780-11787, 2005.

191. N. Li and R.B. Bai. Highly enhanced adsorption of lead ions on chitosan granules functionalized with polyacrylic acid, Ind. Eng. Chem. Res., *In press.*

192. B, Ulrich and W. Rudolf. Module with membrane elements in cross-flow and in a dead-end arrangement, US patent 0111414, 2003.

193. R.L. Machado, E.J. Arruda, C.C. Santana and S.M.A. Bueno. Evaluation of a chitosan membrane for removal of endotoxin from human IgG solutions, Prog. Biochem., *41,* pp 2252-2257, 2006.